



# Hydrodynamic effects of primary vessel waves in a semi-closed groyne field

Master Thesis

S.T. (Sander) Broeders

# Hydrodynamic effects of primary vessel waves in a semi-closed groyne field

Master Thesis

by

S.T. (Sander) Broeders

to obtain the degree of Master of Science  
at the Delft University of Technology,  
To be defended publicly on Monday December 11, 2023 at 3:00 PM



Student number: 4687779  
Project duration: March 8, 2023 – December 11, 2023  
Thesis committee: Dr. ir. B.C. van Prooijen, TU Delft, Chair  
Dr. ir. C.J. Sloff, TU Delft and Deltares, supervisor

*This thesis is confidential and cannot be made public until December 11, 2023.*

Cover: Aerial picture of Groyne Field 9 in the 'Nieuwe Waterweg' (5-4-2023)  
Style: TU Delft Report Style, with modifications by Sander Broeders

An electronic version of this thesis is available at <http://repository.tudelft.nl/>.

# Preface

Submitting this thesis report concludes my Master in Hydraulic Engineering at Delft University of Technology. I am very grateful that I got the opportunity to work on my thesis at the Deltares RIV department.

First, I would like to thank my daily supervisor Kees Sloff for giving me the opportunity to work on this amazing project and for the freedom to choose the path I found most interesting. I got the opportunity to join various fieldwork campaigns for this and other projects. In every field work experience new insights inspired me to study new directions. I want to thank Bram van Prooijen for all the great feedback I received during progress meetings. I found the meetings really pleasant as the three of us were able to discuss all points thoroughly to finish the meeting with a lot of new questions and challenges for the period ahead.

Last but not least, I would like to thank my friends, parents, brother, sister and Marloes for their support during the past 7 years in Delft and the last nine months working on this thesis.

*Sander Broeders  
Delft, December 2023*



# Abstract

The port of Rotterdam is one of the most important ports in Western Europe and via the 'Nieuwe Waterweg' it provides maritime trading between the large hinterland and the rest of the world. To provide port access for the large vessels, the channel and port basins need to be dredged regularly. At the same time, in other locations, sediment is required to fill erosion holes, develop natural habitats and improve water quality. Different stakeholders joined forces to acquire more knowledge about managing the sediment in the system. This resulted in the project called 'Proeftuin Sediment Rijnmond' (PSR). One of the pilot projects of PSR is located in the 'Nieuwe Waterweg' where a longitudinal dam is constructed between groynes to study the effects on nourished sediment. The location used for this pilot is called Groyne Field 9. At the same time, the area around Groyne Field 9 is involved in another project called the 'Groene Poort'. This project focuses on natural development in the areas between groynes. The research in this thesis contributes to knowledge acquisition for the various projects. It studies the effect primary vessel waves have on the hydrodynamic behaviour in the semi-closed Groyne Field 9.

The study answers the research question: *How can primary vessel waves impact the hydrodynamics in the semi-closed Groyne Field 9 in the 'Nieuwe Waterweg' and how can the hydrodynamic conditions be modified with different structural layout designs?* Two different approaches are used to answer the question. First, a data analysis is conducted using 2 relevant data sets and secondly, a numerical model is developed to be able to study the topic in a more controlled environment.

The First part of the research analyses two data sets simultaneously. Water level and velocity measurement data obtained inside the groyne field is combined with Automated Identification System data (AIS data), which contains velocity, location and more information about sailing vessels. Combining these data sets enables the possibility to study the effect of the vessels' characteristics on the water level in Groyne Field 9. A regression analysis is carried out which results in an equation that shows the correlations of all parameters. The most significant parameter influencing the severity of the primary vessel wave is the sailing velocity. Other important parameters that cause water level drawdown are the length, width and draught of the vessel.

In the second part of the research, a numerical model of sailing vessels in the 'Nieuwe Waterweg' is developed in Delft3D Flexible Mesh software. This can be used to analyse the hydrodynamic effect on the groyne field in a controlled way. To simulate vessels passing through the waterway, a local atmospheric pressure field is used. This pressure field simulates the vessels' hull and by moving the pressure field through the numerical domain, a primary wave is modelled. To research the effect of primary vessel waves on the semi-closed groyne field, various simulations are conducted and analysed which can be distinguished by two sets of simulations.

The first set of simulations focuses on understanding the hydrodynamic system by simplifying the bathymetry and other parameters. This simplification is obtained by flattening the bed inside the groyne field. This is then compared to a simulation without this simplification and with the real current bathymetry. The second set of simulations focuses on the properties and effects of different layouts. The different layouts are chosen to be able to research the effect of specific geometrical designs like the situation where more groyne fields are partly closed off by a longitudinal dam.

Both sets of simulations resulted in the general conclusion that the order of magnitude of flow increase caused by vessel-induced waves is about 0.2 m/s and that these magnitudes are most likely to occur near the entrances of the groyne field and near the groynes. In general, the complex bathymetry of the current situation causes more friction compared to the flat bed situation and therefore damping of waves. On the other hand, locally, the velocities can be higher, because flow lines need to contract to flow around a nourished island for example.

The second set of simulations concluded that emerged groynes create much calmer dynamics in the groyne field compared to the simulations with submerged groynes. Next to this, in general, the number

or location of the openings in the longitudinal dam does not result in significant variation in the hydrodynamic properties between the layouts. However, the total size of the openings combined does have an effect.

To conclude, primary vessel waves impact the hydrodynamics in Groyne Field 9 significantly by large vessels sailing at high velocities. These hydrodynamic effects can be managed and modified by making described decisions on geometrical layout designs like groynes or opening size in the longitudinal dam.

The conclusions obtained from this research can be used to further decide on the design of multiple groyne fields in the 'Nieuwe Waterweg'. Different layout elements create different hydrodynamic conditions which can be sufficient for various purposes. Fish species prefer different conditions compared to birds or vegetation development. Additionally, morphodynamic research is necessary to conduct more accurate predictions on different designs and plans. However, the research presented in this thesis provides information on the effect of primary vessel waves from two different analyses which can be used for the development of riverbank projects in the 'Nieuwe Waterweg' and in other locations.

# Samenvatting

De haven van Rotterdam is een van de belangrijkste havens van West-Europa. Via de Nieuwe Waterweg maakt de haven handel mogelijk tussen het uitgestrekte achterland en de rest van de wereld. Om ervoor te zorgen dat grote schepen de haven kunnen bereiken moet de Nieuwe Waterweg regelmatig gebaggerd worden. Tegelijkertijd is er sediment nodig in andere delen van het Rijn-Maas mondingsgebied om bijvoorbeeld erosiekuilen te dichten, voor de ontwikkeling van natuur en het verbeteren van waterkwaliteit. Voor de kennisvergaring over efficiënt sedimentbeheer hebben verschillende partijen de krachten gebundeld. Deze samenwerking heeft geresulteerd in het project 'Proeftuin Sediment Rijnmond' (PSR). Een van de pilot projecten ligt in de Nieuwe Waterweg. In deze pilot is een longitudinale dam aangelegd tussen de kribkoppen om het effect hiervan op sediment suppleties te onderzoeken. Deze locatie wordt 'Kribvak 9' genoemd. Tegelijkertijd is Kribvak 9 ook onderdeel van een ander project dat de 'Groene Poort' heet. Dit project focust zich op natuurontwikkeling onder en boven water in het gebied van de kribvakken. Het onderzoek in dit rapport draagt bij aan het vergaren van kennis voor de verschillende pilot projecten. Het onderzoek focust zich op het effect van primaire scheepsgolven op de hydrodynamica in het gedeeltelijk afgesloten Kribvak 9.

In dit rapport wordt de volgende onderzoeksvraag beantwoord: *Wat voor impact hebben primaire scheepsgolven op de hydrodynamica in het gedeeltelijk afgesloten Kribvak 9 en hoe kunnen die hydrodynamische condities worden aangepast met verschillende structurele kribvak ontwerpen?* Om deze vraag te beantwoorden zijn er twee verschillende benaderingen gebruikt. Allereerst is er een data analyse gedaan door 2 relevante datasets te combineren. Ten tweede is er een numeriek model ontwikkeld die het mogelijk maakt om het onderwerp in een meer gecontroleerde omgeving te onderzoeken.

In het eerste gedeelte van het onderzoek worden twee verschillende datasets tegelijkertijd geanalyseerd. Een dataset met waterpeil- en watersnelheidsmetingen die zijn gemeten in Kribvak 9 wordt gecombineerd met 'Automated Identification System' (AIS) data. AIS data bevat informatie over scheepseigenschappen zoals snelheid, locatie en andere scheepskarakteristieken. Door het combineren van deze datasets wordt het mogelijk om het effect van verschillende scheepseigenschappen op het waterpeil in Kribvak 9. Een regressie analyse is uitgevoerd om een empirische functie te verkrijgen die de data het best beschrijft. Deze functie laat de correlatie van de verschillende karakteristieken zien. Er kan hiermee geconcludeerd worden dat vaarsnelheid is de meest significante parameter dat de intensiteit van de primare golf bepaald. Andere belangrijke parameters voor het veroorzaken van een korte waterpeilverlaging zijn scheepslengte, -breedte en -diepgang.

In het tweede deel van het onderzoek wordt een numeriek model ontwikkeld in het programma Delft3D Flexible Mesh dat schepen kan simuleren die door de Nieuwe Waterweg varen. Dit model kan daarna gebruikt worden om verschillende situaties te simuleren in een gecontroleerde omgeving. Om een bewegend schip door een numeriek domein te simuleren is de atmosferische druk aangepast. Door lokaal de atmosferische druk te verhogen kan een scheepsromp worden nagebootst. Door dit drukveld door het numerieke domein te laten bewegen wordt zo een primaire golf gemodelleerd. Om het effect hiervan op het kribvak te analyseren zijn er verschillende simulaties gedraaid die kunnen worden gecategoriseerd in twee sets simulaties.

In de eerste set simulaties worden de bathymetrie en andere parameters iets gesimplificeerd om zo een beter beeld te krijgen van het hydrodynamisch gedrag in het kribvak. De bathymetrie is gesimplificeerd door de bodem in het kribvak plat te maken. Deze simulatie kan dan vergeleken worden met een simulatie dat wel de iets complexere, maar huidige, bathymetrie bevat. De tweede set met simulaties richt zich meer op het onderzoeken van het effect van verschillende kribvak indelingen. Verschillende indelingen zijn gecreëerd door het combineren van verschillende geometrische opties. Een van de situaties is bijvoorbeeld de situatie waar naastgelegen kribvakken op een zelfde manier zijn afgesloten.

Beide sets simulaties resulteerde in de algemene conclusie dat de orde van grootte van de stromingssnelheidstoename door scheepsgolven is ongeveer 0.2 m/s en dat deze orde groottes meestal optreden in de buurt van de openingen en de kribben van het kribvak. Over het algemeen zorgt een complex

bathymetrie voor meer frictie en het dempen van golven. Aan de andere kant kan er lokaal door het samentrekken van stromingslijnen een snelheidsverhoging ontstaan. Uit de tweede set simulaties kan geconcludeerd worden dat kribben die boven het waterpeil uitsteken zorgen voor een veel rustiger dynamisch beeld in het kribvak vergeleken met wanneer de kribben onder het waterpeil liggen. Daarnaast kan geconcludeerd worden dat de locatie van openingen in de longitudinale dam niet uitmaken voor het dynamica beeld, maar dat de totale grootte van de openingen wel uitmaakt.

Om de algemene vraag te concluderen, hebben primaire scheepsgolven een significante impact op de hydrodynamica in Kribvak 9 door grote schepen die op hoge snelheid varen. Deze hydrodynamische effecten kunnen worden aangepast en gecontroleerd worden door de beschreven beslissingen te nemen in het geometrisch ontwerp van het kribvak, zoals grootte van de opening of hoge of lage kribben.

De conclusies en resultaten die uit dit onderzoek zijn gekomen kunnen worden gebruikt in de besluitvorming van de ontwikkeling van meerdere kribvakken in de Nieuwe Waterweg. Verschillende kribvak indelingen zorgen voor verschillende hydrodynamische condities die kunnen bijdragen aan verschillende doeleinden. Vissoorten gedijen bij andere condities dan vogelsoorten of vegetatie. Daarnaast is morfodynamisch onderzoek nodig om nog accuratere voorspellingen te doen bij verschillende ontwerpen. Echter, het onderzoek in dit rapport biedt inzicht in het effect van primaire scheepsgolven vanuit twee verschillende analyses die gebruikt kunnen worden bij de ontwikkeling van rivieroever projecten in de Nieuwe Waterweg en in andere locaties.

# Contents

<b>Preface</b>	<b>i</b>
<b>Abstract</b>	<b>ii</b>
<b>Samenvatting</b>	<b>iv</b>
<b>1 Introduction</b>	<b>1</b>
1.1 Study area	1
1.2 Motivation and Relevancy	3
1.2.1 Rijkswaterstaat and Rotterdam municipality	3
1.2.2 Port of Rotterdam	3
1.2.3 Nature organisations	3
1.2.4 Rozenburg inhabitants and visitors	4
1.3 Problem analysis	4
1.3.1 Vessel induced waves	4
1.3.2 Natural influence factors	5
1.3.3 Ecological considerations	8
1.4 Research objectives	10
1.4.1 Objective	10
1.4.2 Research questions	11
1.5 Methodology	11
<b>2 Data analysis</b>	<b>12</b>
2.1 Measurement data	12
2.2 Fourier and Wavelet analysis	14
2.2.1 Fourier Transformation	14
2.2.2 Wavelet transformation	15
2.3 Analysing water level signals with AIS data	16
2.4 Natural frequencies in a river	17
2.5 Quantified drawdown effect caused by vessels	18
2.5.1 Sailing velocity effect (1)	19
2.5.2 Vessel length effect (2)	20
2.5.3 Vessel course and distance from groyne effect (3) and (4)	20
2.5.4 Vessel's width and draught effects (5 and 6)	20
2.6 Empirical relation of drawdown caused by vessels	20
<b>3 Primary vessel wave effect model in the 'Nieuwe Waterweg'</b>	<b>23</b>
3.1 Model setup	23
3.1.1 Grid and mesh sizes	23
3.1.2 Bathymetry schematization	24
3.1.3 Boundary conditions	25
3.2 External forces on Groyne Field 9	26
3.2.1 Tidal forcing	26
3.2.2 River discharge	26
3.2.3 Vessel waves	27
3.3 Model verification	28
3.3.1 Verification using measurement data	28
3.3.2 Verification using literature	30
3.3.3 Verification summary	31
<b>4 Hydrodynamics inside Groyne Field 9</b>	<b>32</b>
4.1 Overview simulations	32



4.2	Basic situation (flat bed)	33
4.2.1	Quantitative understanding the basic hydrodynamic system	36
4.3	Complex-bathymetry situation (Current situation)	40
4.3.1	Qualitative analysis complex bathymetry	40
4.4	Tidal background simulation	44
<b>5</b>	<b>Hydrodynamic behaviour in different groyne field layouts</b>	<b>48</b>
5.1	Layout description	48
5.1.1	Layout 1: Closed neighbouring groynes	49
5.1.2	Layout 2: Corner entrances and emerged groynes	49
5.1.3	Layout 3: Single middle entrances and emerged groynes	50
5.1.4	Layout 4: Elongated middle openings and submerged groynes	50
5.2	Alternative layout results	51
5.2.1	General hydrodynamic behaviour	52
5.2.2	Quantitative results	53
5.2.3	Effect of entrance configuration	54
5.2.4	Effect of emerged and submerged groynes	54
5.2.5	Natural frequency	55
5.3	Concluding remarks on the different layouts	55
<b>6</b>	<b>Discussion</b>	<b>56</b>
6.1	Data analysis	56
6.2	Numerical model	56
6.3	Ecological considerations	58
<b>7</b>	<b>Conclusions</b>	<b>59</b>
<b>8</b>	<b>Recommendations</b>	<b>61</b>
8.1	General applications and recommendations	61
8.2	Natural development	62
8.3	Additional research	62
	<b>References</b>	<b>63</b>
<b>A</b>	<b>Study area</b>	<b>65</b>
<b>B</b>	<b>Data analysis appendix</b>	<b>66</b>
B.1	Wavelet signals	66
B.2	Verification selection data	68
<b>C</b>	<b>Numerical methodology</b>	<b>74</b>
<b>D</b>	<b>Numerical simulations</b>	<b>76</b>
D.1	Basic (flat bed) situation	77
D.2	Current (original bed) situation	80
D.3	Tidal flow analysis	84
D.4	Different layout simulations	86
D.5	Quantification tables	89
<b>E</b>	<b>Python sheets</b>	<b>91</b>
E.1	Wavelets	91
E.2	Atmospheric pressure (vessel) input file	93
E.3	Bedlevel file changer	97
<b>F</b>	<b>Sediment analysis</b>	<b>101</b>

# 1

## Introduction

The port of Rotterdam is one of the most important ports in Western Europe and connects the large hinterland with the rest of the world via rails, roads and waterways. An important waterway that serves as the connection between the river mouth and the hinterland is the 'Nieuwe Waterweg'. Yearly, 15,000 vessels of all sizes sail this waterway to transport goods. To provide sufficient draught, the 'Nieuwe Waterweg' is dredged regularly. In the total port of Rotterdam area, 7 - 12 Million cubic meters of sediment is dredged to maintain depths every year. The sediment is mainly transported to and dumped in the North Sea. At the same time, locations within the lower Rhine and lower Meuse, referred to as the Rhine-Meuse estuary, require sediment to fill erosion holes, develop natural habitats and improve water quality. Future sediment management of the Rhine-Meuse estuary is beneficial for various stakeholders, like the port authority, nature organisations and governmental institutions. To obtain more knowledge about the sediment in the system, the project 'Proeftuin Sediment Rijnmond' (PSR) has started. One of the pilot projects of PSR is located in the 'Nieuwe Waterweg' where a longitudinal dam is constructed between groynes to study the effects on nourished sediment. The location used for this pilot is called Groyne Field 9, referring to the groyne field numbering.

Parallel to PSR, another project is ongoing in the same area, called the 'Groene Poort' project. The 'Groene Poort' is a different initiative that has been linked to the PSR project because of the possibilities for a pilot. The 'Groene Poort' project is a project initiated by Rijkswaterstaat, Port of Rotterdam, Rotterdam municipality and the World Wide Fund for Nature. By realising the 'Groene Poort', Rijkswaterstaat can comply with the 'Kader Richtlijn Water' (Hiddema, W., et al., 2013). In 2000, the European Parliament agreed to protect and manage water inside Europe actively. These guidelines for the Netherlands are written in the Kader Richtlijn Water (KRW). The main goal of the guidelines was to secure surface- and groundwater quality in Europe. The exact KRW guidelines and how these are evaluated will be discussed in Section 1.3.

Information about the study area is written in Section 1.1. This section highlights the interventions done in the pilot project that are relevant to this study. To understand the objectives of this research it is important to know about all the different stakeholders. Such an integral project does not have one best solution, but a variety of stakes and objectives. In Section 1.2, all relevant stakeholders and their stakes are discussed. Section 1.3 focuses on the technical and natural considerations in this research. Eventually, the background, different stakeholder objectives and technical considerations result in the main objectives for this research in Section 1.4.

### 1.1. Study area

First, the location of the groyne field will be highlighted, including some historical and important factors within the 'Nieuwe Waterweg'. Secondly, two different projects connected to this research will be explained in more detail: 'Groene Poort' and 'Proeftuin Sediment Rijnmond'.

The Rhine and Meuse rivers flow out to the open sea via the combined Rhine-Meuse estuary located in the southwest of the Netherlands. Via various branches, the water can exit the river through the Haringvliet Sluices or the 'Nieuwe Waterweg'. The 'Nieuwe Waterweg' and 'Het Scheur' are located in the port of Rotterdam and locally connect the branches upstream with the North Sea. The discharge

through the 'Nieuwe Waterweg' is influenced by the discharge in the Rhine River and through the Haringvliet Sluices. The discharge can be managed by opening and closing large gates. If the discharge gets too high in the 'Nieuwe Waterweg', the gates can be opened in order to reduce the discharge in the 'Nieuwe Waterweg'. A geographical layout of the important locations is illustrated in Figure 1.1 and a more zoomed in satellite image is depicted in Appendix A.

The 'Nieuwe Waterweg' is intensively used as a waterway for inland vessels to sail between the Rotterdam port and inland destinations. At the same time, it is used as a waterway for seagoing vessels to sail from the North Sea to port basins upstream of the 'Nieuwe Waterweg'. Yearly, 15,000 vessels with a variety of sizes sail the gateway to the Rhine corridor (of Rotterdam, 2019). In the past few decades, vessel sizes have increased significantly in size due to a growing demand for the transport of goods and technological innovations. In 2016, the new Panama Canal locks were finished which made it interesting to build a new larger fleet of Panamax vessels. These new vessels are called Neopanamax vessels. In response to the increase in vessel sizes, the decision to deepen the 'Nieuwe Waterweg' by 1.5 meters was made by the Port of Rotterdam. This was necessary to allow Neopanamax vessels to navigate through the waterway. The dredging works required to achieve this were carried out in 2018, enabling vessels with a draught of fifteen meters to sail through the 'Nieuwe Waterweg'. (of Rotterdam, 2019).



**Figure 1.1:** The Rhine river system with an overview of the relevant waterways, including the 'Nieuwe Waterweg', Haringvliet sluices and the location of Groyne Field 9 (Rijkswaterstaat).

The river banks of the 'Nieuwe Waterweg' and 'Het Scheur' are made of revetment structures. Along the river bank, groynes reach towards the channel until the deeper dredged part. The groynes are generally submerged, depending on the tide. As already mentioned in the general introduction, Groyne Field 9 is the name of the location studied in this research. Groyne Field 9 is located in 'Het Scheur' as depicted in Figure 1.1. Initially, a longitudinal dam was constructed between the groyne tips to partially block the area between them. In 2016, large rocks dredged from the 'Breddiep' area of the Rotterdam Port were deposited in the groyne field, resulting in the formation of an island that is now visible on maps and is shown in Figure 1.2. In December 2022, additional sediment was deposited within the groyne field using a technique called Rainbowing. Throughout this process, the groyne field is being monitored for both biotic and abiotic factors. Before this nourishment, Kouwenhoven (2023) did Acoustic Doppler velocimetry (ADV) measurements inside the groyne field to research the hydrological behaviour inside the groyne field. This measurement data is used in this study as well. More information about this can be found in Chapter 2.



**Figure 1.2:** Aerial photo of Groyne Field 9 taken on 05-04-2023. The photo was taken at relatively low tide.

## 1.2. Motivation and Relevancy

Significant interest from various stakeholders coincides with multiple projects in and around the Groyne Field 9 area. Each stakeholder has a unique view on the development of the groyne field areas along 'Het Scheur'. Each stakeholder will be discussed separately to highlight the different interests and motivations for the research proposed in this report.

### 1.2.1. Rijkswaterstaat and Rotterdam municipality

Rijkswaterstaat and the Rotterdam municipality are interested in the project for multiple reasons. The already mentioned 'Kader Richtlijn Water' (KRW) is a set of guidelines that the government should make decisions on. Because of this, creating flora and fauna in a highly urbanised area would be in line with the goals of the 'Groene Poort' project. At the same time, the government has an interest in the Port of Rotterdam for its economic benefits. The government works for society and should lobby for its interests as well. The governmental stakeholders aim for the best solution for all other stakeholders.

### 1.2.2. Port of Rotterdam

For the Rotterdam Port Authority, the 'Nieuwe Waterweg' is important for the port infrastructure. The waterway is vital for port operations and therefore, future natural development should not hinder vessels sailing in the waterway. Another possible inconvenience for port operations is that sediment will flow back into the channel. If this happens, the channel has to be dredged more often which causes downtime and costs money. However, natural development is something that the port authority encourages. The port authority created a vision of nature development in the port and states that the port will put effort into maintaining and recovering nature and biodiversity in the port (of Rotterdam, 2022). The 'Groene Poort' is an example that will help the port authority achieve this vision. The project 'Proeftuin Sediment Rijnmond' aims to reuse dredged material from the waterways in the same system to reduce the sailing distance for dredging vessels. By reducing this sailing distance for the disposal, the costs of dredging works will be reduced. This will be beneficial for the port authority.

Another factor that is a possible threat from the port authority's perspective is the fact that natural development could put limitations on future port development and activities. If nature flourishes, protected species could settle in the area. This possibly harms the port because, for protected species, certain rules exist to not disturb them. This situation is not likely to occur in the short term, but theoretically, it is possible.

### 1.2.3. Nature organisations

Natural organisations will encourage the plan to develop more nature in the area. However, different animals and species will flourish in slightly different environments. For example, fish will benefit from a groyne field with deeper areas in order for the fish to rest along their journey upstream. On the other hand, birds will benefit more from large flats so they can rest and feed.

### 1.2.4. Rozenburg inhabitants and visitors

The 'Landtong Rozenburg', which is the land area south of a large part of the 'Nieuwe Waterweg', contains a lot of nature in the middle of a highly urbanised environment. People who visit the area and people who live nearby often have a strong opinion about everything that is going on there. The inhabitants want to preserve nature and therefore they predominantly support projects like the 'Groene Poort'.

## 1.3. Problem analysis

Section 1.1 and Section 1.2 provides background information about the projects and the future vision of the pilot project in Groyne Field 9. This section focuses on the influence factors that impact Groyne Field 9. By examining these factors, the main objective is to formulate relevant research questions for the study conducted in this thesis. Additionally, the information provided in this section provides some literature background for the relevant subjects of this study.

### 1.3.1. Vessel induced waves

The 'Nieuwe Waterweg' is a dredged channel that facilitates vessel navigation between the downstream-located port basins and upstream-located areas. The 'Nieuwe Waterweg' is the only open connection from the Rhine and Waal rivers to the sea, which makes it a popular channel for cargo vessels to sail. Yearly, 15,000 vessels sail the 'Nieuwe Waterweg' and create waves that impact the river bank and Groyne Field 9. The section below provides theoretical background on vessel-induced waves inside a channel.

In Figure 1.3, the hydrological effects caused by a vessel sailing through a channel are illustrated. The arrows represent hydrodynamic flow patterns.

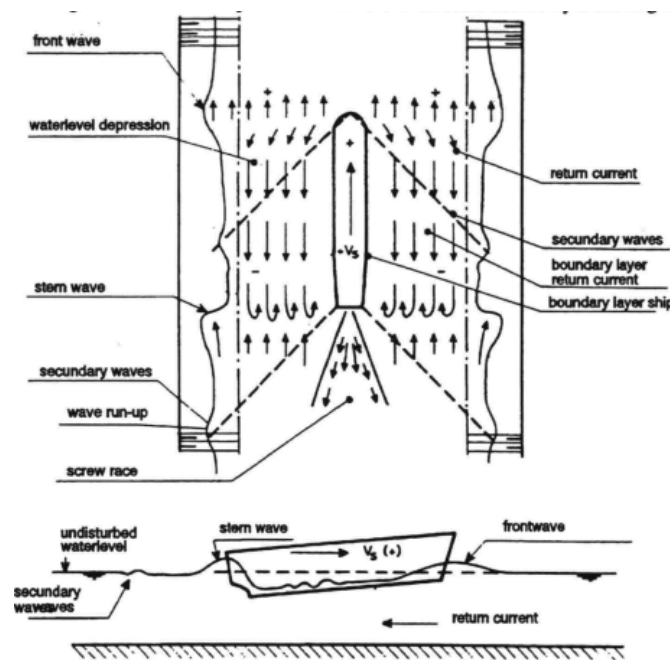


Figure 1.3: Different vessel-induced currents and vessel-induced waves (Schiereck, 1993).

The waves induced by a sailing vessel can be classified into two distinct categories. The primary wave refers to the water level reduction resulting from the return current. The return current is created by a sailing vessel that pushes the water level up at the bow of the vessel and creates space for water at the stern of the vessel as visualized in Figure 1.3 and illustrated by the black arrows. The return current reduces the pressure alongside the vessel according to Bernoulli's principle, which states that the water level reduces because the water mass has velocity. The reduction of the water level will eventually travel through a water body and this is referred to as the primary wave (Ten Brinke, 2003, Engineering and of Germany, 2010, Dempwolff et al., 2022). This primary wave has a wavelength proportional to

the length of the vessel and is therefore different from the secondary waves.

If a vessel moves through a channel, secondary waves, also referred to as the Kelvin Wake or Kelvin wave systems are the most visible waves (Soomere, 2007). Secondary waves can be distinguished by their V-shape wave pattern behind the sailing vessel.

Kouwenhoven (2023) studied the velocities caused by vessel-induced waves in the hydraulically already dynamic groyne field. He found that the average velocity increase at a particular location is 0.23 m/s.

Figure 1.4 illustrates a measurement signal of Acoustic Doppler Velocimeter 3 (ADV 3) from the field campaign of Kouwenhoven (2023). The signal shows in detail how a vessel passage results in a water level variation and how the passage increases the velocity magnitude significantly. It can be obtained that the velocity at the location increases up to 0.5 m/s. Before conclusions can be drawn from the data on the effect on sediment transport, it is necessary to check if other influences impact the same effect.

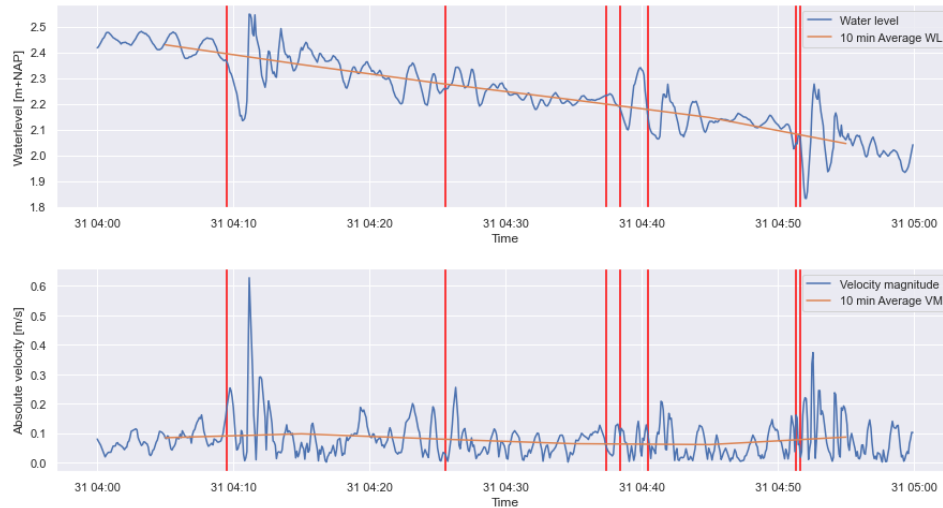


**Figure 1.4:** Water level and velocity signal of ADV 3 at a particular interval on the 30th of March 2022. The blue lines represent the water level and velocity magnitude signals. The red lines represent vessel passages.

### 1.3.2. Natural influence factors

In addition to vessel-generated waves, the groyne field hydrodynamics are significantly influenced by various estuary characteristics, including tidal forcing and river discharge. The research conducted for this thesis focuses on vessel-generated waves. However, it is important to be aware of all possible influential factors. Four contributing factors are briefly discussed in this section.

#### Tides

The 'Nieuwe Waterweg' connects the North Sea with the Rhine-Meuse river system. It means that the tidal forcing present at the North Sea impacts the water level inside the estuary resulting in two high and two low waters each day. This tidal signal goes hand-in-hand with in- and outflow of water at the river mouth. In his research, Kouwenhoven (2023) analysed ADV data that resulted in general tidal flow patterns within the groyne field geometry. As illustrated in Figure 1.5, the flow direction varies between high and low tide. The figure shows the significant influence the tidal forcing has on the flow direction inside the groyne field. Therefore, it is one of the factors that should be taken into account while conducting hydrodynamic or morphodynamic studies at the location.



**Figure 1.5:** Flow patterns during low and high tide according to Kouwenhoven (2023).

Figure 1.6 shows a random selection of the velocities measured by the ADVs during low and high tide. The velocity caused by the tidal forcing will rarely exceed 0.6 m/s, as depicted in the figure. From the measured data plotted in Figure 1.4, it can be obtained that velocity magnitudes around vessel passages exceed the average velocity caused by the tidal forcing. However, tidal forcing has a significant role and can not be ignored. If the vessel wave effect is analysed by using a model, tidal effects must be taken into consideration. It depends on the focus of the research, but the model can, for example, be run for different scenarios with changing tidal phasing.

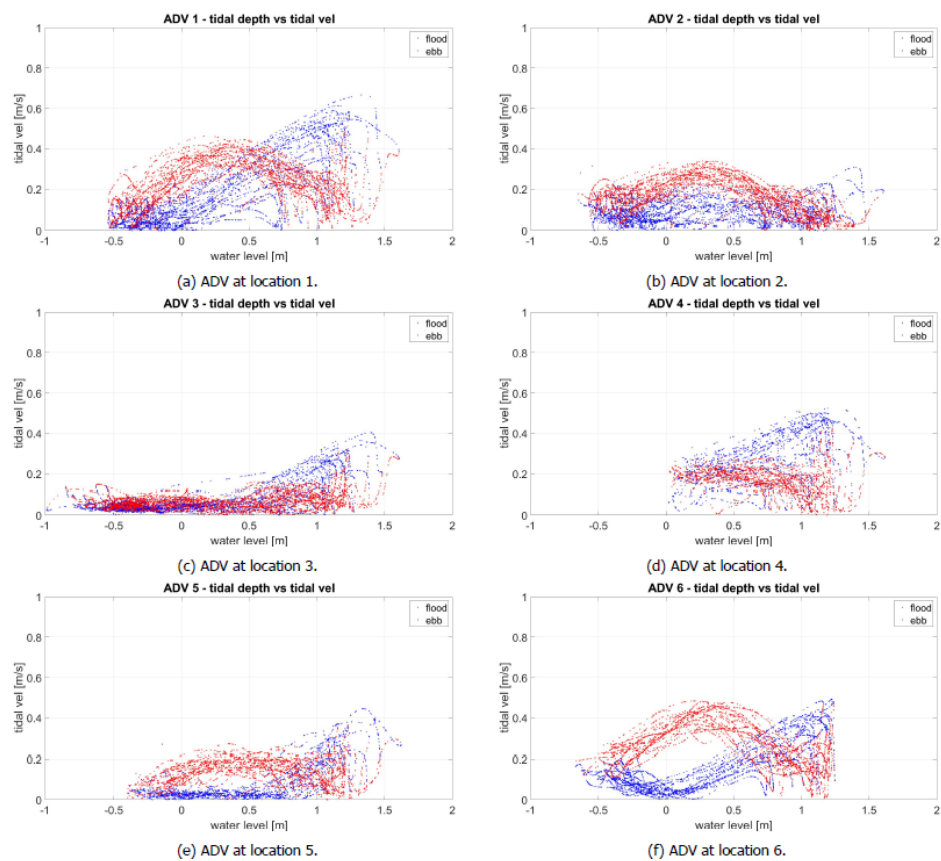


**Figure 1.6:** The tidal velocities and water levels for 10,000 random moments. Red dots represent low tide moments and the blue dot the moments during high tide (Kouwenhoven, 2023).

### River discharge

The Rhine River enters the Netherlands at Lobith, from where the river bifurcates into several branches and eventually, the water exits the system through the 'Nieuwe Waterweg' or the Haringvliet sluices. The Haringvliet exit is controlled by a dam with sluices, so the discharge through this location is controlled manually by monitoring the discharge at Lobith. Managing this discharge influences the discharge through the 'Nieuwe Waterweg'. Since 2019, the gates of the Haringvliet sluices have been partially open to allow for salt water to intrude in the Haringvliet and to allow fish migration. The discharge through the 'Nieuwe Waterweg' is regulated to be equal to  $1500 \text{ m}^3/\text{s}$  for a discharge between  $1700$  and  $3900 \text{ m}^3/\text{s}$  in the Rhine at Lobith. Together with the tidal forcing, the discharge results in a dynamic system with constantly changing flow velocities in the area where Groyne Field 9 is located.

### Salinity

Additionally, the tidal forcing and the river discharge impact the average salinity in the area. The 'Nieuwe Waterweg' is the mixing zone between sweet fresh water from the river and salt water from the sea, which is called brackish water. Depending on the discharge or tidal phase, the salinity levels change constantly. A large discharge causes the boundary from fresh to salt water to be more seaward-directed and a smaller discharge causes the opposite situation. During fieldwork, it is observed that the water at Groyne Field 9 tastes quite fresh compared to the seawater. Additionally, salt water has a higher density, which influences the flow patterns by creating higher-density layers near the bed and lower-density layers near the water surface. Fresh water from the river flowing in a seaward direction flows over the salt water layer intruding the river, also known as the salt tongue. The two-dimensional model uses the depth-averaged velocity assumption which is not able to take this into account. Therefore, in this research, this effect will be neglected because of the complexity and lack of measurement data and instruments. Additionally, the salinity is important for the natural ecology analysis because the variation between fresh and salt water creates specific habitats for particular species.

### Wind

Wind is a factor that is almost always present in the area and which causes potential wave loads in the groyne field. These waves need a certain fetch or distance to develop. If the fetch is longer, the wind has more distance and time to develop and amplify a wave. Therefore, the longer the fetch, the higher the wave. Groyne Field 9 is partially closed most of the time which causes negligible wave heights because the fetch only has the length of the groyne field. When the groynes are submerged during high tides and the wind comes from the seaward direction, the fetch has its maximum length. Kouwenhoven (2023) compared his measured data with wind data and concluded that the difference in water levels between periods with strong wind with a large fetch and periods with little wind influence is limited. Figure 1.7 shows the effect of strong wind conditions compared to the effect of moderate wind conditions. From the absolute values of wave heights in Figure 1.7a, it can be concluded that strong winds have a relatively small effect on the wave conditions and are therefore neglected in this study.

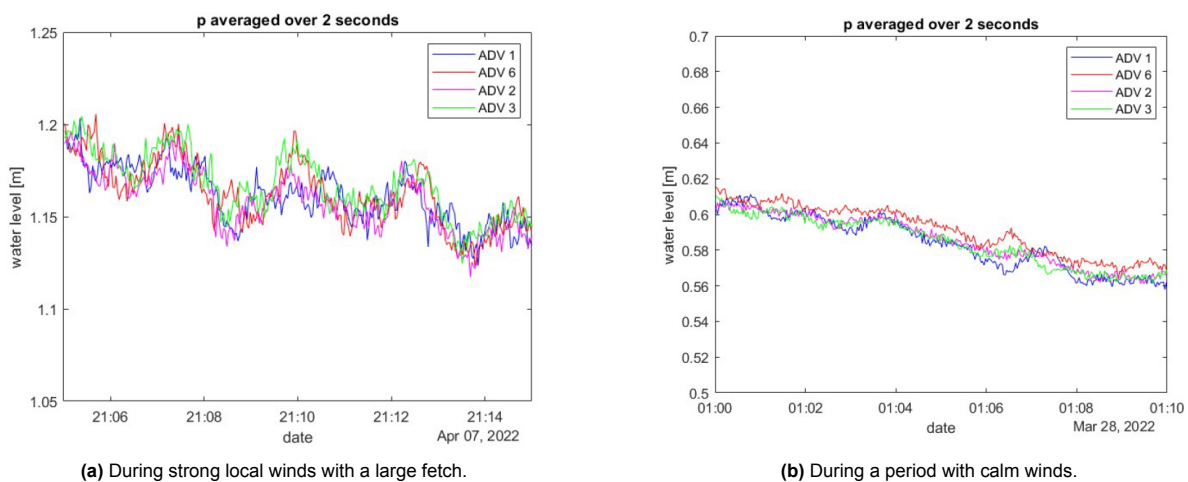


**Figure 1.7:** Measured water level signals under different wind conditions (Kouwenhoven, 2023). Water level signals are averaged over 2 seconds.



### 1.3.3. Ecological considerations

Researching the hydrodynamics in Groyne Field 9 increases knowledge about abiotic factors. The stakeholders involved are mainly interested in the biological considerations because the important objectives of the projects are often based on a biological aspect. This thesis will hardly treat these biological aspects, however, before the research is conducted, it is important to have an idea of certain biological backgrounds. First, the governmental objectives of the natural system in its water areas are highlighted. Then, the fish and vegetation details considered in the 'Groene Poort' project are explained. Finally, this section explains a reference project where longitudinal dams have been placed in a river and which contains similarities with the objectives considered in the projects 'Proeftuin Sediment Rijnmond' and the 'Groene Poort'.

#### 'Kader Richtlijn Water'

In the Netherlands, the 'Rijksinstituut voor Volksgezondheid en Milieu' (RIVM) has the task of advising the government in implementing the KRW into daily government. As already explained, one of the main objectives of the 'Groene Poort' project is to create tidal parks along the riverbank. Creating more natural value in waterfront areas is advised in the 'Kader Richtlijn Water' (KRW), which translates and transposes European guidelines to apply these in the Netherlands. These guidelines aim to improve the biological water quality. To evaluate these guidelines, four different categories are tested: Macrofauna, other water flora, fishes and phytoplankton. The requirements are set to have a desired amount of flora and fauna present at a location, for example, Groyne Field 9. Each of these categories gets a score according to the Ecological Quality Ratio (EKR), scored zero to one which shows the situation of the category according to its reference level (1). A score below 0.6 is considered insufficient. For the 'Nieuwe Waterweg', the scores of macrofauna, other water flora, fishes and phytoplankton are 0.35, 0.05, 0.6 and 0.6 respectively (van Infrastructuur en Milieu, 2015). It is important to note that the KRW has guidelines for the Netherlands and that the 'Groene Poort' project translated these into objectives specifically for the 'Nieuwe Waterweg' area (Parlement and council, 2000; Hiddema, W., et al., 2013).

#### Intended fish species

The 'Groene Poort' project focuses on migratory fish such as sturgeon, eel, houting, allis shad, and twaite shad. These fish rely on estuaries for food, shelter, and a gradual transition between fresh and salt water. While salmon focuses on reaching spawning grounds in high-altitude mountain areas, sturgeon uses the estuary not solely as a transportation route but also as a place for young fish to grow and adult fish to find food. The 'Groene Poort' project aims to contribute to the improvement of the habitat for migratory fish, specifically for sturgeon, by developing new inter-tidal areas (Hiddema, Zwakhals, et al., 2013). In practice, this means that behind the dam, a 1-meter depth must remain during low tide. Additionally, during low tide, fish must be able to pass the dam in order to enhance migration.

#### Vegetation

In the 'Nieuwe Waterweg', a couple of hundred meters upstream from Groyne Field 9, a small intertidal area is located, which is called 'Gors van Rozenburg'. An areal picture of the area is illustrated in Figure 1.8. The area contains already a variety of vegetation species. Therefore, it could be used as a reference area for what is expected in Groyne Field 9. The nature in this area probably developed in the 20<sup>th</sup> century, because its location became more sheltered after construction works near Rozenburg. It is located in the outer bend of the channel which could create different hydrodynamic conditions, but from an ecological aspect, the environment is similar to the area of Groyne Field 9.



**Figure 1.8:** Aerial picture of reference area: Gors van Rozenburg (Hiddema, Zwakhals, et al., 2013)

#### Reference project: Longitudinal training walls in the river Waal

Between 2016 and 2020, newly constructed longitudinal training walls (LTWs) located in the river Waal have been monitored. This campaign focused on all kinds of areas such as fish population, vegetation, macrofauna and morphodynamics. Three longitudinal training walls that have been constructed from 2014 until 2016 serve as a pilot project where the effects of long LTWs can be investigated. Between 1993 and 1997, a somewhat similar project was conducted on a much smaller scale in the Waal near Opijnen en Beneden-Leeuwen. This project consisted of a small parallel channel next to the main navigational channel. The evaluation clearly showed that the side channels contribute to the rehabilitation of the habitat for river organisms (Simons et al., 2000).

The subsequent project of the longitudinal training dams (LTWs) was expected to be more beneficial than traditional groynes for flood safety, channel navigation, nature and sweet water supply (Collas et al., 2020). The years after construction were used to monitor and check whether these expected effects were correct. One of the conclusions was that the LTWs reduced vessel wave effects. Figure 1.9 illustrates a whisker plot of the flow velocities measured at different locations for a set time range (A) and solely when vessels pass the locations (B). In this figure, the longitudinal training walls are abbreviated to LTDs instead of LTWs. In the left graph, the flow velocity difference is hardly visible but present. The location in a groyne field with no LTW shows higher velocities, but as shown in the figure, most of the difference is in the outliers of the data. The effect is much more visible in the right figure, which shows that the effect of vessels sailing in the main channel is reduced by a significant amount. Next to the reduction of vessel waves, the vessel noise intensity is reduced by the LTWs, Collas et al. (2020) concluded.

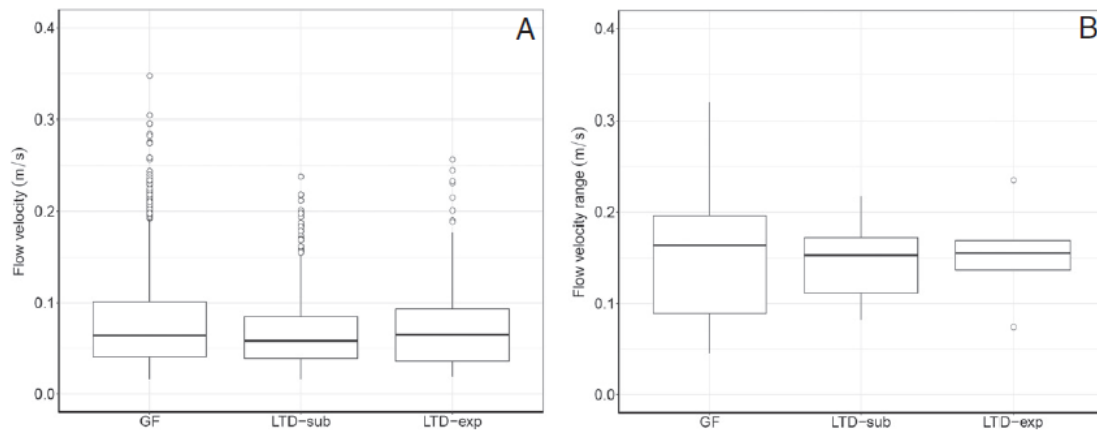


**Figure 1.9:** Whisker plots of measurements at the groyne field location (GF), submerged lowered LTW location (LTD-sub) and emergent lowered LTW location (LTD-exp) of A) all flow measurements and B) range in flow velocity during the passage of vessels. The bands in the middle of the boxes are the median; the lower and upper bands of the boxes are the 25th and 75th percentiles, respectively; and the dots represent outliers (Collas et al., 2018).

After the construction of the LTWs, the riparian channels became hydromorphologically active. At the moment of evaluation of Collas et al. (2020), the long-term equilibrium effects could not have been considered, because it was too early for the river to reach an equilibrium state, which makes it difficult to predict future development. Many conclusions about natural development have been specified in this research. One of the most important conclusions about habitat diversity and development is that the riparian channel has a variety of steep and shallow banks and fast and moderate-flowing water. This makes the habitat diversity in this location higher compared to the normal groyne field locations. The riparian channels primarily indicate erosion. However, the erosion magnitude is lower than the groyne fields used for reference. The report also concluded that the reduction of vessel influence is beneficial for the habitat environments.

Moreover, Collas et al. (2020) looked at the development of fish species at the locations where LTWs are constructed. The most significant conclusion from the monitoring campaigns is the fact that the diversity of fish species is higher in these parallel riparian channels and that the densities of all fish species are higher inside the riparian channel than outside. Another conclusion on fish species is that riparian channels are primarily important as a growing habitat for young fish. Furthermore, macrofauna flourishes at locations where the LTWs are constructed.

The Longshore Training Dam project has some key differences with the 'Groene Poort'. First, the location of the LTWs is much more upstream, which means that river discharge mainly determines the water level. In the 'Nieuwe Waterwet', tidal forcing is the process that predominantly determines the water level. Together with the salinity differences, it causes the habitat to be significantly different which has an impact on the species that may flourish there. Certain influences, like the fluctuation of water level, could be specifically beneficial for a certain species. Despite the differences between the two projects, the LTW project gives a certain indication of what can be expected when longitudinal dams are constructed in the 'Nieuwe Waterweg'.

## 1.4. Research objectives

This section provides an overview of the specific objectives and research questions that this report aims to address. The research objectives are developed based on a thorough review of the literature, careful consideration of the possible research directions and of the authors' own interests.

### 1.4.1. Objective

The projects 'Proeftuin Sediment Rijnmond' and the 'Groene Poort' encompass a range of areas, including the development of nature and the reuse of dredged material. To develop viable research objectives, it is necessary to narrow down the focus of the study.

The primary objective of this thesis is to study the impact of vessel waves on the hydrodynamics of groyne fields and to assess the extent to which these effects can be modelled. At the same time, it

is interesting to research the applicability of longitudinal dams in other groyne fields of the 'Nieuwe Waterweg'. The objectives are purely based on hydrodynamics. This thesis will not study morphology and ecology, however, it is treated in the introduction and will be considered shortly in the discussion.

#### 1.4.2. Research questions

The research report aims to address the main research question: *How can primary vessel waves impact the hydrodynamics in the semi-closed Groyne Field 9 in the 'Nieuwe Waterweg' and how can the hydrodynamic conditions be modified with different structural layout designs?* To achieve this objective, the main research question is divided into sub-questions. The following sub-questions will be addressed in the study to eventually answer the main research question:

1. *Which vessel characteristics are important for creating the primary vessel waves that impact semi-closed groyne fields, based on measurement data?*
2. *How can primary vessel waves be modelled numerically in a clear but realistic manner?*
3. *How does the hydrodynamic system behave in a semi-closed groyne field?*
4. *What structural layout design decisions can modify the hydrodynamic conditions in a semi-closed groyne field?*

### 1.5. Methodology

This section briefly discusses the methodology that is used to answer the question: *How can primary vessel waves impact the hydrodynamics in the semi-closed Groyne Field 9 in the 'Nieuwe Waterweg' and how can these effects be managed to create particular intended conditions?* A brief summary of the methodology is given below.

1. First, existing measurement data, consisting of Acoustic Doppler Velocimetry (ADV) and Automatic Identification System data (AIS), will be analysed to study the influence of individual vessel waves in Groyne Field 9. By analysing the measurement data, the impact of different vessel parameters on the primary vessel wave is researched. This part is discussed in Chapter 2. This information is used in the development of the numerical model in a later phase of the study. Additionally, the measurement data is used to validate the model.
2. A Delft3D Flexible Mesh model is developed to model the hydrodynamic influence of primary vessel waves in a semi-closed groyne field. The moving atmospheric pressure method is used to model the vessel in the Nieuwe Waterweg. This is explained in detail in Chapter 3. The objective of this model is to be able to create a controlled environment where specific factors can be changed to study their influence. Factors like bathymetry, vessel frequency, and the geometrical groyne field layout are checked. The model will be validated with the existing measurement data.
3. The validated model will be used to analyse different simulations. Simulations treated in Chapter 4 focus on understanding the hydrodynamic driving forces in the groyne field, caused by the primary vessel waves. This is done by modelling a simplified situation and comparing this to the real situation. The theory of having more vessels sailing behind each other is considered to obtain the effects of multiple vessels. The last part of this chapter highlights the tidal background with a simulation solely containing tidal input.
4. Chapter 5 uses the model already treated in Chapters 3 and 4, but focuses on managing the hydrodynamics by changing layout components. For example, it compares the current situation to the situation where the neighbouring groyne field is partially closed off by a longitudinal dam.

# 2

## Data analysis

Kouwenhoven (2023) obtained water level and velocity data from six different instruments placed inside Groyne Field 9 using Acoustic Doppler velocimeters (ADV). In this chapter, the data is processed and analysed with a focus on primary vessel waves. The main objective for conducting these analyses is to obtain an answer to the following question: *'What parameters are important for creating the primary vessel waves that impact semi-closed groyne fields, based on measurement data?'* First, wavelet analysis is done to check whether this is a valid way to research vessel waves. Afterwards, different parameters are checked for correlation to eventually come up with an empirical formula to describe the drawdown resulting from vessels passing the Groyne Field 9.

### 2.1. Measurement data

The analysed data consists of two different data sets. The first set is measurement data obtained with six different ADVs located at various locations inside Groyne Field 9, depicted in Figure 2.1. The ADVs measure pressure (water level) and velocities. The signals are measured with a frequency of 8 Hertz, but because of the low primary vessel wave frequencies, the data is resampled to a period of 5 seconds. To include vessel parameters in the analysis, Automatic Identification System (AIS) data is used. AIS data is created by all vessels with a length above 15 meters and it contains information about dimensions, course, velocity and (GPS) location. ADV and AIS data are used simultaneously to check the effect of vessel characteristics on hydrodynamic effects.



**Figure 2.1:** Measurement locations of six Acoustic Doppler velocimeters (ADV) (Kouwenhoven, 2023).

The AIS data is gathered by adding all kinds of different information to a single dataset. On one hand, information is provided automatically, like the GPS data, sailing velocity and the vessel's course. On the other hand, some information in the data relies on manual input. The most important example of such a parameter is the vessel's draught. The vessel's crew needs to add this information manually before each departure because of the varying load of the vessel. A quick check of the dataset shows that this information is regularly missing. In the analysis, this information is in most cases not used, but it suggests the possibility that the manual data is not as accurate as preferred. Inaccurate AIS data has been obtained by Brouwers (2022) in his research on the effect of vessel waves on groynes in the Waal. Another issue that he faced, was the fact that the GPS data of the used AIS data was not always accurate. As he mentioned, "some vessels appeared to be sailing on land due to a lack of GPS data". The research on the vessels in the 'Nieuwe Waterweg' used the GPS data at the moment it was the closest to the measuring instrument in the groyne field. If the GPS data of all of these vessels is plotted in one image, like in Figure 2.2, the GPS data appears to be quite accurate because no vessels appear to sail on land. Clearly, the locations are quite stretched out over a certain range of the channel, but this can be explained by the fact that the GPS location of the vessels is only known every 10 seconds. Which of these GPS locations is closest can therefore vary around the vessel's velocity in meters per second times 10 seconds.

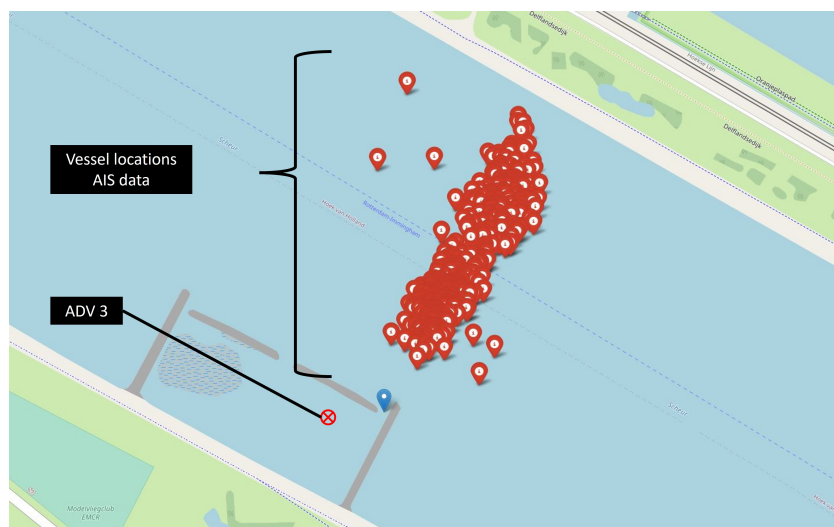


**Figure 2.2:** Selection of vessel locations from the dataset. The red markers show the point in the data where each vessel has the closest distance to the blue marker. At this moment, at this location, the vessel data is used for analyses.

Ideally, the data is known at the exact same point, because if one vessel is pinged at a location 100 meters further than another vessel, the primary wave obtained in the ADV data arrives at a different time span after the vessel passage which may influence the drawdown obtained in the data. The severity of these AIS data inaccuracies is moderate since the quantity of the data is large enough to have a stable amount of valid data.

A similar problem is the fact that the locations of the GPS transmitter inside the vessel are different on each vessel. If a vessel has its AIS transmitter located at the bow, it is different than if it is located at the stern. This information is known and included in the AIS data. Still, the accuracy it brings by including it in the analysis is unnecessary when the GPS data brings an even larger inaccuracy.

Another relevant factor is the exact location of the ADV inside the groyne field. The data is relatively good in showing clear drawdowns resulting from vessel passages, but in some cases, a wave signal is observed which is inexplicable from the AIS data. At the same time, sometimes a large wave is expected from the AIS data, and no wave is defined in the signal. This could hypothetically be explained by the fact that the location in the groyne field causes the ADV to receive waves that are reflected multiple times between boundaries. The theory of oscillating behaviour in the groyne field is further explained in Sections 2.4 and 4.2.1.

## 2.2. Fourier and Wavelet analysis

The pressure signal of the ADV can be analysed using wavelets. Wavelet transformation is a way to locate the place in a time series where certain frequencies occur, instead of solely obtaining the presence of a certain frequency. To understand the underlying principle of wavelet transformation, Fourier transformation (FT) is explained first.

### 2.2.1. Fourier Transformation

To analyse a signal, Fourier Transformation (FT) can be used. The FT decomposes a function (time-dependent signal) into sines and cosines to check what frequencies exist in the signal. The mathematical function of this Fourier analysis is shown in Equation 2.1. For visualisation, in Figure 2.3, a time series is depicted which can be represented as the sum of two sine waves with frequencies 1 and 2 Hertz. Figure 2.4 shows the corresponding power spectrum of the FT of the signal in Figure 2.3a. In theory, every possible signal can be described by the sum of infinite sine and cosine functions.

$$f(k) = \int_{-\infty}^{\infty} f(x)e^{-2\pi ikx} dx \quad (2.1)$$

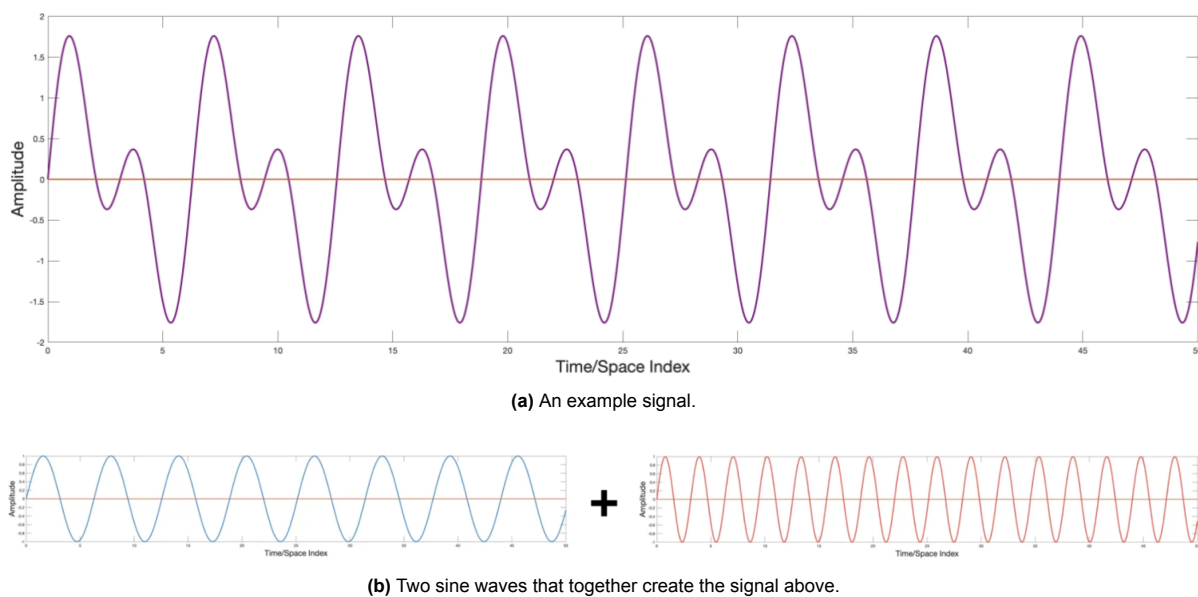


**Figure 2.3:** Simple example of Fourier transformation (Talebi, 2020). The signal of image (a) can be created by adding the signals from (b).

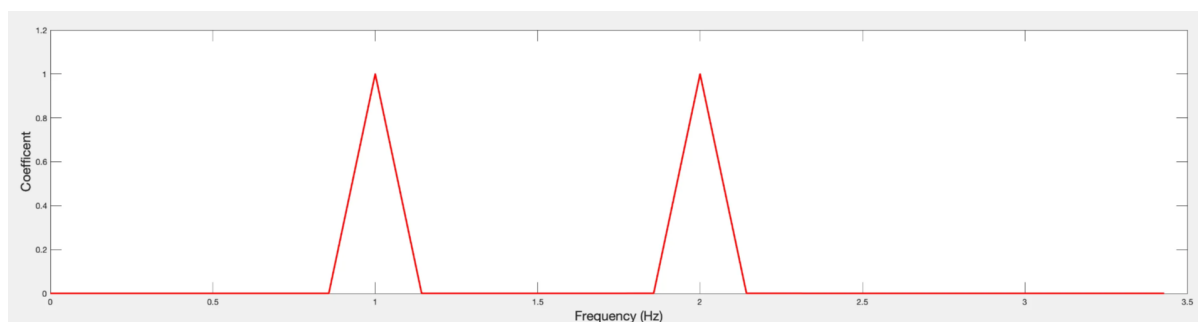


**Figure 2.4:** Corresponding power spectrum from the signal from Figure 2.3a (Talebi, 2020).

The FT provides insight into the wave conditions at specific locations. It is widely used in coastal engineering to determine wave climates by analysing wave spectra. What these spectra do not show, is the moment in time at which certain frequencies occur. This is because sine waves are continuous

and therefore the power spectrum only tells whether or not certain frequencies occur.

For analysing vessel waves in the 'Nieuwe Waterweg', knowing the location within the signal and power of particular frequency components is crucial. Locating existing frequencies in a signal is achieved using wavelet analysis.

### 2.2.2. Wavelet transformation

Wavelet Transformation (WT) is similar to Fourier Transformation. A WT decomposes a signal into a set of wavelets instead of sine functions. A wavelet is a function of a wave that is localised in time. The mathematical function is shown in Equation 2.2 and a wavelet is visualised in Figure 2.5.

$$y(t) = -(x - b)e^{\frac{-(x-b)^2/(2a^2)}{\sqrt{2\pi}a^3}} \quad (2.2)$$

The a-variable in the equation represents the scale of the wavelet. A lower value of the a-variable will cause the wavelet to look more squished. Therefore, this can capture higher-frequency information from a signal. A high a-variable will make the wavelet look more stretched and will capture low-frequency information.

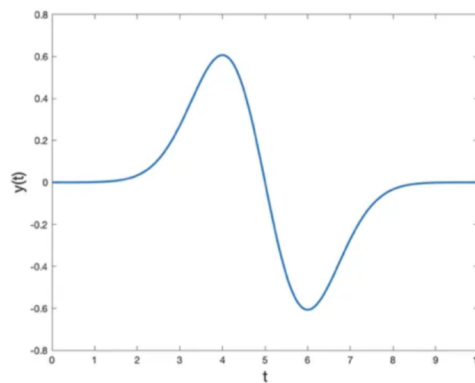
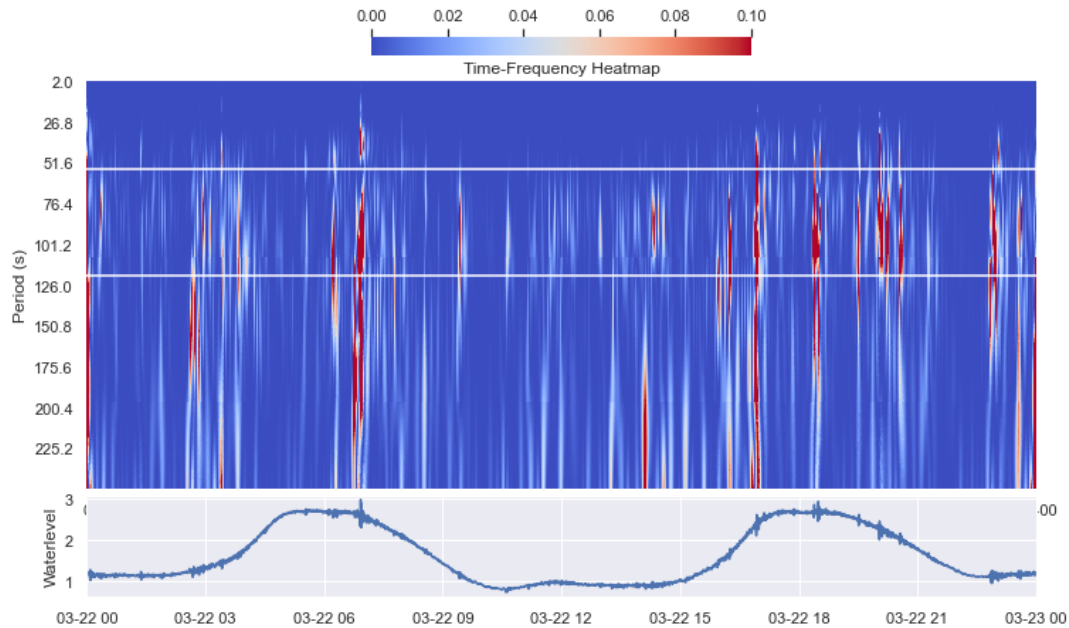


Figure 2.5: Wavelet shape

Similar to the Fourier analysis, different wavelets are compared along the measured signal. In this way, a frequency occurrence and the location of where this frequency occurs can be checked resulting in a power spectrum, such as illustrated in Figure 2.6, which illustrates a wavelet analysis of a pressure signal of ADV 3. The time domain (horizontal axis) is chosen to be around one day to clearly show two tidal waves and to be able to see small wiggles in the signal. ADV 3 is chosen to analyse because it is the ADV that is located at the lowest level. It means that, even during low tide, the instrument is located below the water level, which results in the most complete measurement dataset. The ADVs at other locations were often above the water level during low tide, which caused neglecting vessel waves during low tide. The location of ADV 3 is depicted in Figures 2.2 and 2.1. The vertical axis in the wavelet spectra represents the frequency recalculated to the wave period, to make it more intuitive. It means that red hot spots at the top of the figure represent short-period waves (high frequency) at the corresponding time. The two horizontal white lines in the power spectrum represent the period boundaries of 55 and 120 seconds. According to Kouwenhoven (2023), the period of a primary vessel wave is between 55 and 120 seconds. The figure shows that a large number of hot spots are located between these horizontal boundaries, but in some cases, these spots stretch out below the 120-second boundary.





**Figure 2.6:** Frequency to time heat map of the pressure signal from ADV3 created by wavelet analysis. The y-axis is transposed to wave period instead of frequency. Red spots correspond to the presence of the corresponding wave period in the water level signal at this location in the signal.

### 2.3. Analysing water level signals with AIS data

To connect wave signals to individual vessels, AIS data is included. In this way, the causality between a drawdown and vessel characteristics can be proved. To visualise this causality, an interval is plotted in Figure 2.7 where the vertical yellow and black lines represent vessels that pass Groyne Field 9 at the corresponding moment in time. The northeast corner of the groyne field is chosen as point of passage as it is the closest entrance to the location of ADV 3, the location where the signal is measured.

The variation between the effect of different vessels is visible in the pressure signal, by looking at the power spectra. The majority of the vessel passages hardly cause a water level change, but at the same time, some particular vessels cause a very large change in water level. The colour of the vertical line refers to the vessel's velocity. The yellow line indicates a velocity larger than 14 knots ( $=7.2$  m/s), while the vertical black line represents a vessel that is sailing slower than 14 knots. It shows that at the locations where vessels sail faster, the influence on the water level inside the groyne field is much higher.

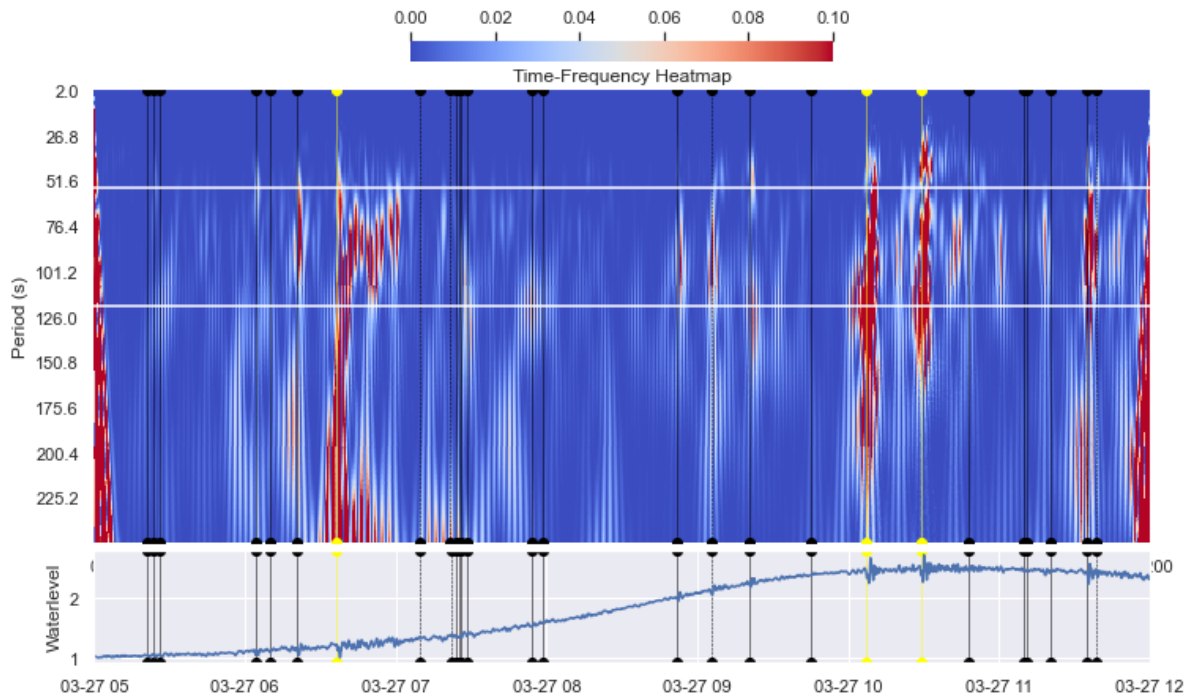


**Figure 2.7:** Time-period graph of the pressure signal from ADV3. Compared to Figure 2.6, the time interval is smaller to better visualise vessel wave effects. The vertical lines represent vessels passing by the groyne field. Red spots correspond to the presence of the corresponding wave period in the water level signal at this location in the signal.

Similarly, plots have been created for other parameters, like vessel length, draught and distance from the groyne field, which are depicted in Appendix B.1. The main conclusion is that vessel dimensions do have an influence on the intensity of the wave and that the distance from the groyne field does not have a significant influence. This manual analysis is done by analysing a short interval and therefore it does not represent the entire measurement campaign. The conclusions from this small analysis would be qualitative instead of quantitative. Valid and accurate conclusions rely on an analysis of the entire data set. Wavelets could be used in analysing quantitatively by making a sum of the power analysis after a vessel passage that gives a certain severity of each vessel passing the groyne field. An uncertainty to this approach is the fact that the power output includes a significant amount of noise. Instead, another quantifiable approach is used. At every vessel passage, the drawdown is obtained by subtracting the lowest water level in a range around the vessel passage from the average water level. This drawdown magnitude is added to the AIS data and will be analysed in Section 2.5.

## 2.4. Natural frequencies in a river

In the wavelet power spectra, sometimes small hot spots are visible at locations where no vessel has sailed by. It is visible in the water level signals that some vessel waves cause water level fluctuation for a long time after the vessel has passed.

A possible explanation for this phenomenon is natural oscillatory movements inside a river or groyne field. This effect in a river with groynes is already explained by Juez and Navas-Montilla (2022) and Meile et al. (2011). To explain this effect, a simplified river is assumed with a homogeneous depth. If this river oscillates in the first natural frequency, the wave has one node and 2 anti-nodes. According to this theory, anti-nodes are located at the river banks and the node is present in the middle of the river. Unfortunately, no measurements are done on the other side of the channel to be able to analyse possible oscillatory behaviour along the river width. Without this information, the theory can be used to see whether or not this effect could occur. In this theoretical situation, the width of the river is equal to half of the wavelength. This assumption results in an equation that calculates the wave period and wave frequency of this wave. The 'Nieuwe Waterweg' has a specific bathymetry because the sailing channel has been dredged quite extensively compared to conventional river channels. The depth in the channel can be up to twenty meters, while the depth between the groynes is not larger than six or

seven meters. Additionally, tide has an influence on the water depth. To get an idea of the oscillation effect, the width is estimated at 420 meters and the depth at eighteen meters.

$$T = \frac{2L}{\sqrt{gd}} = \frac{2 * 420}{\sqrt{9.81 * 18}} = 63.2s \quad (2.3)$$

It is calculated that a natural wave period is 63 seconds, which is in the same order of magnitude as vessel wave periods (Kouwenhoven, 2023). In line with the same theory, natural frequencies could occur at other locations. For example, let's consider the groyne field as a closed basin. If the water level is dropped or raised at one side, a standing wave could occur in the first natural frequency of the system. In the same way as Equation 2.3, the length of the (closed) basin would be the dimensions of the groyne field. Two directions of oscillations could be considered. The direction perpendicular to the river and the direction longitudinal to the river. The natural frequencies become respectively:

$$T = \frac{2L}{\sqrt{gd}} = \frac{2 * 110}{\sqrt{9.81 * 1}} = 70s \quad (2.4)$$

$$T = \frac{2L}{\sqrt{gd}} = \frac{2 * 290}{\sqrt{9.81 * 1}} = 185s \quad (2.5)$$

These calculations assume a constant water depth and a closed homogeneous basin. In reality, the water depth varies due to tidal effects. The groyne field bathymetry is not homogeneous and has openings at all sides. This makes it difficult to apply the assumptions necessary to calculate the system in the way of a homogeneous closed basin. However, the resulting periods from the Equations 2.4 and 2.5 are in the same order of magnitude as vessel wave periods. It qualitatively shows that 'in-explainable' hot spots in the wavelet analysis can be explained. The system and its oscillatory behaviour are studied more extensively in a numerical way in Chapter 4.

## 2.5. Quantified drawdown effect caused by vessels

A recognisable effect of primary vessel-induced waves is the drawdown of the water. The moving vessels result in local water level reduction which results in water retracting from the groyne field. This eventually leads to the reduction in water level at the measurement instruments referred to as drawdown. To analyse the effect of different parameters on drawdown, the data has been processed to obtain a quantified drawdown for every vessel passage. The considered parameters and characteristics are the vessels' velocity, length, width, draught, course and distance from the groyne field. The effect of the vessel parameters of all vessels on the drawdown can be visualised in six graphs, which are depicted in Figure 2.8. The different characteristics are explained separately.

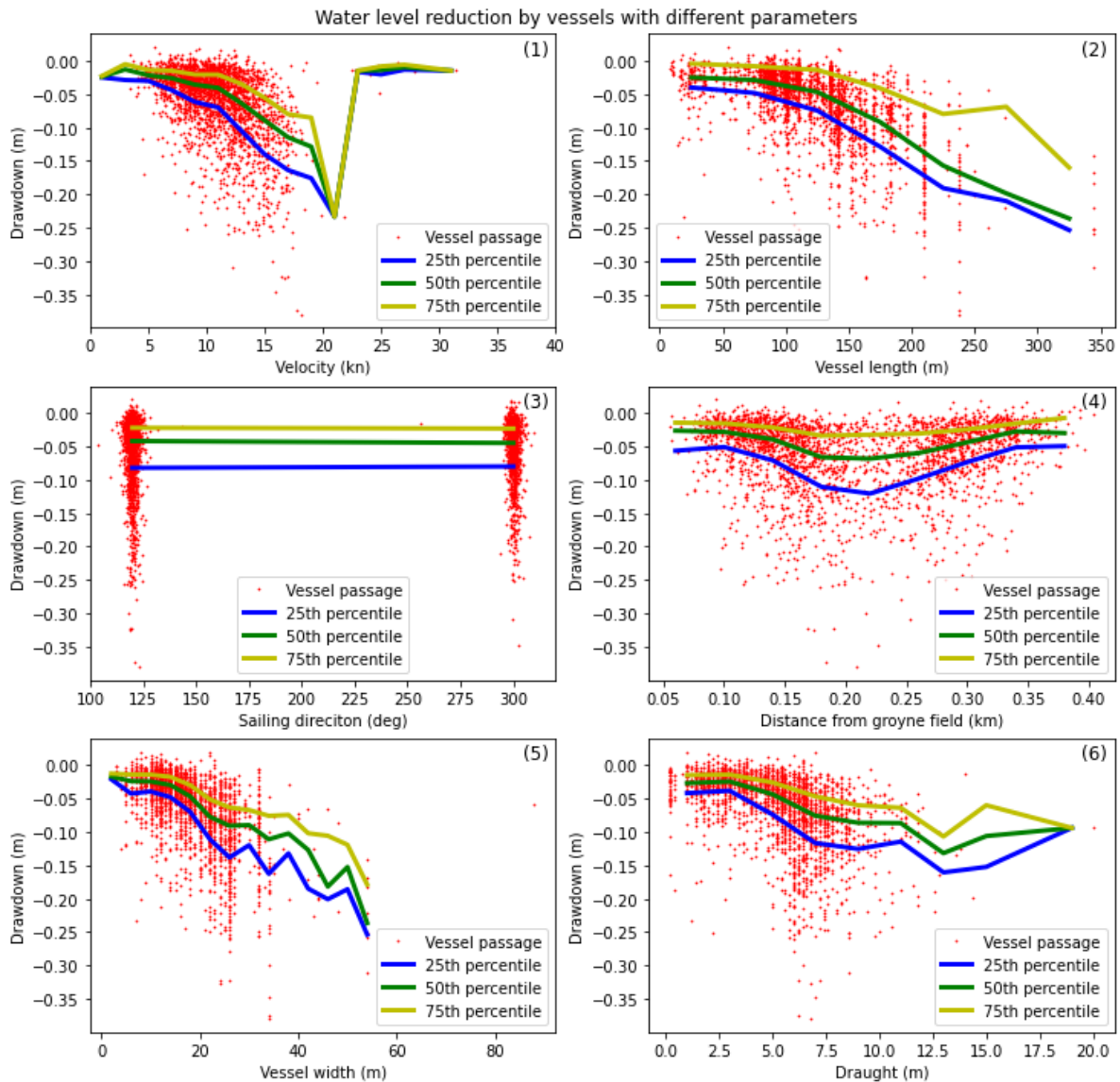


**Figure 2.8:** Drawdown plotted against different vessel characteristics. Drawdown data is obtained from ADV data and the vessel parameters are obtained from AIS data. Each red dot represents one vessel passage, the lines are different percentiles of the data.

### 2.5.1. Sailing velocity effect (1)

The first graph from Figure 2.8 illustrates that water level reduction is limited at lower vessel velocities and increases with the vessel velocity parameter. Only for vessels sailing above 20 knots, the drawdown reduced back to almost zero. This sudden change in correlation can have multiple reasons. First of all, far fewer vessels with velocities above 20 knots exist in the dataset. Only 22 out of 2585 vessels from the data set sailed by faster than 20 knots. 9 of these vessels have a velocity of exactly 102.3 knots (190 km/h), which is an unrealistic velocity for vessels and can only be explained by an error in the data. Another indication as to why these particular data points have been filled in incorrectly is that their course is all set to 360 degrees, which is a strange direction to sail to in that location. The rest of these 22 'fast' vessels all have a velocity between 20 and 30 knots. A noticeable observation is the fact that all of these 13 vessels have relatively small dimensions. Normally, smaller vessels have lower velocities compared to larger vessels. The explanation for why these particular vessels have such high velocities lies in the hull speed theory. According to the theory, vessels are unable to sail faster than their so-called hull speeds, which depend on the primary wave the vessel creates. The wavelength of this wave depends on the length of the vessel and therefore, the vessel length corresponds to the

maximum velocity a vessel can sail. Equation 2.6 describes a calculation to how this limit velocity can be calculated (Schierreck, 1993).

$$[H] \left. \begin{array}{l} c = \frac{gT}{2\pi} \tanh \frac{2\pi h}{L} \\ L = cT \end{array} \right\} V_l = c = \sqrt{\frac{gL}{2\pi} \tanh \frac{2\pi h}{L}} \quad (2.6)$$

In shallow water, the limit velocity is proportional to the water depth and the vessel length. Assuming a depth of 17 meters in the 'Nieuwe Waterweg', a vessel of 300 meters would have a limit (hull) speed of 12.6 m/s (24 kn) and a vessel of 25 meters would have a limit speed of 6.2 m/s (12 kn). Vessels actually never sail at their hull speed, because of energy costs. Vessels typically sail at 90% of their limit speed. In the data set, all vessels that sailed faster than 20 knots have lengths of around 25 meters. Under 'normal' conditions, according to the theory of Equation 2.6, it is very unlikely for a vessel to sail faster than 20 knots.

However, in reality, it is possible for a vessel to sail faster than its hull speed. High-speed boats are able to sail faster by applying a lot of energy and lifting their hulls above the water. In this way, the drag reduces because the boat is able to skim across the water surface. In this situation, the theory from Equation 2.6 is invalid. This explanation corresponds to the observation that all vessels that have high velocities are relatively small. The fact that these boats are lifted from the water and skim the water surface explains the fact that for these velocities the drawdown is small because less water is pushed out of the vessel's way.

### 2.5.2. Vessel length effect (2)

The second graph depicts the drawdown caused by a vessel with respect to the length of that particular vessel. It shows that higher vessel lengths result in more significant drawdowns. However, as explained in the previous section, longer vessels have higher hull speeds which means they are able to sail with a higher velocity. This correlation between sailing velocity and vessel length is integrated within the data, and therefore, from this image, it can not be concluded with 100% certainty whether vessel length or sailing velocity is the main driving force.

### 2.5.3. Vessel course and distance from groyne effect (3) and (4)

Graphs (3) and (4) from Figure 2.8 show results from two parameters that are highly correlated and therefore are explained similarly. The parameter plotted against the drawdown in graph (3) represents the course of each vessel. The vessels with a course of around 120 degrees are heading in a landward direction and the vessels with a course of around 300 degrees are heading in a seaward direction. In graph (4), the 2 dense clouds of red markers can be explained by the fact that sailing vessels tend to keep at the right side of the channel to be able to pass vessels sailing in the opposite direction. This explains the fact that one 'cloud' of red markers is sailing at a certain distance from the groyne field, and another cloud is sailing at a larger distance. Therefore, in most cases, vessels sail closer to the groyne field when sailing in landward direction compared to vessels sailing to the sea. Both graphs (3) and (4) show that distance does not influence the drawdown magnitude in the groyne field.

The fourth graph shows, however, that vessels sailing in the middle of the channel cause a greater drawdown magnitude. This observation could indicate that the river has some sort of natural frequency that is amplified by vessels sailing in the middle of the channel.

However, a straightforward explanation for this observation is that larger vessels often sail more to the middle of the channel to reduce the risk of collision by creating as much space between the vessel and the river banks as possible. Previous sections have shown that larger vessels create larger drawdowns.

### 2.5.4. Vessel's width and draught effects (5 and 6)

The width and draught parameters, depicted in graphs (5) and (6), both correlate to the length of the vessel which explains the same curve shape as the second graph of Figure 2.8. The number of 'large' vessels is significantly lower compared to 'smaller' vessels which means that the percentile lines in the graphs have higher inaccuracies if the dimensional parameters increase.

## 2.6. Empirical relation of drawdown caused by vessels

The previous section treats the analysis of the measured data and it shows that various parameters influence the drawdown magnitude in the groyne field. This section empirically explains the process of

drawdown by vessels by conducting regression analysis on the data to come up with the best coefficients to fit a proposed empirical formula. Similar research from Almström and Larson (2020) is used to decide on which parameters are considered in the empirical formula. To create a correct formula, certain parameters are divided to create dimensionless components. It would be interesting to compare the data with all kinds of empirical formulas derived in the past, but this is something outside the scope of this thesis. Only two empirical equations are considered. One created with the data of this research and one of Almström and Larson (2020) created with other data.

Regression analysis includes creating a semi-empirical formula where the coefficients are created to fit the data best. These coefficients are derived using a simple model consisting of the main driving parameters considered in previous sections and used in similar research conducted by Almström and Larson (2020). In their research, they measured and analysed primary vessel waves in the Stockholm Archipelago and included vessel parameters and drawdown. To see if a similar empirical formula can describe the vessel waves from the 'Nieuwe Waterweg', the same non-dimensional components are used. The non-dimensional terms included in the empirical formula are the depth-based Froude number ( $U/\sqrt{gD}$ ), the ratio between the distance to the bank and the width of the vessel ( $x/W$ ), the ratio between the width of the vessel and the channel width ( $W/W_{ch}$ ), the ratio between the draught and the water depth ( $ds/D$ ), and the ratio between the vessel length and the vessel draught ( $L/ds$ ) (Almström and Larson, 2020).

Using the dataset, regression analysis is performed resulting in Equation 2.7. The equation is manually checked and validated using smaller samples of the dataset, which showed no errors or strange results. The predictive results are compared to the observed drawdown from the dataset and plotted in Figure 2.9a. In addition to this empirically obtained function, the function created by the dataset of Almström and Larson (2020) (Equation 2.8) is analysed with the data obtained in this research. This is done to analyse the differences and similarities between the two formulas. The result is depicted in Figure 2.9b.

The fitness of both empirical approximations can be calculated by the mean average error (MAE) and the  $R^2$ . The MAE is lower and the  $R^2$  is higher for the approximation by the formula obtained from the data set used in this research compared to the use of the empirical formula from Almström and Larson (2020). The model has a mean average error of 0.024, which can be interpreted as a good fit. However, relatively, this conclusion is questionable because an error of 0.02 [m] for an observed drawdown of -0.02 [m] drawdown is relatively seen as a large error compared to the same error for an observed drawdown of -0.15 [m].

Empirical equation resulting from the analysis of the data set in the 'Nieuwe Waterweg':

$$\frac{S_D * 2g}{U^2} = 0.051 * \left(\frac{U}{\sqrt{gD}}\right)^{-0.36} * \left(\frac{x}{W}\right)^{-0.80} * \left(\frac{W}{W_{ch}}\right)^{-0.17} * \left(\frac{ds}{D}\right)^{0.98} * \left(\frac{L}{ds}\right)^{0.57} \quad (2.7)$$

Empirical equation resulting from the analysis of Almström and Larson (2020) in the Sweden archipelago:

$$\frac{S_D * 2g}{U^2} = -0.22 * \left(\frac{U}{\sqrt{gD}}\right)^{0.42} * \left(\frac{x}{W}\right)^{-0.85} * \left(\frac{W}{W_{ch}}\right)^{0.32} * \left(\frac{ds}{D}\right)^{1.46} * \left(\frac{L}{ds}\right)^{0.80} \quad (2.8)$$

The equations both contain non-dimensional terms created by dividing the right parameters. The non-dimensional terms make it easier to conduct the regression analysis, but it complexifies analysing the resulting terms in this formula separately because some parameters exist in different terms. For example, the velocity parameter has at the right side of the equation a power of -0.36 in Equation 2.7 and a +0.42 in Equation 2.8. This could intuitively create the image that the velocity has a negative correlation in one equation and a positive in the other. This is not the case, because, in both equations, the velocity is negatively squared at the left side of the equation. This means that the total power of the velocity on the drawdown is 1.64 and 2.42 for respectively Equations 2.7 and 2.8. Equations 2.9 and 2.10 captures the proportionality of all parameters of both Equations 2.7 and 2.8. It shows that the velocity has the most influence on the resulting drawdown in both equations, but the difference in influence is still very high. It is good to note that the locations have different characteristics. The location Almström and Larson (2020) did their measurements have no river or tidal flow, like in the 'Nieuwe Waterweg'. In both studies, the absolute velocity drawn from GPS data is used. If the water flows in the

channel, the relative velocity with respect to the water movement can vary quite extensively. Because the drawdown is created by the interaction between the vessel and the water, this can influence the results. This uncertainty in the data could explain the fact that the direct influence of the sailing velocity on the drawdown is lower compared to the influence it has in the analysis of Almström and Larson (2020).

Empirical function proportionality:

$$S_D \propto U^{1.64} * x^{-0.80} * W^{0.63} * ds^{0.41} * L^{0.57} \quad (2.9)$$

Empirical function Almström and Larson (2020) proportionality:

$$S_D \propto U^{2.42} * x^{-0.85} * W^{1.17} * ds^{0.66} * L^{0.80} \quad (2.10)$$

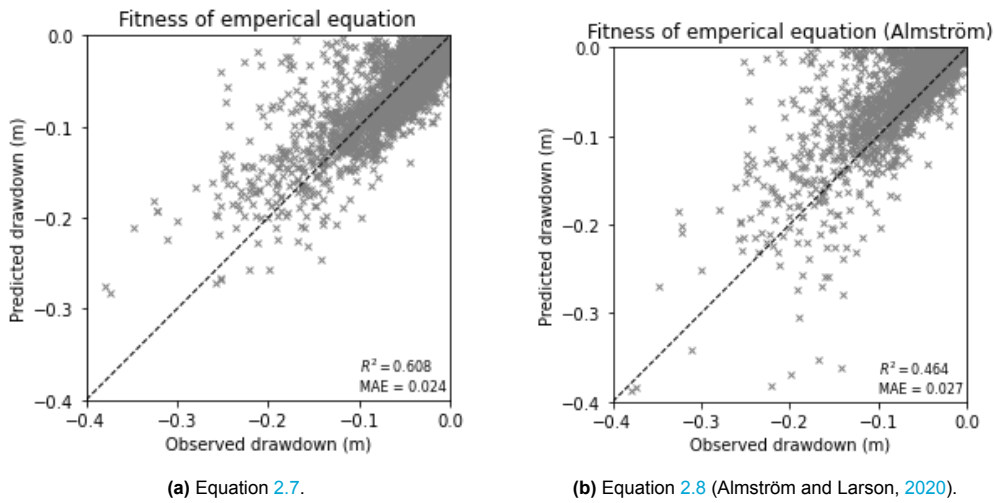


**Figure 2.9:** Predicted drawdown calculated with respectively Equation 2.7 and 2.8 plotted against the observed drawdown from the dataset of vessels sailing near the groyne field in the 'Nieuwe Waterweg'.

The resulting plots in Figure 2.9 show the accuracy of the fitness of both equations. Basically, both empirical relations give a good indication of reality apart from the fact that Equation 2.8 gives generally less conservative results when the data from the 'Nieuwe Waterweg' is checked. This slight difference can be explained with the background of where Equation 2.8 is developed from. The information used to develop this equation is from a different data set, obtained at a different location with different vessel composition. The shallow location of the measurement instrument in Groyne Field 9 could amplify the primary wave locally, resulting in different drawdown magnitudes.

# 3

## Primary vessel wave effect model in the 'Nieuwe Waterweg'

A numerical model is created and used to study the hydrodynamic effect of primary vessel waves on a semi-closed groyne field like Groyne Field 9. This chapter explains different individual elements concerning the numerical model setup, implementation of hydraulic forcing, and how the model has been verified. It serves as a background for the following chapters where the results of the simulations are considered. Therefore, this chapter answers the question: *How can the influence of primary vessel waves be modelled using a numerical model?*

### 3.1. Model setup

This section describes how different choices and assumptions are made to make the model as realistic as possible. It focuses on the bathymetry setup, grid and mesh setup and boundary conditions. For various parameters, like the viscosity, values are used by the advice of experts. The values are stated in Appendix C. In some cases, the goal of the model is to make a simulation as realistic as possible, but in some cases, the reality is simplified. This is done to study the hydrodynamic system and describe and explain the governing natural processes.

#### 3.1.1. Grid and mesh sizes

The numerical grid is created with the program Delft3D Flexible Mesh (Delft3D FM), which is developed from one of its predecessors Delft3D Flow. These software versions work in a similar way, but the most noticeable difference is the use of unstructured grids in Delft3D FM. This function allows the grid to use triangles, pentagons and hexagons in order to couple large regions with quadrangles, which allows for detail at interesting locations and saves computational time. Another difference is the grid setup. In Delft3D FM, the grid no longer has true grid 'rows' and 'columns', but each cell is labelled with a unique number. Just like Delft3D Flow, Delft3D FM implements a finite volume solver on a staggered grid (Deltares, 2022). This concept states that the different quantities like water level and velocity should not be located at the same location in the numerical grid. It means that the water level is defined in the centre of each computational cell and the velocity components are calculated perpendicular to the grid cell faces. This particular arrangement of variables is called the Arakawa C-grid. The advantages of using this staggered arrangement are as follows (Deltares, 2018):

- Rather simple implementation of boundary conditions.
- Compared to democratisation on non-staggered grids, it is possible to use a smaller number of discrete state variables in order to obtain the same accuracy. This means a more efficient computation.
- Staggered grids for shallow water solvers prevent spatial oscillations in the water levels (Stelling, 1984).

The Delft3D models solve 2D or 3D non-linear shallow water equations. To solve the derived Navier-Stokes equations, several assumptions are made. The first important assumption is the Boussinesq



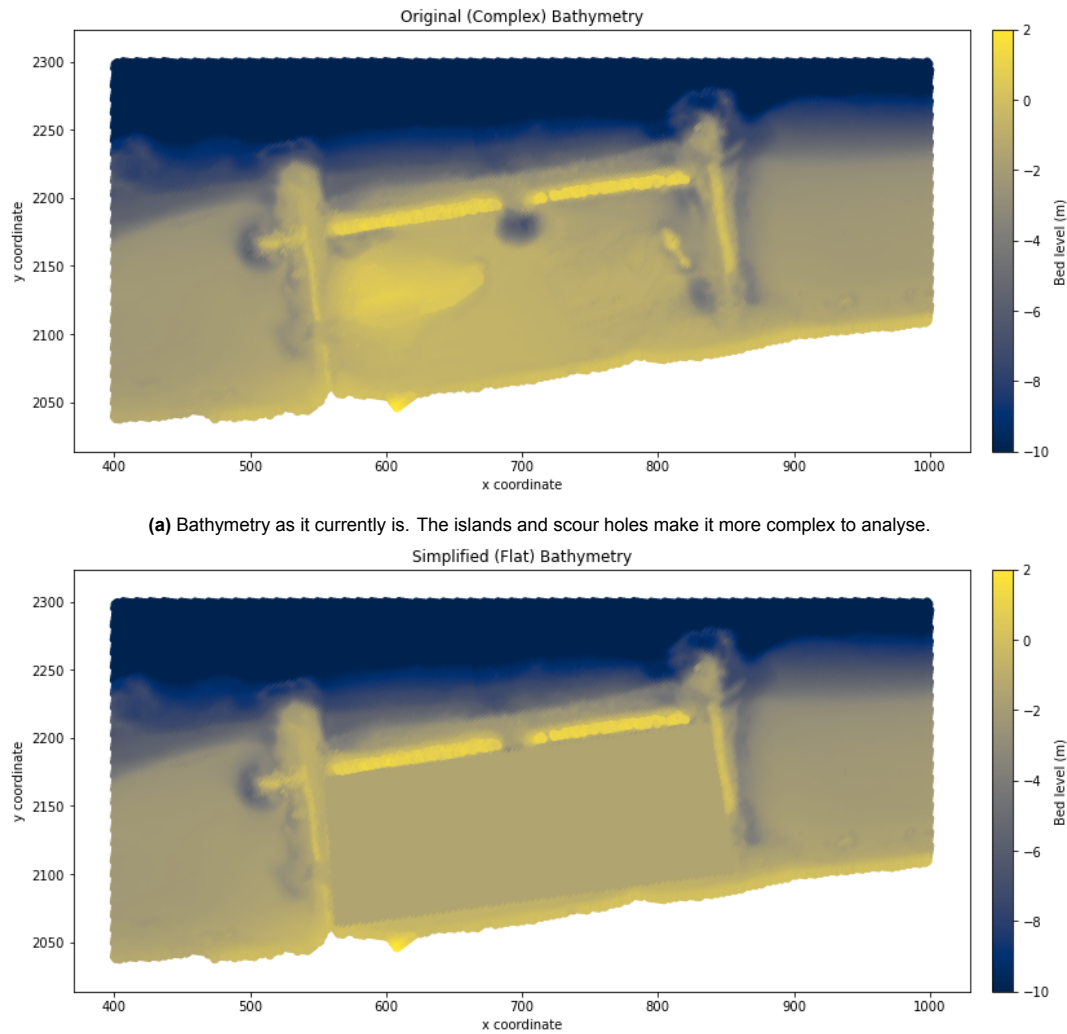
assumption which states that the fluid is in-compressible. Next to this, shallow water is assumed by which the vertical momentum equation is reduced to a hydrostatic pressure equation. (Deltares, 2018). The unstructured grid function allows certain areas to have a much finer mesh to obtain more detailed results in a shorter time period. In the model, two areas are the most important. The most important focus area is the area around Groyne Field 9. In this area, the hydrodynamic behaviour needs to be assessed as detailed as possible. Grid size in this area is created with a size of around 1 meter x 1 meter. Another important area is the area around the vessel's trajectory. The vessels are modelled in 3D, which means that the vessel needs a fine grid around its hull to model the shape of the vessel as realistic as possible. Modelling the moving vessel will be explained in more detail in Section 3.2.3. An image of the unstructured grid is shown in Appendix C.

### 3.1.2. Bathymetry schematization

Bathymetry data is obtained from the measurements done by 'Rijkswaterstaat' (RWS) in the 'Nieuwe Waterweg'. The implemented file contains three sets of information. An x-coordinate, a y-coordinate and a z-value correspond to the bed level at different locations in the computational domain. The points are located two meters from one another which is more accurate than a large part of the computational grid as explained in the section above.

The bathymetry data is able to provide data for most of the computational domain. However, the data lacks information at a few important locations. This can be explained by the fact that these measurements are conducted by boat. Various locations in the domain cannot be reached by floating vessels. One example is the island in Groyne Field 9 which is either emerged or submerged depending on the tide. To create the most realistically possible bathymetry model, data from the 'Algemeen Hoogtebestand Nederland' (AHN) is used to fill the empty spaces in the data. AHN is an organisation that maps out the height of all the land surfaces in the Netherlands. These measurements are obtained by laser altimetry which solely measures the land surface. In this case, one slight uncertainty remains. Because the two measurements were conducted in two different ways and at two different moments in time, differences in accuracy or a sudden offset in the combined data could occur. The possible inaccuracy has not been observed in the results and model.

Initially, two different bathymetry situations will be considered, depicted in Figure 3.1, where one will be the current more complex bathymetry and one will be a simplified bathymetry to serve as a generic simulation to obtain knowledge on the hydrodynamics in general closed groyne field systems. More information on the different simulations is explained in Chapter 4. The last part of the numerical research focuses on different layouts. The layouts and bathymetries are explained extensively explained in Chapter 5.



(a) Bathymetry as it currently is. The islands and scour holes make it more complex to analyse.

(b) Modified bathymetry where the bed is flat within the groyne field. This makes it better to analyse for general conclusions. In this thesis it is sometimes referred to as the basic situation.

**Figure 3.1:** Two considered bathymetries for the first set of simulations.

### 3.1.3. Boundary conditions

In the 'Nieuwe Waterweg', both the upstream and downstream boundaries are open, meaning at these boundaries, water can flow in or out and waves can travel in or out of the domain. For example, both the tidal forcing originating at open sea or the river discharge at the upstream boundary determine the water level and basic current properties. The simulations in this research focus on the effect of vessel waves. Therefore, in most simulations, forcing types like these are not applied at the boundaries because it is numerically hard to combine vessel forcing with tidal forcing. However, a single simulation containing solely tidal forcing is run. The results of this simulation are treated in Section 4.4.

For the vessel wave impact studies, different solutions at the boundaries are necessary. If boundary conditions are omitted in the model, the upstream and downstream boundaries of the domain would represent closed boundaries which are able to reflect waves, resulting in unrealistic results. To reduce the reflection at the upstream river boundary, a Riemann boundary condition is applied. The Riemann invariant attenuates most of the waves that would otherwise be reflected. The theory behind the Riemann invariant is not explained in this report. While the most important waves are attenuated, test simulations show that some waves are still reflected at the upstream boundary. Simulating a moving pressure field, which will be further emphasised in Section 3.2.3, creates a complex situation because the pressure field needs to travel through the boundary. This creates a conflicting situation at the boundary which cannot be solved. However, the waves that are reflected from the boundary have an insignificant influence on the results at the groyne field location. The Riemann boundary condition is

not applied at the seaside (left) boundary because test simulations show that at the moment the vessel (pressure field) enters the domain, a large wave is initialised at the bow of the vessel. Instead, a large deep sea is modelled at the seaside of the domain to attenuate the waves that would otherwise be reflected. Moreover, the presence of this large sea is beneficial for the gradual entrance of the vessel into the domain, which contributes to a realistic model.

## 3.2. External forces on Groyne Field 9

Different hydraulic forces influence the hydrodynamic behaviour in Groyne Field 9. This research simplifies the situation by neglecting tidal forcing and river discharge in the simulations where vessel waves are analysed. In theory, these factors can be implemented in the same mode, but this would create hard-to-explain results. Therefore, tidal forcing is analysed in a separate simulation. The theoretical background on tidal forcing and river discharge is explained below. Next to tidal forcing and river discharge, vessel wave forcing is explained in this section.

### 3.2.1. Tidal forcing

Tidal forcing can be modelled in Delft3D by implementing components A0, M2, M4 and M6. A more detailed explanation of how tidal forcing is implemented in the single simulation is explained in Section 4.4. Measurement data in the groyne field location shows the real existing tidal cycle in Figure 3.2. The water level signal is influenced by other factors like discharge, but it depicts the tidal cycles relatively well. Moreover, it shows the flow velocity magnitude at the location of Acoustic Doppler Velocimeter (ADV) three in the research of Kouwenhoven (2023). In the analysis of vessel wave impact, the decision is made to look at the influence at a low water level of -0.5 meters because visual research shows that the hydrodynamic behaviour is active under these conditions. A more extensive numerical analysis is conducted in Section 4.4.

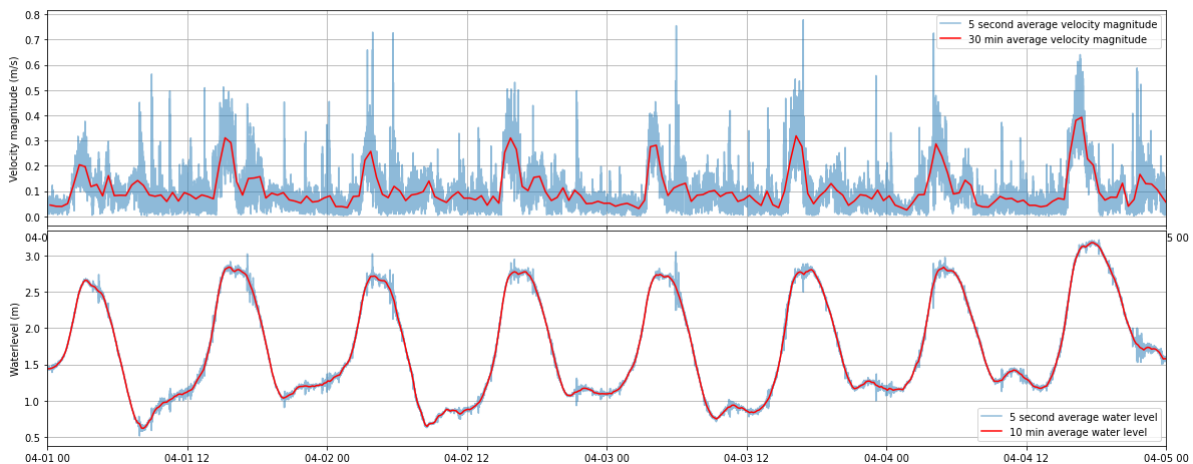


**Figure 3.2:** Tidal signal measured in the groyne field. The top figure shows the velocity magnitudes and the lower graph shows the water level signal.

### 3.2.2. River discharge

River discharge is another factor influencing the water level near Groyne Field 9. The combination of discharge upstream and the tidal forcing downstream decide how the overall water level and currents behave. This has already been researched to some extent by Kouwenhoven (2023). The precise influence of the discharge on the 'Nieuwe Waterweg' is difficult to explain because the discharge is only measured at Lobith. After Lobith, the water flows westward where the river bifurcates multiple times. A certain part of the water flows to the North Sea through the Haringvlietdam. Together, these influences make it hard to predict the exact flow at the groyne field location in the 'Nieuwe Waterweg'. Figure 3.3a shows the discharge at Lobith during the time for which measurements were conducted. In Figure 3.3b, the 30-minute average water level and velocity signals are illustrated. The signals do not

show significant changes 4 days after the discharge increases, which indicates that changing discharge at Lobith hardly influences the water level in the 'Nieuwe Waterweg'. Note that by the time the really high peak in discharge reaches the groyne field, the measurement campaign already ended. In this study, discharge is not taken into consideration.

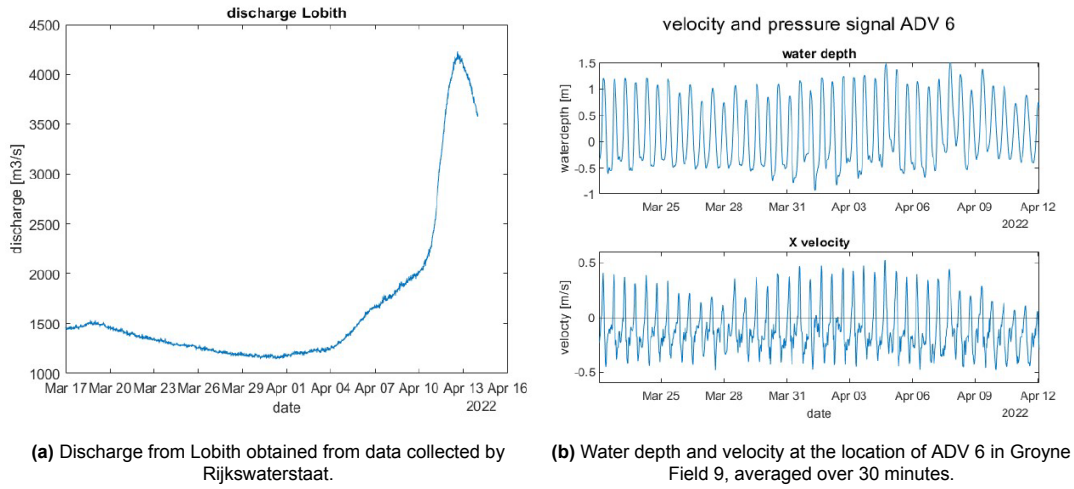


**Figure 3.3:** Discharge at Lobith together with the corresponding signal from one of the ADV's. (Kouwenhoven, 2023)

### 3.2.3. Vessel waves

Vessel waves are modelled by applying the moving pressure method. This method is based on the fact that an increase in air pressure reduces the water level. In reality, high-pressure zones in the atmosphere influence the water level on a large scale as the atmospheric pressure does not vary much locally. In the model, however, air pressure is locally increased to cause a reduction in water level. By translating the pressure field every time step in the direction of the (modelled) vessel's course, it is possible to simulate a moving object in the numerical grid. The input file that is necessary for Delft3D is created with Python and can be checked in Appendix E. When creating these input files, different elements need to be considered. The most important are explained below.

First, a vessel sails along a certain trajectory. In the model, it would be beneficial to be able to change this trajectory to see the effect of a vessel sailing close by or far away from the groyne field. From the AIS data, coordinates of all vessels that sailed by during the measurement campaign in 2022 are available. This information is used to create a path for the pressure field to translate every time step in the model. By interpolating the inserted coordinates, time steps and velocities can be changed in the model. Figure 3.4a depicts what this step can do in a simple visualisation. In this image, just a rectangular shape is shown. This can be representative if, for example, a push barge is sailing a waterway. However, often, vessels have different shapes. Every vessel shape is different, but for this research, a standardised vessel shape is used and shown in Figure 3.4b. The shape that will be used as a standard vessel is calculated by Equation 3.1. Previously, this equation has already been used in similar research to model vessels with the moving pressure method (Samaras and Karambas, 2021).

$$(\psi_S)_{i,j} = D_p \left[ 1 - c_L \left( \frac{x_i - 0.5L_p}{L_p} \right)^4 \right] \left[ 1 - c_B \left( \frac{y_i - 0.5B_p}{B_p} \right)^2 \right] e^{-a \left( \frac{y_i - 0.5B_p}{B_p} \right)^2} \quad (3.1)$$

With  $D_p$ ,  $L_p$ , and  $B_p$  representing the draft, length, and width of the pressure respectively. With  $D_p = 10^5 * D_s$ , where  $D_s$  is the corresponding vessel draught. The variables  $a$ ,  $c_L$ , and  $c_B$  are set to respectively 16, 2, and 16. These parameters result in the slender body that is shown in Figure 3.4b. In future research, these parameters can be changed according to the research objective.

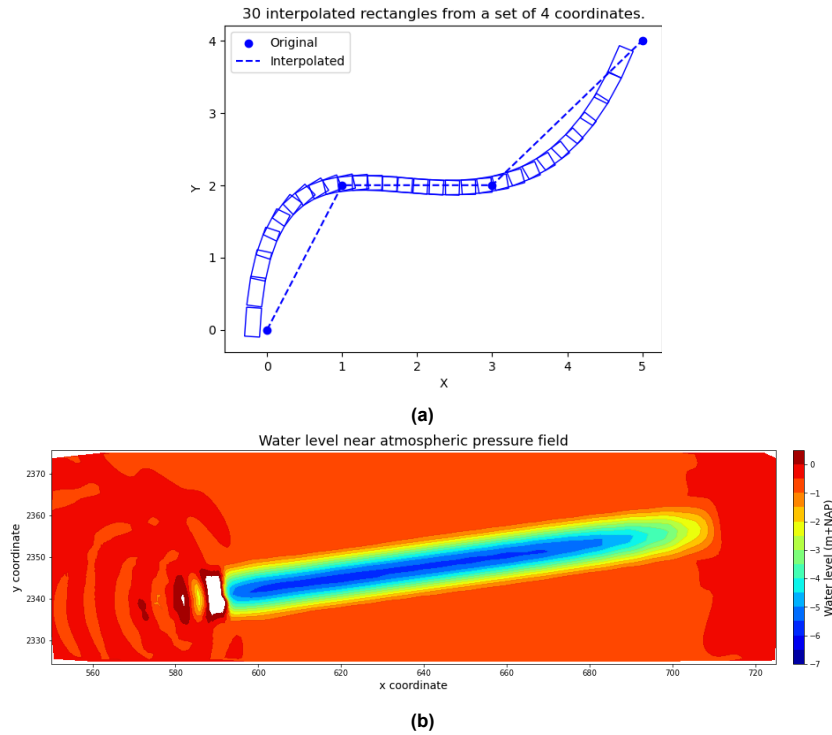


**Figure 3.4:** (a): Schematic visualisation to show the concepts of how the moving pressure field travels through the domain. The blue dots are input coordinates and the model interpolates the blue rectangles in a smooth line through the coordinates. (b): The vessel that is added in the square has a shape that corresponds to this shape. Here it shows the vessel from above and the waterline. In the middle, the draught is around -7 meters.

The pressure fields are automatically interpolated over the grid of the Delft3D FM model. It is therefore preferable that the grid used to create the pressure field is finer compared to the hydraulic grid in the Delft3D FM model. At the same time, the hydraulic grid size of the model must be sufficiently small to be able to recreate the vessel's shape. For uniformity, in all of the simulations, the vessels are sailing from west to east. It opens up space in the modelled open sea for the pressure field to be applied gently in multiple steps.

For the simulations with Delft3D Flexible Mesh, certain parameters are necessary. For most of the numerical parameters, the default settings are used. Each parameter can be researched thoroughly, but in this case, parameters are chosen practically.

Parameter	Value	Unit
Initial water level	-0.5	m
Vessel length	90 - 100	m
Vessel width	20	m
Vessel draught	5	m
Vessel velocity	15	knots

**Table 3.1:** Vessel parameters used in the model

### 3.3. Model verification

The numerical model is verified in two different ways. First, model results are compared to the measurement data and second, the results are compared to the literature study of Ten Brinke (2003). In this way, the model is verified from two different perspectives to obtain the best results.

#### 3.3.1. Verification using measurement data

The available data to calibrate and validate the model is the already analysed measurement data obtained by Kouwenhoven (2023). It is possible to compare the numerical simulation to similar situations

in the data to check if the model can represent reality. To do this, all vessels with similar lengths, widths, draughts, velocities and courses as the numerical pressure field have been selected from the AIS data. This leaves a selection of 32 vessels. Their signals are plotted in Figure 3.5. The moment the vessel passes Groyne Field 9 is taken as point zero in time and is visualised as the vertical black line in the graph.

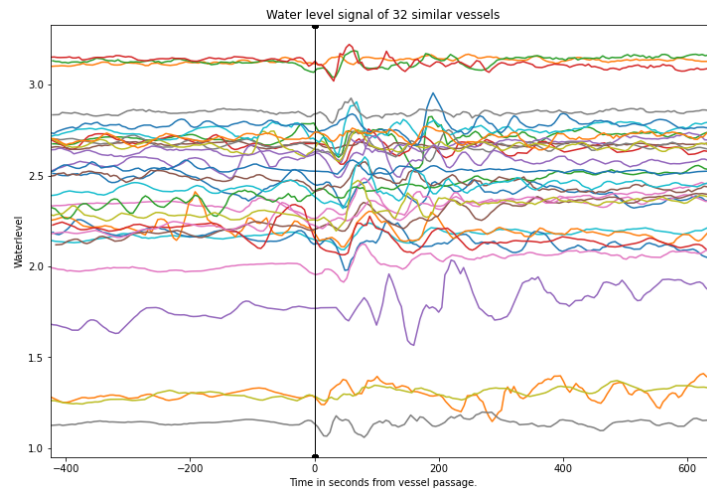


**Figure 3.5:** Water level signal of eleven similar vessels as the modelled vessel. The black vertical line is the moment the vessel passes the groyne field according to the data. All the passage moments are aligned to moment  $t = 0$  to compare signals.

To be able to validate the numerically obtained water level signals, the numerical signals are compared to the signals from the data above. Figure 3.6a illustrates the average of all the measurement signals from ADV 3. Figure 3.6b depicts the model output around the same location in Groyne Field 9 as where ADV 3 was located. As can already be observed in Figure 3.5, the 32 individual vessels each have quite some variety in their signals. This indicates that more complex processes play a role in developing the primary wave. For this step in the verification process, it is sufficient to check if the order of magnitude of the drawdown is around the average magnitudes measured by the ADVs. When the Figures 3.6a and 3.6b are compared, it can be concluded that the drawdown in the measured signals is around the same order of magnitude as the drawdown in the modelled signal. The green dashed line in the figures represents the point in time three minutes after the vessel passes the groyne field. It can be concluded that the frequency of the measured wave is higher compared to the frequency of the modelled wave. As can be obtained from the signals of the 32 individual vessels, after around 100 seconds, the variety in the measured signals becomes high. From this point, it is difficult to conclude about the model's performance.

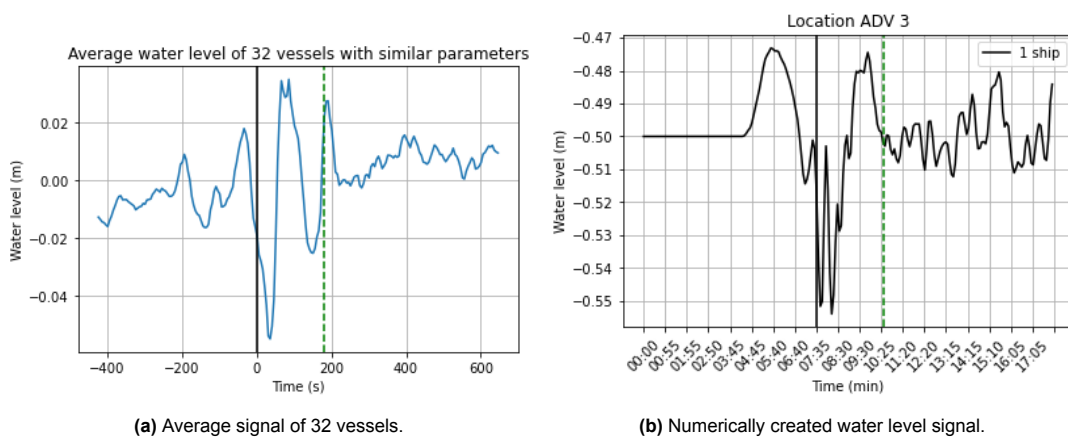


**Figure 3.6:** Comparison between the average primary wave from the measurements (blue line) compared to the numerical signal (black line). The green dashed line corresponds to the equal time after the black passage time in both graphs.

### 3.3.2. Verification using literature

Another way to validate the model is by comparing the results with existing literature. Ten Brinke (2003) described the flow inside an open groyne field during vessel passage. He described the passage of a vessel in six phases. The initial phase (zero) is the situation without a vessel and solely containing discharge, which is different from the numerical situation to be verified, as river discharge is neglected in the numerical model. In phases one and two, the bow of the vessel enters the area in front of the open groyne field. Phase three describes the situation where the vessel is fully in the area in front of the groyne field. Important to note is that in his theory, Ten Brinke (2003) uses a push barge that has around the same length as the distance between the groynes. This causes some differences in results since the vessels used in the numerical model are less than half the length of the groyne field. In phases four and five, the vessel leaves the area in front of the groyne field. In Figure 3.7, three of the six phases of Ten Brinke (2003) are shown, together with the vector plots of the numerical model. As already mentioned, the dimensions of the vessel used in the theory of Ten Brinke (2003) are much larger. The numerical model uses a much shorter vessel which only creates a return flow near the vessel. This may affect the flow inside the groyne field. Another difference between the theory and the numerical simulation is the circulation in the groyne field. Multiple factors can explain this. First, the theory assumes a river flow in all phases of the situation. In the numerical model, no river discharge is assumed for simplicity. Another difference is the groyne field dimensions. The groyne field in the theory is much more stretched whereas the groyne fields in the 'Nieuwe Waterweg' have more of a square-like shape. Furthermore, the groyne fields in the 'Nieuwe Waterweg' are partly submerged, depending on the tide. This impacts the hydrodynamic behaviour significantly. Despite the differences, comparing the numerical situation with the literature confirms the presumption that the numerical model represents a realistic situation.

For each phase, the most important features are explained separately.

1. During the first phase (Figures 3.7a and 3.7b), the vessel starts to sail in front of the open groyne field. The return flow and corresponding drawdown by the vessel cause a flow from the groyne field to the main channel. According to the theory, the flow at the west side of the groyne field is directed in the opposite direction as the direction the vessel sails in. This is the case in the numerical model as well. However, the flow at the east side is not the same as Ten Brinke (2003) described. This can be explained by the fact that the theory assumes a river discharge, while in the numerical model, the water is stationary at the start of the simulation.
2. In the third phase, the vessel sails directly in front of the groyne field and the return current of the vessel affects the hydrodynamics between the groynes. Ten Brinke (2003) describes a flow from the east side to the west side, in the opposite direction as the vessel's sailing direction. Figure 3.7d predominantly shows this behaviour. However, the numerical result shows that the return current does not extend the full width of the groyne field. This effect can be explained by the fact that the groyne field is less stretched out like the groyne field in the theory. The relatively short vessel can cause a limited return current that will have less effect closer to the river bank.
3. The last two figures represent the sixth phase of the theory (Figures 3.7e and 3.7f). This phase is directly after the vessel has passed the groyne field. The main similarity between the model and the theory is the large circular flow within the groyne field. On the west side, the secondary waves enter the groyne field again, whereas on the east side, the water is still withdrawn because of the vessel's return current. A main difference is in the groynes. The groynes are partly submerged in the numerical model whereas the theory of Ten Brinke (2003) considered emerged groynes. Additionally, the theory shows much smaller eddies resulting from the closed groynes. These secondary eddies relate to the size of the groyne field (Yossef, 2005). This will not be treated in this report, but it is important to realise that it plays a role.

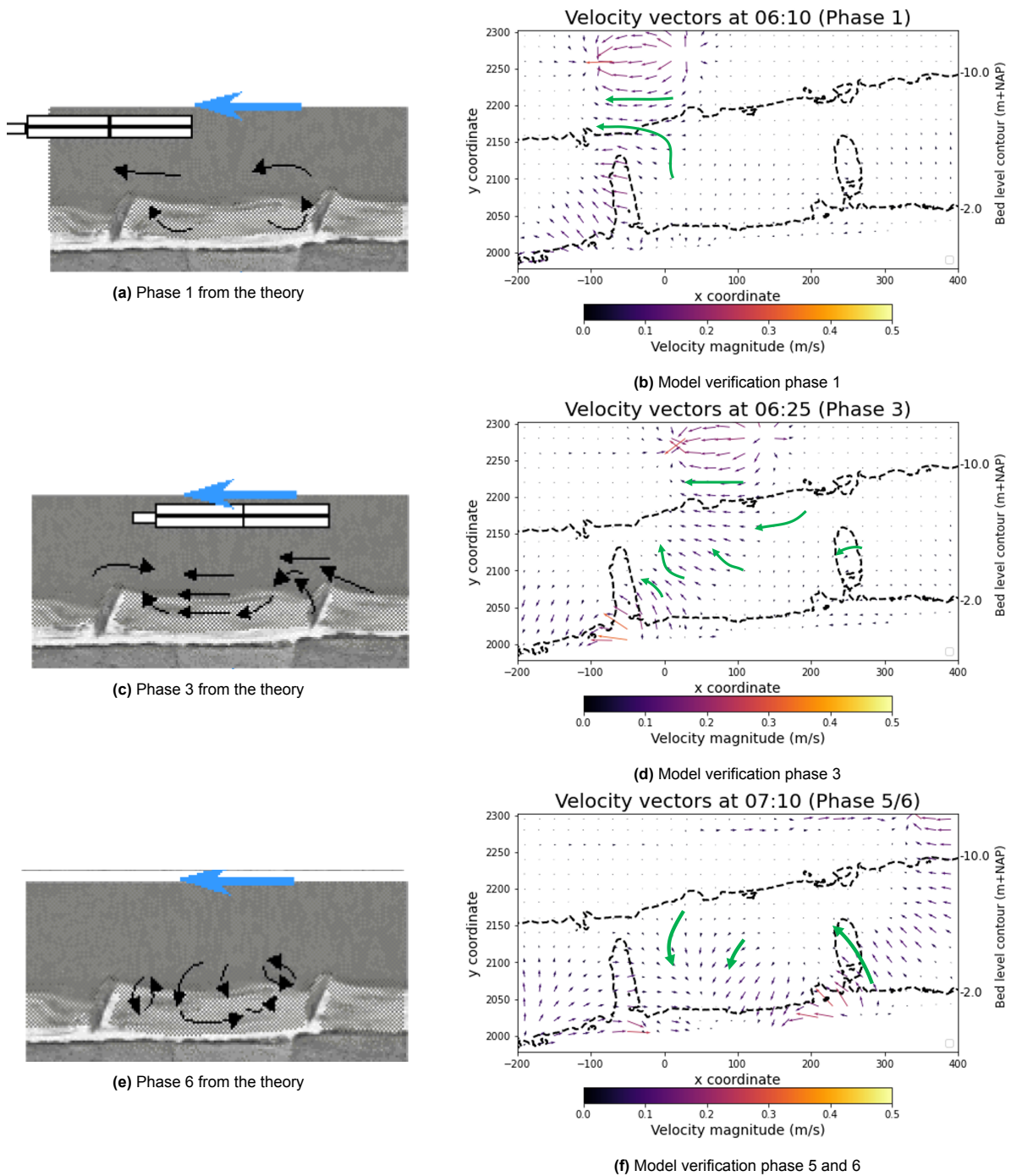


**Figure 3.7:** a, c and e) Different phases during the passage of a vessel near an open groyne field in the river Waal. The black arrows represent the hydraulic flow and the blue arrow represents the discharge direction of the river. b, d and f) Corresponding vector in the simulation if a vessel passes one of the open groyne fields in the 'Nieuwe Waterweg'. The location of this groyne field is depicted in Appendix A. The green arrows summarise other vectors and make the similarities with the theory more visible. Note that the groynes in this model are submerged, which is different from the theory. (Ten Brinke, 2003).

### 3.3.3. Verification summary

The numerical model is verified by comparing the model to water level and velocity magnitude measurement data, and by comparing velocity vectors to existing literature from Ten Brinke (2003). Despite the consideration of some assumptions, the model is sufficiently verified to study the effect of primary vessel waves on the semi-closed Groyne Field 9 in the 'Nieuwe Waterweg'. The hydrodynamic system and properties of the groyne field are researched in Chapter 4 and in Chapter 5 different geometrical layouts are run to study the effect of different design decisions on the hydrodynamic activity.



# 4

## Hydrodynamics inside Groyne Field 9

The verified model is used to analyse different model configurations. This chapter focuses on four simulations that serve to gain more knowledge on the hydrodynamic system in Groyne Field 9. The chapter answers the question: *How does the hydrodynamic system behave in a semi-closed groyne field?*

### 4.1. Overview simulations

First, a basic situation is modelled that represents a simplified situation where one vessel sails with a constant velocity next to the groyne field. In this simulation, the bathymetry in the groyne field is simplified to a flat bed. This allows for a better analysis of 'general' situations and a better understanding of the hydrodynamic system. In the next steps, the results from the basic situation can be used to compare different simulations to.

Next to the simplified basic simulation, a model is run containing the current real bathymetry. This adds specific complexity to the model unique for Groyne Field 9. However, it contributes to understanding the general hydrodynamic behaviour in such semi-closed groyne fields, because it shows smaller local effects that occur in such complex systems. Another advantage of this simulation is that it can be compared to the measurement results of Kouwenhoven (2023) which have already been analysed in Chapter 2. The same situations are run with 2 vessels sailing at a defined time interval from each other to check the possible oscillatory effect first proposed in Section 2.4.

The research in this report focuses on the effect of vessel waves, but to analyse the total system behaviour, the tide needs to be considered. Therefore two separate simulations are run solely containing tidal boundary conditions. For these simulations, the flat bed level from the basic situation as well as the complex bathymetry are used. In Table 4.1, an overview of the differences between the simulations is shown. The difference between the flat bed and the current bed situation is illustrated in Figure 4.1. This figure contains additional elements, which will be discussed in a later section.

Layout/situation	Vessel configuration
Basic situation	1 vessel
	2 vessels (60s in between)
	2 vessels (120s in between)
	2 vessels (180s in between)
	2 vessels (150s in between)
Additional	
Complex-bathymetry situation (current situation)	1 vessel
	2 vessels (60s in between)
	2 vessels (120s in between)
	2 vessels (180s in between)
Tidal background (Flat bed)	0 vessels
Tidal Background (Current bed)	0 vessels

**Table 4.1:** Overview of the different simulations ran for this chapter.

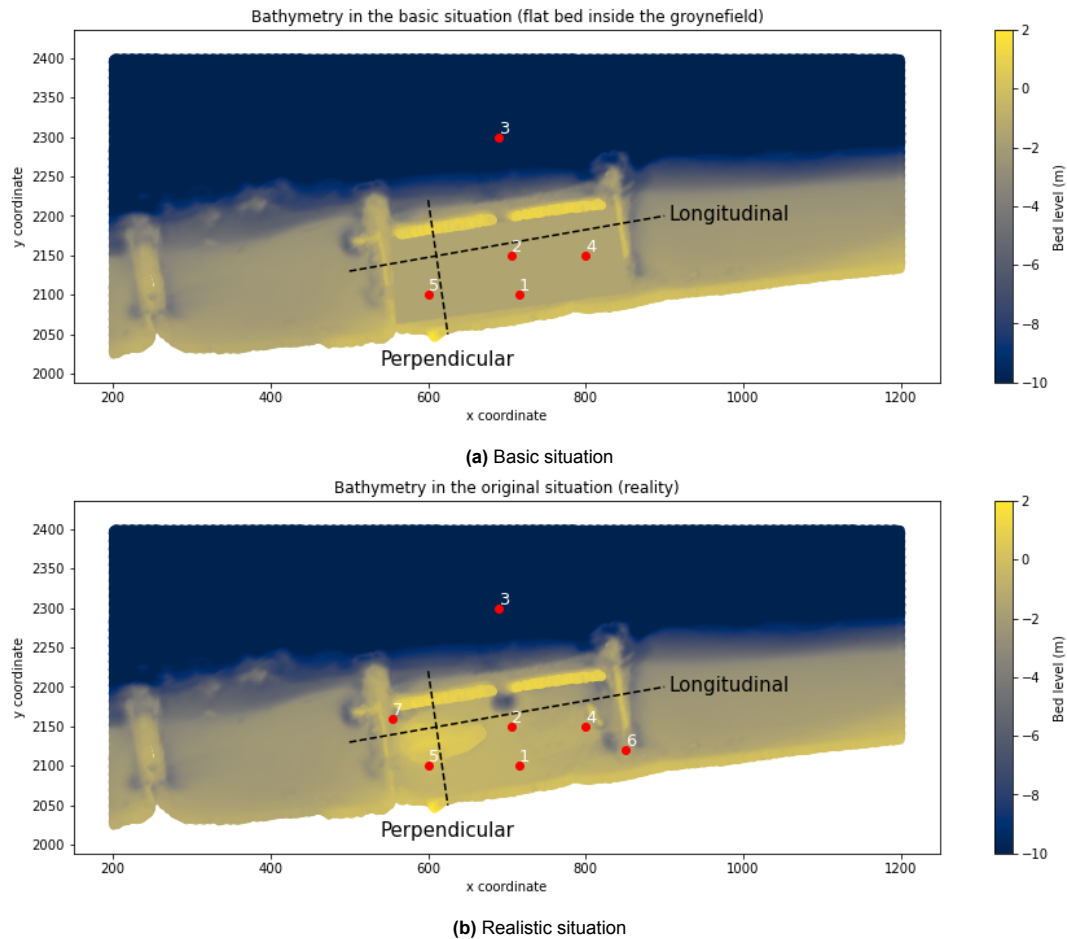


**Figure 4.1:** Bathymetries of respectively the simplified flat bed situation and the current complex situation. The colour scale represents the bed level. The red markers illustrate the locations of the analysed points in the groyne field and the dashed lines represent slices where Figures 4.2 and 4.10 are based on.

## 4.2. Basic situation (flat bed)

Groyne Field 9 has a specific bathymetry. Because of the different disposal activities that have been undertaken in the past, the bed level is higher around the island near the west of the groyne field while at the same time scour holes exist near the openings of the longitudinal dam. To be able to understand the general hydrodynamic system, the bathymetry is simplified inside the groyne field by applying a homogeneous bed level. In this simplification, the hydraulic effects of the groynes and longshore dam can be analysed, without the interference of the complex bathymetry caused by nourishments. Figure 4.1a depicts a map of the bathymetry of the simplified groyne field. Additionally, it shows the points where water levels and velocity magnitudes will be measured for the analysis. Figure 4.2 illustrates the corresponding intersections.

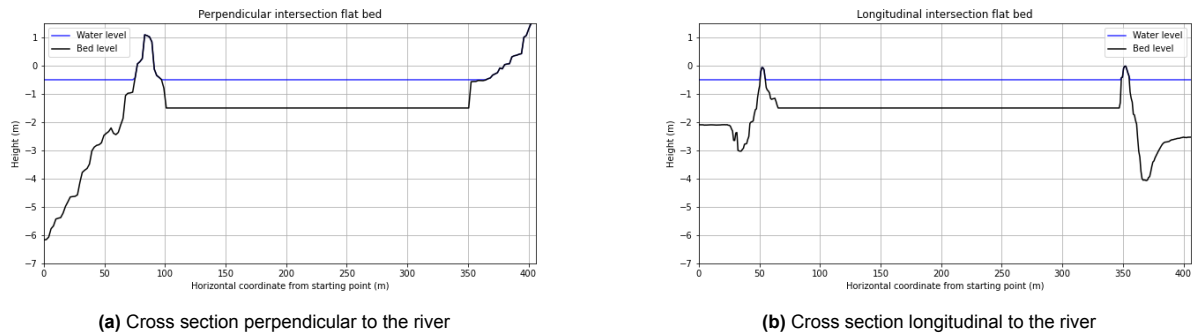


**Figure 4.2:** Overview of the bathymetry used in the simplified model. Slices correspond to the dashed lines in Figure 4.1a. Black lines represent bed level across a line and the blue line represents the water level used in the numerical models at  $t = 0$ .

Figure 4.3 shows the water level of the 'Nieuwe Waterweg' at different moments in time while one modelled vessel passes the groyne field. The colours represent different water levels. The scale is illustrated at the right of the middle image. It is qualitatively visible that next to the vessel's hull, the water level is lower compared to the initial -0.5 meters. This can be explained by the theory of primary vessel waves, discussed in Chapter 1. The figure shows that the water level reduction is not only present next to the hull of the vessel, but the effect extends much further from the vessel in the direction of the river bank. Figure 4.4 visualises the transport of the water around the same points in time by plotting the vectors along the domain. The image indicates how the water behaves around a vessel, as well as inside the groyne field, but it does not provide clear quantitative data which could be analysed. To further analyse the effects of the vessel in a quantitative way, the water levels and velocity magnitudes are obtained at different points in the domain. The geographical locations of these points are depicted in Figure 4.1. For the rest of this chapter, not all plots of all simulations are shown. All relevant images, which are not used in the text are shown in Appendix D. The following section selects and explains the most important features of the first set of simulations.

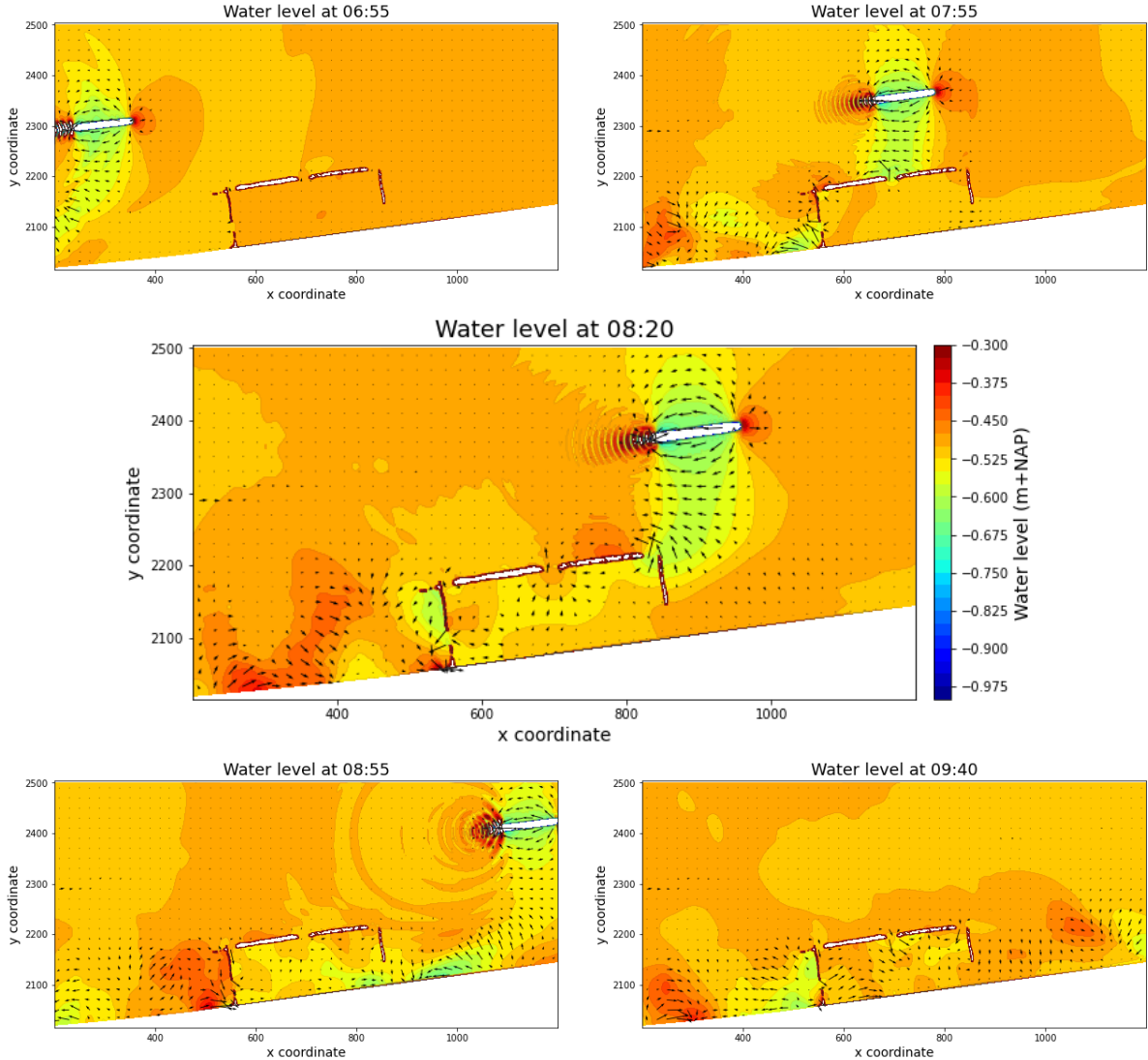


**Figure 4.3:** Water level around the groyne field at different moments in time while a vessel passes the groyne field. The colours represent the water level ranging from -1 to -0.3 meters +NAP. Initial (calm) Water level =-0.5 m. The black arrows show the flow direction at the corresponding points in time and indicate the magnitude. The vessel sails in the direction from left to right.

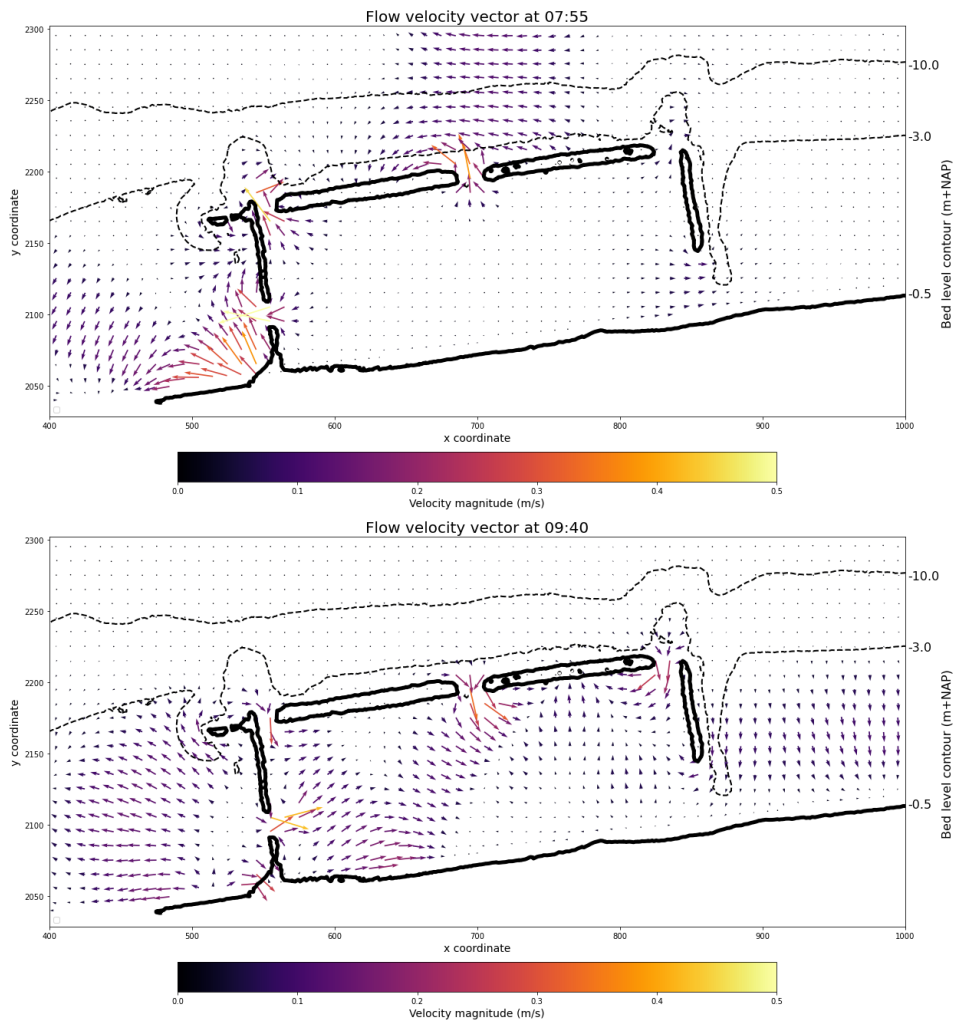


**Figure 4.4:** Visualisation of the flow in and around the groyne field for two moments in time. The top figure represents the moment when a vessel sails in front of the groyne field and the lower graph represents the moment in time when the vessel already has passed the groyne field. The colours represent the velocity magnitude and the arrows show the flow direction. The black lines illustrate the bathymetry and layout in a simplified way. The vessel sails in the direction from left to right.

#### 4.2.1. Quantitative understanding the basic hydrodynamic system

To be able to obtain more quantitative results, water level and velocity magnitude signals are drawn at different locations in and outside the groyne field. The analysis of the configuration containing a flat bed inside the groyne field is separated into three parts. First, a signal outside Groyne Field 9, location 3, is analysed (see Figure 4.5) to check the primary vessel wave effect without the interference of the groynes or longitudinal dams. Next, a hump visible in most of the water level signals is explained. Lastly, the theory from Section 2.4 where the groyne field is assumed to be a closed basin is checked.

##### Effect without interference

Location 3, which refers to a location outside the groyne field, is the first location to be analysed because the location shows signals that are not influenced by the longitudinal dams or the groyne field. The graphs in Figure 4.5 clearly show the water level drop of around eight centimetres and a velocity increase of 0.12 meters per second caused by vessels passing the groyne field. After the vessel has passed, the signals show relatively small oscillations compared to the other locations as can be obtained from the figures in Appendix D. This confirms that drawdown effects can take longer to fade away inside the groyne field compared to outside the groyne field.

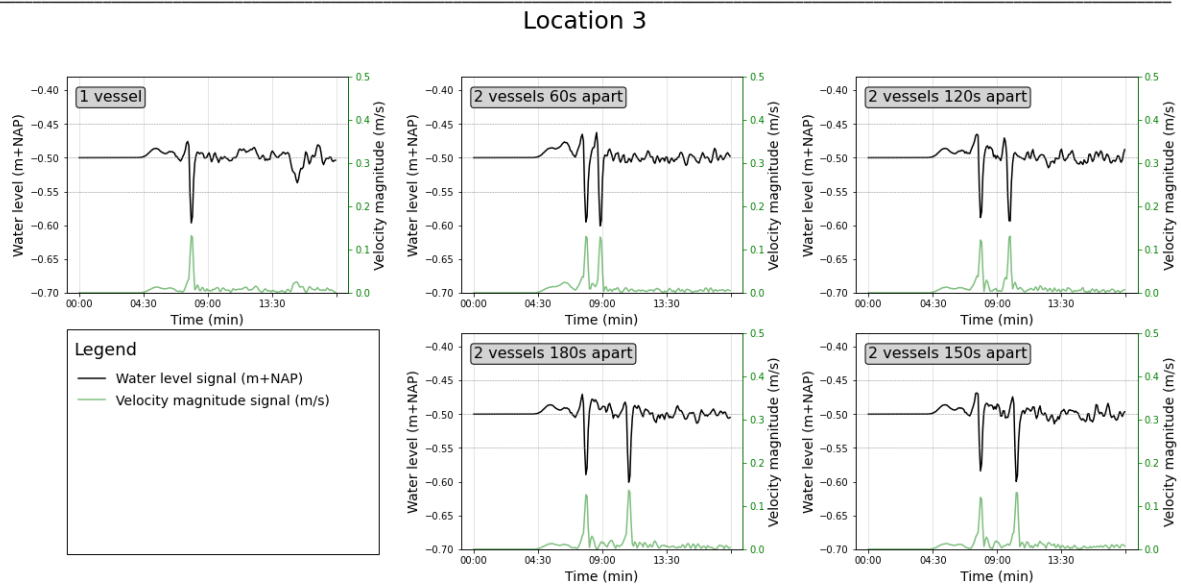


**Figure 4.5:** Two different graphs of five different simulations. The black line represents the water level signal at location 3. The green line represents the velocity magnitude at location 3. The different graphs represent different simulations. The graphs clearly show the moment the numerical vessels pass the location.

#### Initial water level increase

For all water level signals, Fourier analysis is conducted to check which wave frequencies occur from a vessel sailing next to the groyne field. At almost all locations, these Fourier signals show a high power of wave period around 215 - 270 seconds. At the same time, all water level signals contain a relatively long positive wave the minutes before the vessel passes the groyne field. Figure 4.6 shows that these waves correspond to this peak in the Fourier signals. The dashed green and red lines correspond to an interval of 215 and 270 seconds. The Fourier analyses are used in a later section, but this already explains the peaks at high periods.

These results show that vessels in the computational domain are able to cause a wave minutes in advance by pushing water forward. To avoid an initial shock wave in the model, the vessel forcing is applied to the model in gentle steps. This resulted in a reduction of the initial shock wave, but it did not remove the initial wave. It does not prove the initial wave is fully caused by numerical flaws, so it is possible that in reality, a small wave is generated at the bow that influences the water level at a large distance. Either way, the small analysis shows that whether or not the vessel forcing is applied gently, the rest of the signal does not vary significantly. This means that the rest of the water level and water velocity signals can be interpreted separately without the 'fear' of the possibility that the full signal is influenced by an 'unrealistic' numerical effect.

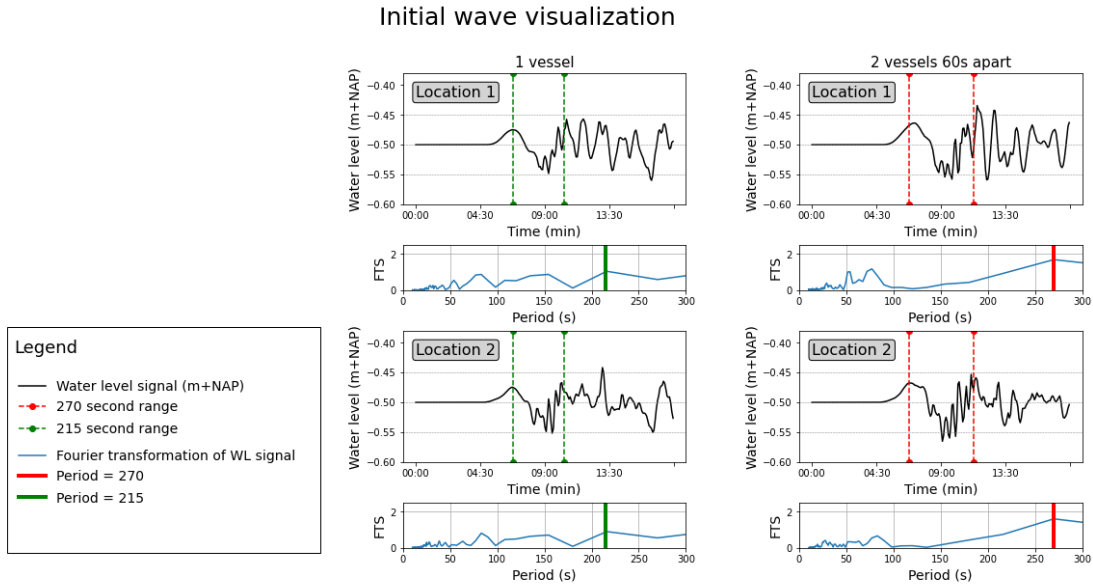


**Figure 4.6:** Graphs of two different simulations at two different locations. A single vessel and two vessels with 60 seconds in between configurations. The black line represents the water level signal at location 1 or 2. The blue line shows all the wave periods that occur within the water level signal by conducting Fourier transformations. The Fourier analysis shows a peak at 270 seconds. The dashed green lines show the corresponding range of 270 seconds in the water level signal.

### Oscillatory behaviour

The theory of natural frequencies influencing water level hydrodynamics in the groyne field is verified in the numerical simulations. The results confirm the theory explained in Section 2.4 where the semi-closed groyne field partially behaves as a first mode oscillating closed basin. The validity of this theory can be shown by the signals from locations 4 and 5, which are located near the east and west groynes of the basin. In the graphs shown in Figure 4.7, green vertical lines are plotted at the moments where the water signals at these locations are in opposite phases. Likewise, this oscillatory behaviour is even more prominently visible in Figure 4.8 as the water level along the longitudinal line of Figure 4.1a is plotted. The Fourier transformation of locations 4 and 5 shows the presence of equal frequencies of waves with a period of around 150 seconds. These results all confirm the existence of the oscillatory behaviour in Groyne Field 9. However, the period of the oscillatory movement in the model deviates from the theoretical period calculated in Equation 4.1. According to the theory, the period should be 185 seconds.

$$T = \frac{2L}{\sqrt{gd}} = \frac{2 * 290}{\sqrt{9.81 * 1}} = 185s \quad (4.1)$$

As illustrated in Appendix D, this peak at 150 seconds in the Fourier analysis is less noticeable at locations 1 and 2 because they are located in the middle between the east and west boundaries of the groyne field. According to the theory, the oscillations in a closed basin are milder in the middle compared to near the boundaries like locations 4 and 5. The groyne field is multi-dimensional, so the water in the basin could oscillate in a crosswise direction. Theoretically, the oscillation period in this direction is calculated as in Equation 4.2.

$$T = \frac{2L}{\sqrt{gd}} = \frac{2 * 110}{\sqrt{9.81 * 1}} = 70s \quad (4.2)$$

Figure 4.7 illustrates another peak in the Fourier analysis at the yellow dashed line point in time. This line represents the peak around a period of 80 seconds which is similar to the theoretically calculated 70-second period. It is possible that the 150 and 80-second peaks correspond to these natural modes, but that the frequencies and periods are influenced by the openings, making the length over which the water oscillates shorter. The effect in the direction perpendicular to the river would be less because it has one closed boundary at its riverbank. The longitudinal cross-section has two openings that are not fully closed which makes the assumption of a closed basin less accurate. Another possible influence factor is that the two-dimensional oscillatory movements in both directions will result in one three-dimensional oscillatory movement.

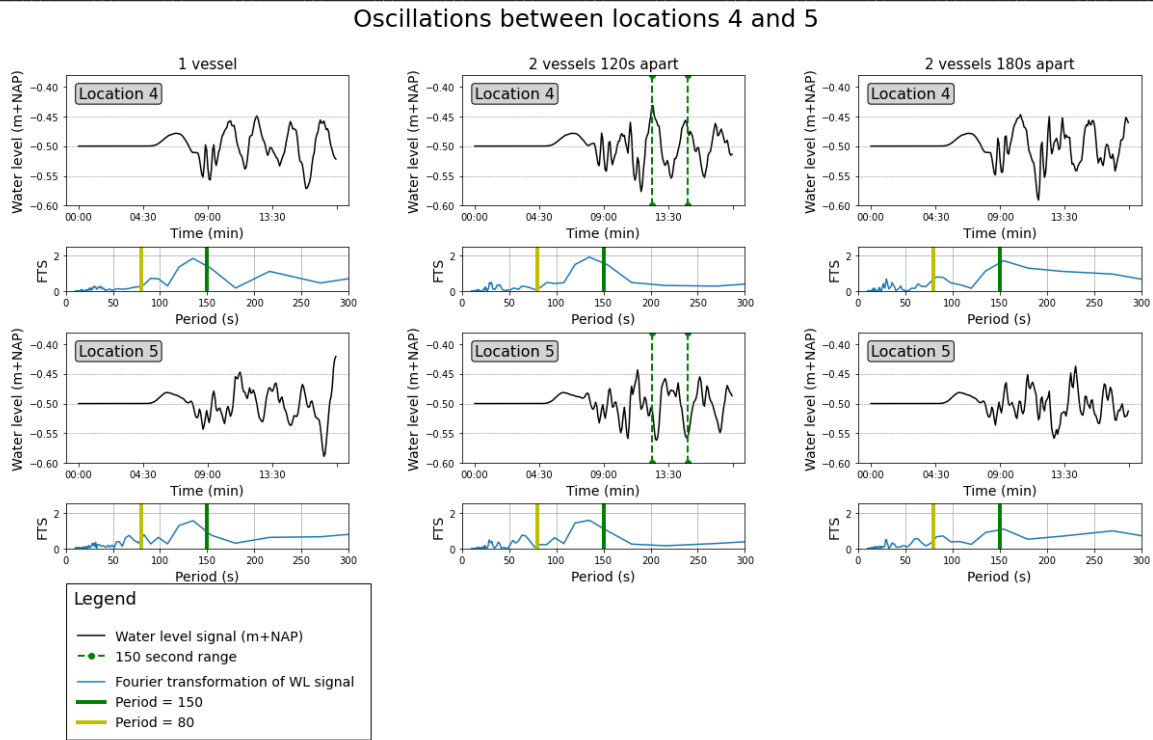


**Figure 4.7:** Graphs of three different simulations at two different locations. The black line represents the water level signal at location 4 or 5. The blue line shows all the wave periods that occur within the water level signal by conducting Fourier transformations. The Fourier analysis shows a peak around 80 and 150 seconds. The dashed green lines show the corresponding range of 150 seconds in the water level signal.

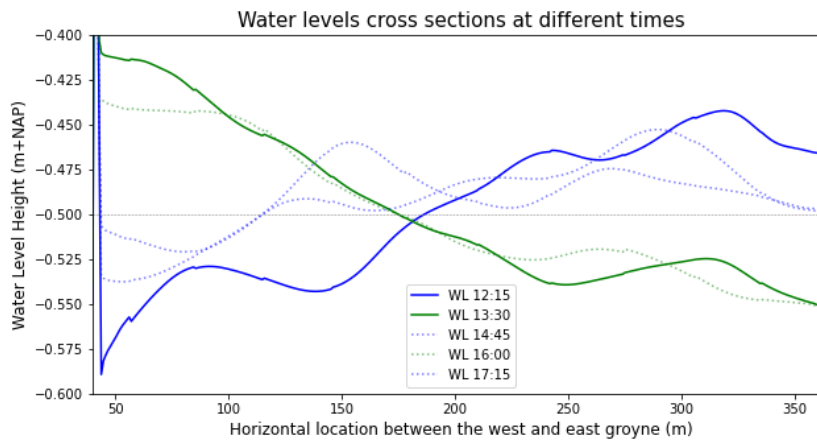


**Figure 4.8:** Five water level cross sections along the longitudinal line shown in Figure 2.4 that show the oscillatory movement in the groyne field. The slices are taken from the model each 75 seconds apart. The total period of the oscillatory movement is 150 seconds.

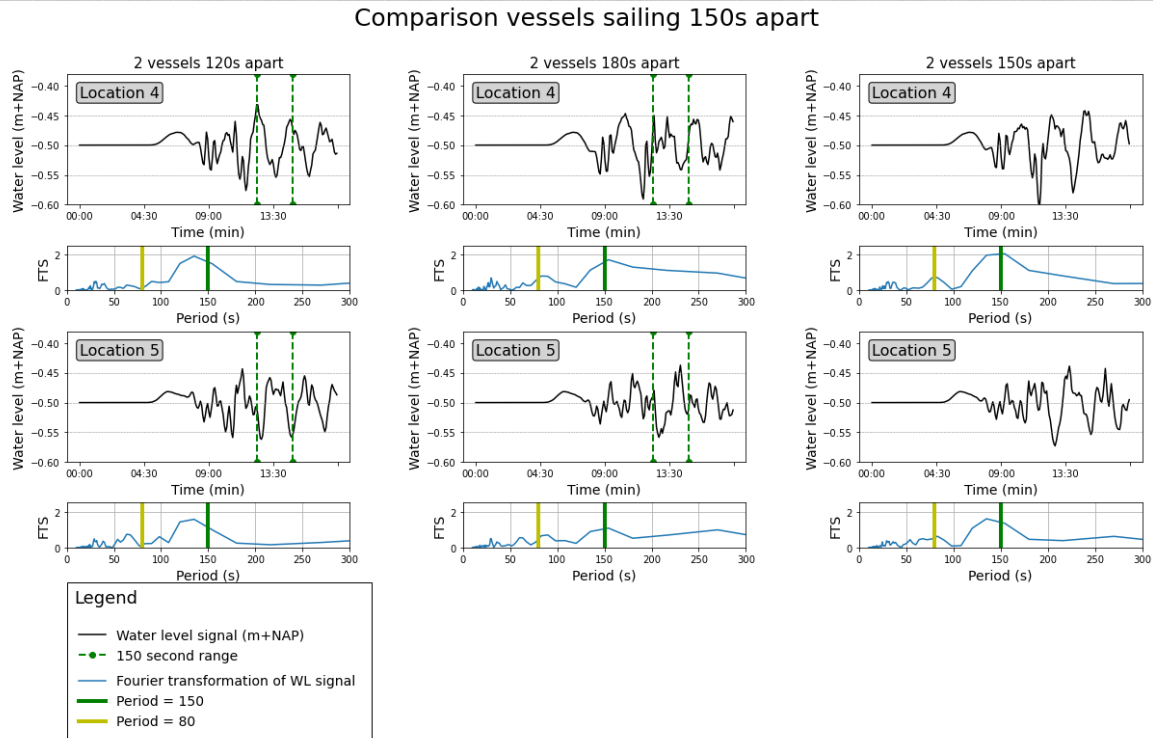
**Check for resonance**

Figure 4.7 suggests the possibility of a natural frequency in the groyne field because of the fact that a frequency peak occurs when the primary waves of 2 vessels are almost in phase with this frequency. To verify the possibility that resonance occurs if the vessels sail exactly 150 seconds apart, an additional simulation is run. Figure 4.9 illustrates the results of this simulation together with the simulations where the vessels sail respectively 120 and 180 seconds apart.

According to the Fourier transformations of the water level signals, the presence of a 150-second period signal is higher in the simulation where the vessels sail 150 seconds apart compared to the other simulations. However, the water level amplitudes at locations 4 and 5 are not significantly different in



one of the simulations. Next to this, the velocity magnitude is not significantly different in one of the simulations, which accounts not only for locations 4 and 5 but for all locations. These observations indicate resonance is unlikely to occur in this system. It can be explained by the fact that the theoretical basin is not fully closed, as soon as the amplitudes increase, the water level difference between the inside and outside of the groyne field increases, which leads to a higher outflow and therefore damping of the oscillatory movement.



**Figure 4.9:** Graphs of three different simulations at two different locations. The black line represents the water level signal at location 4 or 5. The blue line shows all the wave periods that occur within the water level signal by conducting Fourier transformations. The Fourier analysis shows a peak of around 80 and 150 seconds. The dashed green lines show the corresponding range of 150 seconds in the water level signal. The simulation with two vessels sailing 150 seconds apart is compared in this image.

### 4.3. Complex-bathymetry situation (Current situation)

The simulations analysed in this section have one difference to the basic simulations treated in the previous section. In this model, the current bathymetry inside the groyne field is used. This bathymetry is more complex, and heterogeneous, but very specific for this particular location. The bathymetry is illustrated in Figure 4.1b and the corresponding cross sections are depicted in Figure 4.10. These figures give a visual representation of the heterogeneous and more complex bathymetry compared to the considered flat bed in the basic simulation. To analyse the differences between the simulation results, the signals from different locations are analysed.

#### 4.3.1. Qualitative analysis complex bathymetry

For the analysis of the simulations with the current groyne field bathymetry, 7 observation locations are used. These locations are illustrated in Figure 4.1. For homogeneity, locations 1 until 5 are similar to the locations in the previous analysis. The reason for adding two locations is the complex bathymetry. For example, location 5 does not give a signal, because it is located at a location above the water line. The basic simulation showed that the hydrodynamic behaviour could be described using closed-basin assumptions. In this more complex situation, this assumption is not valid. Instead, interesting points in the groyne field are selected by looking at specific elements in the bathymetry that stood out during visual inspection. These locations are the area in the northwest corner above the island (location 7) and the area in the southeast corner (location 6), as shown in Figure 4.1. All locations are analysed,

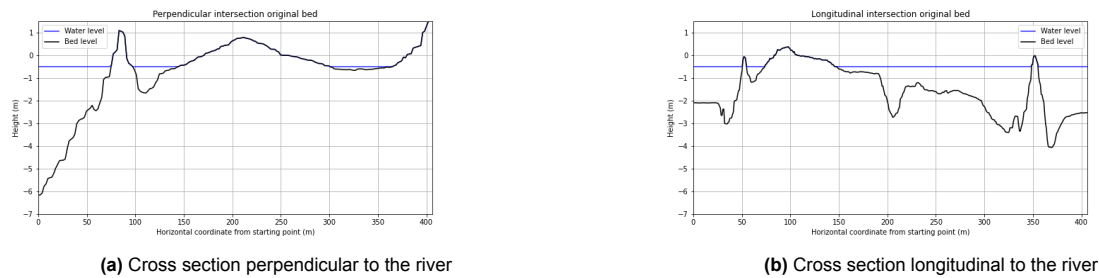


**Figure 4.10:** Overview of the bathymetry used in the model where the current complex bathymetry is used. Slices correspond to the dashed lines in Figure 4.1b. Black lines show the bathymetry along a line and the blue line shows the used initial water level in the model.

but the most notable results are discussed in this section.

### Location 2

The first obvious difference between the resulting signals of the basic simulation and the complex-bathymetry simulation is visible in the water level and velocity magnitude signals of location 2. Location 2 is located in the middle of Groyne Field 9 below the middle opening of the longshore dam and right next to the 'tip' of the disposed island in the current (complex) bathymetry. The signals are illustrated in Figure 4.11 and show significantly higher velocities for the complex-bathymetry situation compared to the basic situation, while the water level oscillations are more or less the same. An indication of why the velocity magnitudes are higher in the complex bathymetry situation is illustrated in Figure 4.14 which illustrates the flow patterns at two points in time. It shows that the geometrical layout of the disposed island causes the water to increase velocity at the tip of the island which is where location 2 is located.

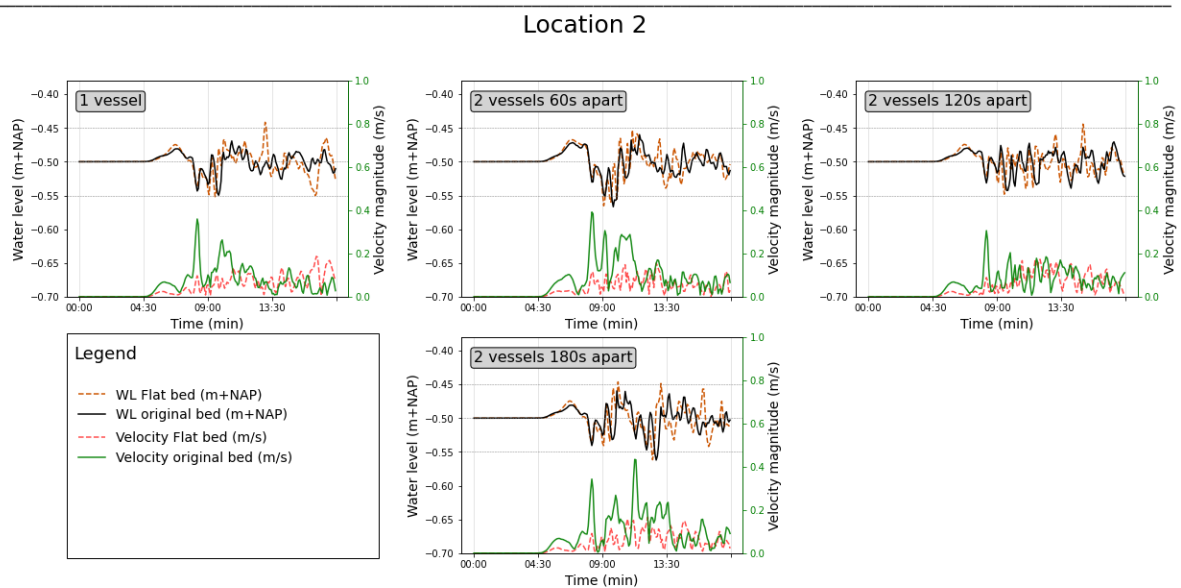


**Figure 4.11:** Graphs of the water levels and velocity magnitudes of 2 simulations at location 2. Red and orange dashed lines indicate signals from the simulation with a flat bed and the black and green lines represent the signals from the simulation of the original bed.

### Location 4

Location 4, which is located further away from the large island, shows different results. Figure 4.12 illustrates lower amplitudes for the water level oscillation compared to the simulation with a homogeneous bed. This effect can be explained by the fact that the complex bathymetry adds obstacles to the bed that cause friction compared to the 'empty' basin in the basic simulations. These obstacles limit the oscillatory behaviour in the groyne field, explained in Section 4.2.1. Apart from this, the velocity

magnitude is almost equal, which indicates that, at location 4, the bathymetry does not limit the flow velocity. This is emphasised by the fact that the area around location 4 is relatively open and no large nourishment or obstacle influences the flow compared to the basic situation.

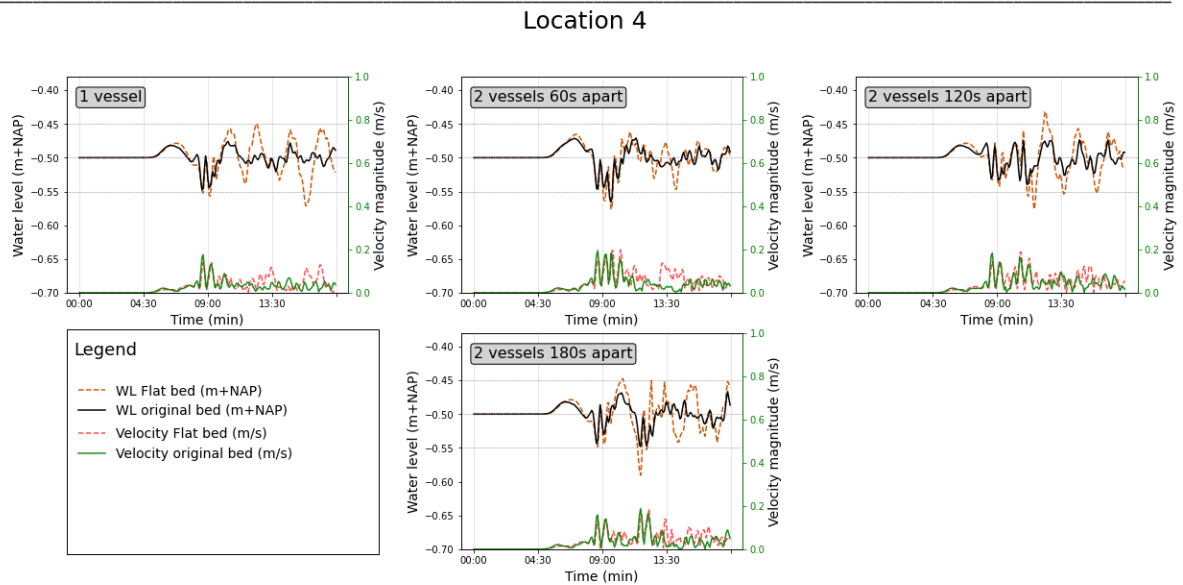


**Figure 4.12:** Graphs of the water levels and velocity magnitudes of 2 simulations at location 4. Red and orange dashed lines indicate signals from the simulation with a flat bed and the black and green lines represent the signals from the simulation of the original bed.

#### Locations 6 and 7

Visual observations are conducted several moments in time and these observations suspect the water in the southeast corner to behave dynamically the moment a vessel passes the groyne field. The east groyne is partly submerged which creates an even more turbulent hydrodynamic environment. Location 6, which is located next to the east groyne in a small scour hole, is introduced to research the behaviour in this area of the groyne field. Another interesting area in the groyne field is the northwest corner, introduced and analysed as location 7, located between the northwest opening of the longitudinal dam and the disposed island. The exact locations of locations 6 and 7 are depicted in Figure 4.1b and the corresponding signals are illustrated below in Figure 4.13.

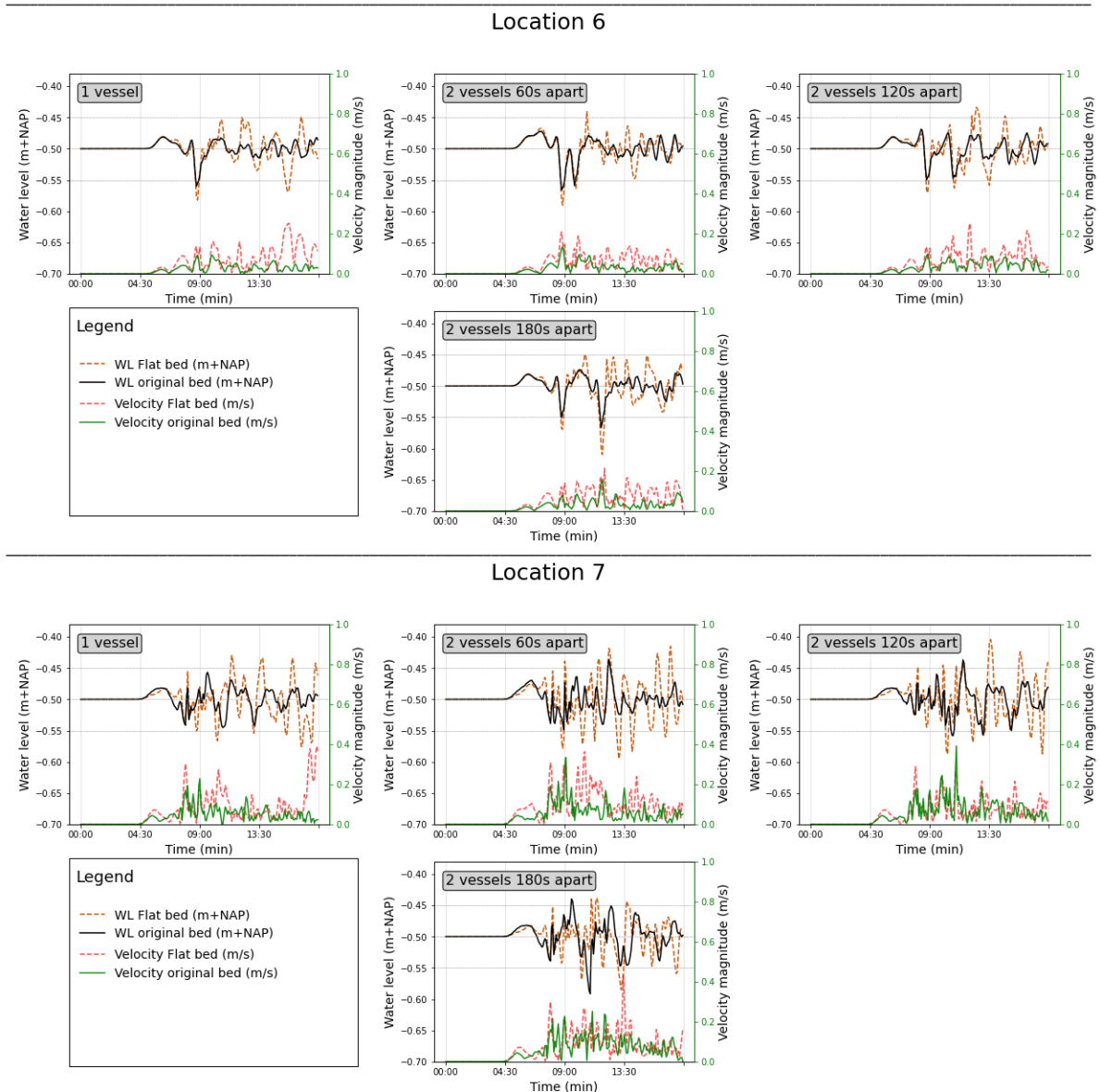


**Figure 4.13:** Graphs of the water levels and velocity magnitudes of 2 simulations at locations 6 and 7. Red and orange dashed lines indicate signals from the simulation with a flat bed and the black and green lines represent the signals from the simulation of the original bed.

Just like at other locations, the water level oscillation amplitudes in locations 6 and 7 are smaller in the situation with the current bathymetry compared to the situation with the flat bed. However, the velocity magnitudes in locations 6 and 7 are lower in the complex bathymetry situation, which is different with respect to locations 1 and 2. This can be explained by the fact that friction plays a role in limiting overall velocity magnitudes, except in locations where local bathymetry causes flow line contraction resulting in a velocity increase, like location 2. The local bathymetry around locations 6 and 7 does not vary much from the basic situation, which explains why the velocity is only decreasing instead of increasing. For locations 1 and 2, this conclusion is invalid due to the suspected local geometrical properties that cause the velocity to increase locally.

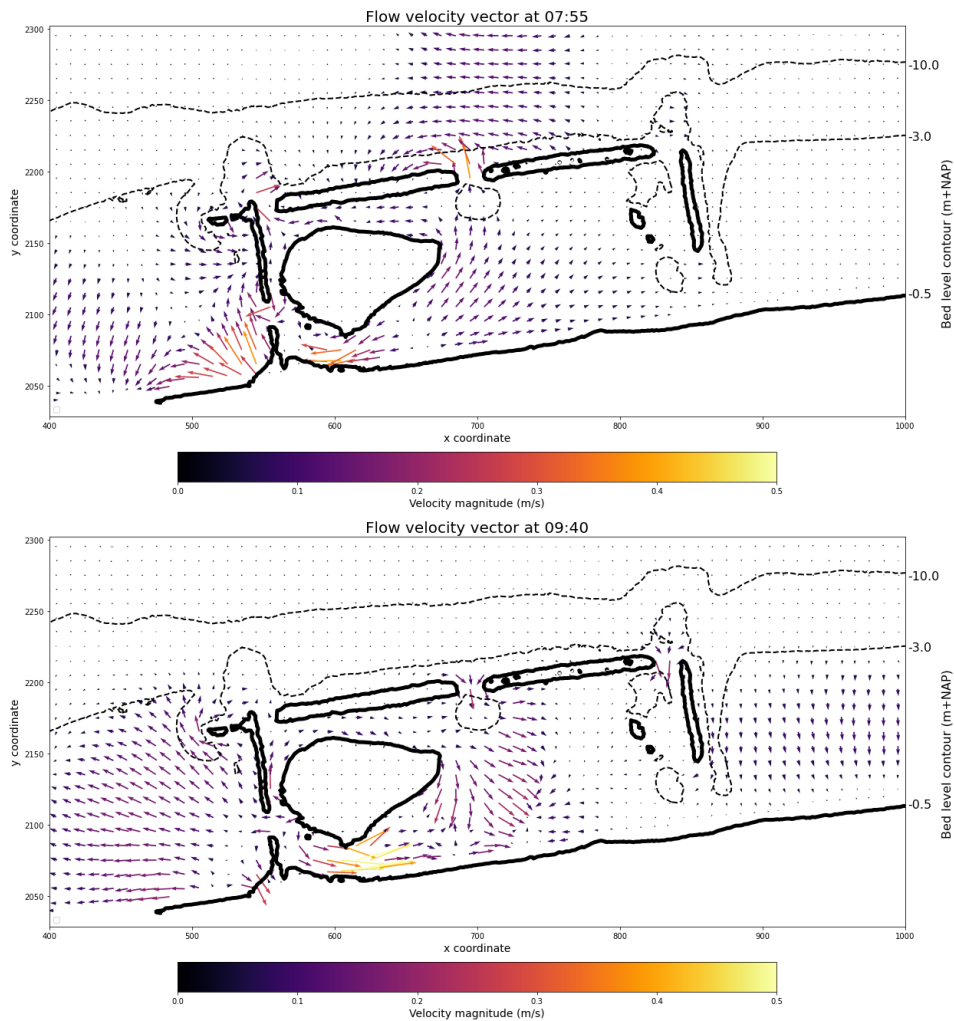


**Figure 4.14:** Visualisation of the flow in and around the groyne field for two moments in time. The top figure represents the moment when a vessel sails in front of the groyne field and the lower graph represents the moment in time when the vessel already has passed the groyne field. The colours represent the velocity magnitude and the arrows show the flow direction. The black lines illustrate the bathymetry and layout in a simplified way.

#### 4.4. Tidal background simulation

The research conducted in this report mainly focuses on the effect of primary vessel waves in the semi-closed groyne field. However, tidal effects play a big role in the 'Nieuwe Waterweg'. Conclusions on effects on this particular location can only be used if tidal forcing is taken into account. Therefore, a simulation that exclusively addresses tidal forcing is modelled.

The tidal boundary condition at the left side includes tidal components A0, M2, M4 and M6 according to Sloff et al. (2012). The numerical representation of the longitudinal dam becomes less realistic when the water level is higher, because, in the numerical model, it becomes possible for water to flow through, and eventually over the dam. In reality, this does not happen every tidal cycle and therefore, for this simulation, a small offset of -0.4 meter is applied. The effect on the general flow pattern for low and high tides will be limited because of the offset because there is already a large variation between different water level situations.

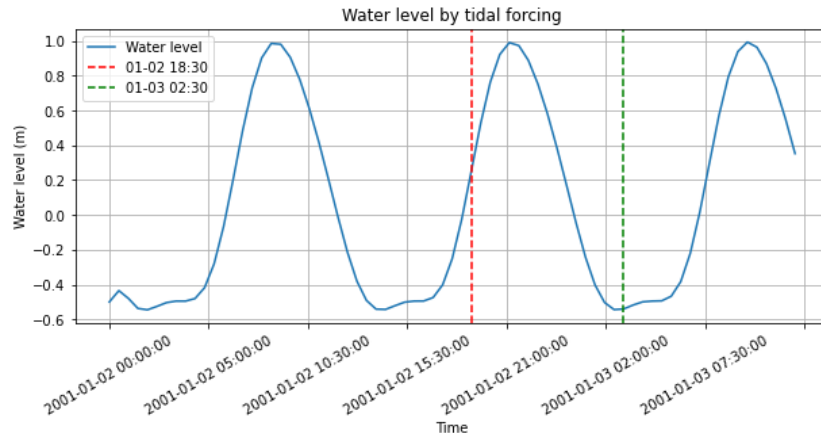


**Figure 4.15:** Modelled tidal signal. The blue line shows the water level and the red and green lines refer to the moment the plots in Figure 4.16 are shown.

Figure 4.16 depicts the numerical flow velocities during the high and low tide compared to the conclusive flow obtained by Kouwenhoven (2023). Almost all proposed flow directions are depicted in both the left and the right images, which means the numerical model represents a real situation quite sufficiently. The left vector plots are derefined for clarity, but more detailed images are depicted in Appendix D.3. One difference between the measurement result and the numerical result is the flow during low tide from the northeast of the groyne field to the middle north, depicted as a dashed line. The numerical model shows an outflow of water, whereas the measurement analysis concluded in an inflow.

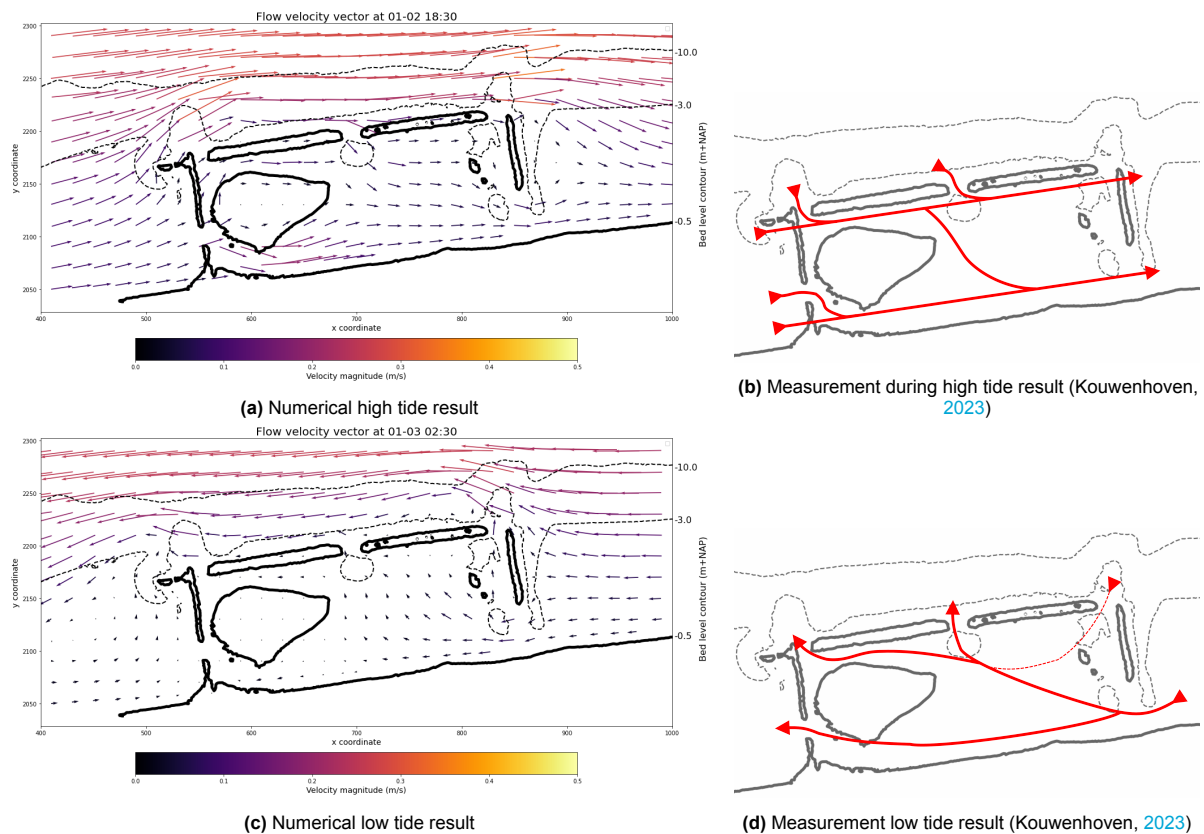


**Figure 4.16:** Left: Vector plots from points in time during high and low tide situations. The arrows show flow direction and velocity and the black lines give a schematic overview of the bathymetry. More detailed images are shown in Appendix D.3. Right: Flow pattern conclusions by Kouwenhoven (2023).

To be able to conclude on the numerical tidal flow, four situations from two simulations are analysed.

The different simulations contain different bathymetries, the original bed and the flat bed inside Groyne Field 9. From each simulation, flow during high and low tide is analysed. All four vector plots are shown in Appendix D.3, but to illustrate an example, two situations with a flat bathymetry are depicted below in Figures 4.17 and 4.18. The corresponding moment in the tidal cycle where the vector plots are taken from is shown in Figure 4.15.

During both high and low tide, the hydrodynamic activity is most active near the partly submerged groynes. During high tide, depicted below, the overall velocities and magnitudes are higher, as well as the presence of significant flow through the middle opening in the longitudinal dam. For these simulations, river discharge has not been taken into consideration, which causes the low tide flow velocity magnitudes to be lower as illustrated in Figure 4.18. The main objective of these simulations is to understand the hydrodynamic behaviour instead of the flow magnitudes, therefore assuming no discharge is allowable.

Near the river bank, higher flow is shown by longer arrows. The largest differences between low and high tide flow can be observed by the flow velocities near the groyne field entrances. During high tide, more activity is observed at the openings in the dam because apparently in this situation, the west side groyne is obstructing enough for the water to flow a different way into the groyne field. These plots confirm the observations gathered during the visual survey which suspected that if the water level is high enough to be able to surpass the groynes, less water flows through the longitudinal dam entrances and if the groynes obstruct enough flow, the entrances in the longitudinal dam become the important connections between the water level outside and inside the groyne field.

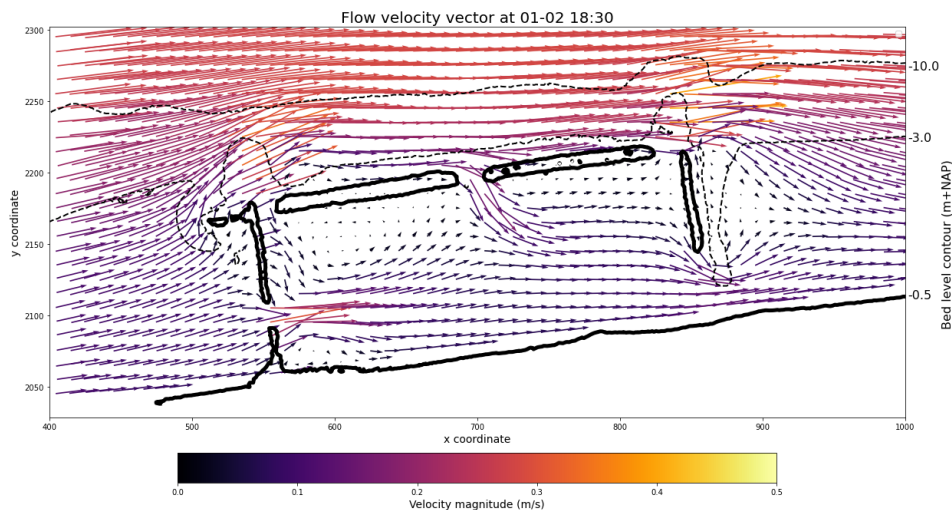


**Figure 4.17:** Vectorplot of the flow velocities around Groyne Field 9 during flood tide. The colours represent the velocity magnitude and the arrows show the flow direction. The black lines illustrate the bathymetry and layout in a simplified way.

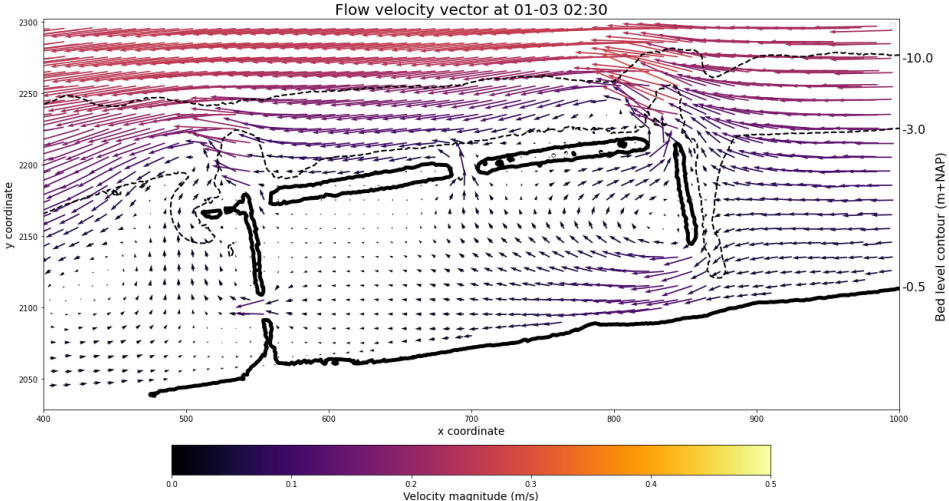


**Figure 4.18:** Vectorplot of the flow velocities around Groyne Field 9 during low tide. The colours represent the velocity magnitude and the arrows show the flow direction. The black lines illustrate the bathymetry and layout in a simplified way.



# 5

## Hydrodynamic behaviour in different groyne field layouts

The previous chapter focused on understanding the hydrodynamic behaviour in the groyne field using a simplified situation and a situation containing the original bathymetry. This chapter answers the question: *What structural layout design decisions can modify the hydrodynamic conditions in a semi-closed groyne field?* To answer this question, different layout designs are developed from visual research, literature and the background knowledge obtained in the previous chapters. The simulation results provide hydrodynamic insight into the impacts of certain layouts and can be used for future decision-making. Four layouts, which are all variations of the basic layout, are analysed. In this way, each geographical component can be analysed separately. The geographical elements that are studied are the opening configuration in the long-shore dam and the height of the groynes. Various alternatives are combined to eventually the following layouts:

1. In the first layout, the groyne fields next to Groyne Field 9 are partially closed off in the same way to represent the situation when the project is scaled up to the whole waterway and to check whether this influences the results compared to the basic situation.
2. The second layout contains only entrances in the groyne field corners and has emerged groynes. It analyses the effect of fewer opening points in the longshore dam together with higher groynes.
3. Layout 3 contains only one middle entrance and has emerged groynes. This layout can be compared to the more open basic situation from Chapter 4 and to the second layout.
4. In layout 4, the groyne fields have elongated openings in the middle and submerged groynes to check the third layout results with a situation where the groynes are partially submerged. This situation can be compared to longshore dams in the Waal (Chavarrias et al., 2020).

The four different layouts will be extensively described and explained in the following sections.

### 5.1. Layout description

This section will describe and explain the considerations made into the design of each of the four different layouts. The layouts are implemented into the simulations by changing the bed levels. The bed level consists of a file with x, y and z coordinates which creates a grid of points with a certain height. Delft3D software interpolates this grid to create a virtual bed level. To vary layouts, the grid points in the input file at certain locations are changed to a higher z-value. This generates a local increase in bed level that results in a representation of a dam-like structure. This causes a vertical slope at these locations, but for research and simplifying purposes, this is intended. It is useful, however, to be aware of the fact that in reality, a slope of for example rocks damps waves and flows. In these simulations, this is not the case. The layouts all have a flat bed within Groyne Field 9 because in this case, the results can be compared to the basic simulation with the flat bed from the previous chapter. The vessel trajectories, as well as boundary conditions, and bed levels, are identical with respect to the basic simulations, except for the added dams.

### 5.1.1. Layout 1: Closed neighbouring groynes

The project 'Proeftuin Sediment Rijnmond' is using Groyne Field 9 as a pilot area where ideas can be tested. However, the original future planning is to (partially) close off more groyne fields in the 'Nieuwe Waterweg'. At the same time, measurement data, the numerical model and observations show that the flow on the east and west sides of the groyne field is hydro-dynamically active when a vessel passes the groyne field. The question arises whether the closing of neighbouring groyne fields in the same way will change the hydrodynamic behaviour significantly. To answer this question, the neighbouring groyne fields are partially closed as illustrated in Figure 5.1. The effects of this layout are useful for future development of the groyne field projects in the 'Nieuwe Waterweg'.

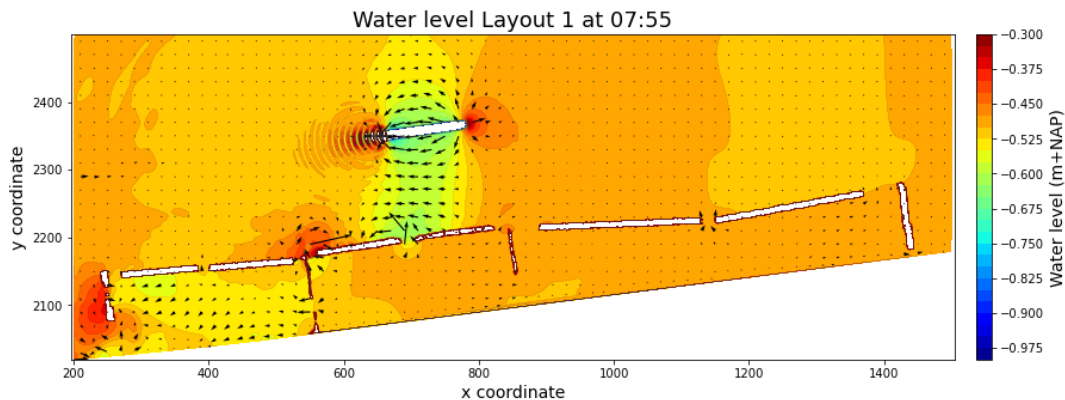


**Figure 5.1:** Water level around the groyne field at different moments in time while a vessel passes the groyne field considering layout 1. The colours represent the water level ranging from -1.8 to 0.0 meter +NAP. Initial (calm) Water level = -0.5 m. The black arrows show the flow direction at the corresponding points in time and indicate the magnitude. The vessel sails in the direction from left to right.

### 5.1.2. Layout 2: Corner entrances and emerged groynes

The second and third layouts highlight the effect of the number and location of the openings in the longitudinal dam. Groynes have been modelled so that they emerge above the water level. In the basic situation, the groynes are partially emerged, but it is still possible for water to flow through or over the groynes. The absence of the opening in the middle of the longitudinal dam together with the emerged groynes results in a situation where the closed basin assumptions become much more valid with respect to the basic simulation.

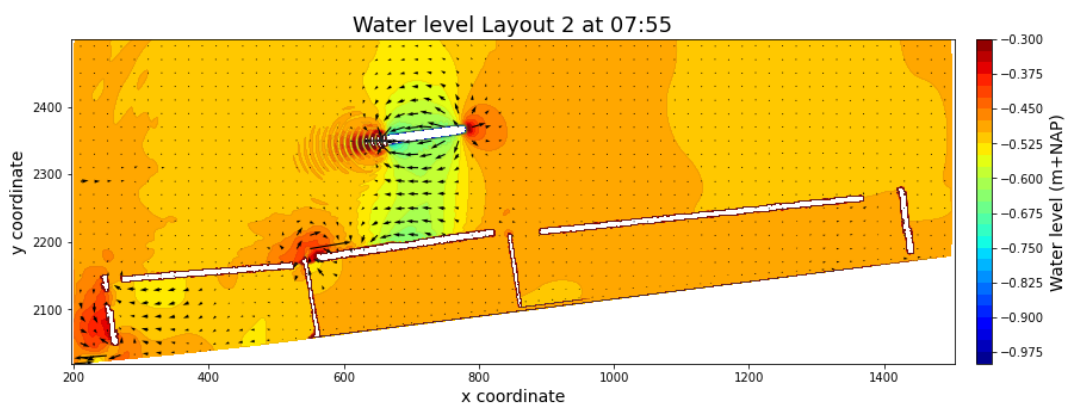


**Figure 5.2:** Water level around the groyne field at different moments in time while a vessel passes the groyne field considering layout 2. The colours represent the water level ranging from -1.8 to 0.0 meter +NAP. Initial (calm) Water level = -0.5 m. The black arrows show the flow direction at the corresponding points in time and indicate the magnitude. The vessel sails in the direction from left to right.

### 5.1.3. Layout 3: Single middle entrances and emerged groynes

Layout 3 is similar to layout 2 because they both contain emerged groynes which almost excludes the influence of the neighbouring groynes. The difference with respect to the second layout is the opening layout in the longitudinal dam. In layout 3, the openings at the corners are closed off, creating a calm area in the top corner of the groyne field. At the same time the entrance in the middle of the dam, similar to the basic situation, was added to check if this has any influence on the hydrodynamic activity in the groyne field.

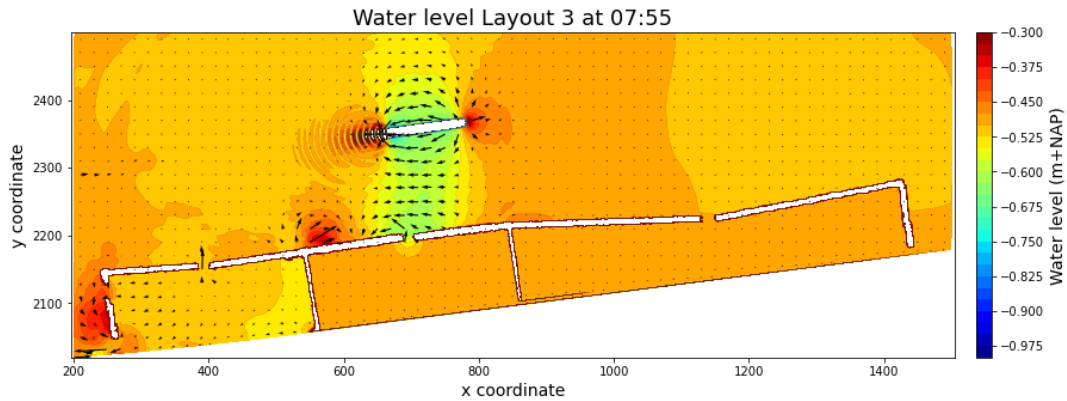


**Figure 5.3:** Water level around the groyne field at different moments in time while a vessel passes the groyne field considering layout 3. The colours represent the water level ranging from -1.8 to 0.0 meter +NAP. Initial (calm) Water level = -0.5 m. The black arrows show the flow direction at the corresponding points in time and indicate the magnitude. The vessel sails in the direction from left to right.

### 5.1.4. Layout 4: Elongated middle openings and submerged groynes

The design for Layout 4 is based on the idea that, to create larger deeper areas, the entrance needs to be elongated. In this scenario, the water that enters the groyne field flows through a small channel instead of just an opening of a dam. Theoretically, this results in a larger area. Figure 5.4 illustrates the differences between the layout entrances. Openings between two dams cause the water to separate directly after passing the opening, while the flow separation in the fourth layout happens at the end of the elongated entrance.

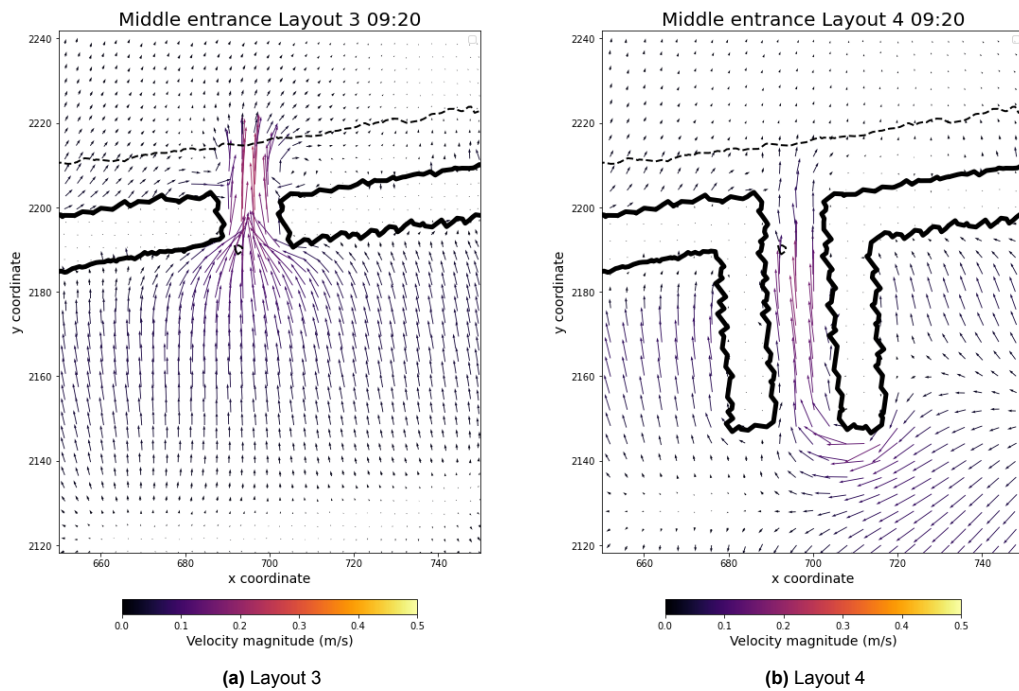


**Figure 5.4:** Zoomed image of the middle entrances of the groyne field for layouts 3 and 4. The coloured arrow represents flow velocity and direction and the black lines represent bathymetry and show the geometrical layout of the groyne field entrance.

Additionally, layout 4 contains the original submerged groynes. Using submerged groynes and limiting the number of openings on the riverside creates a situation that has similarities to longitudinal training dams in the Waal. Recently, these dams were constructed as a pilot project to research this new idea for river training. These longshore dams are located at three locations on the inner bend of the river Waal, contain openings at certain locations and are meant to improve navigability, overall bed incision, improved ecological conditions and more safety against flooding (Chavarrias et al., 2020).

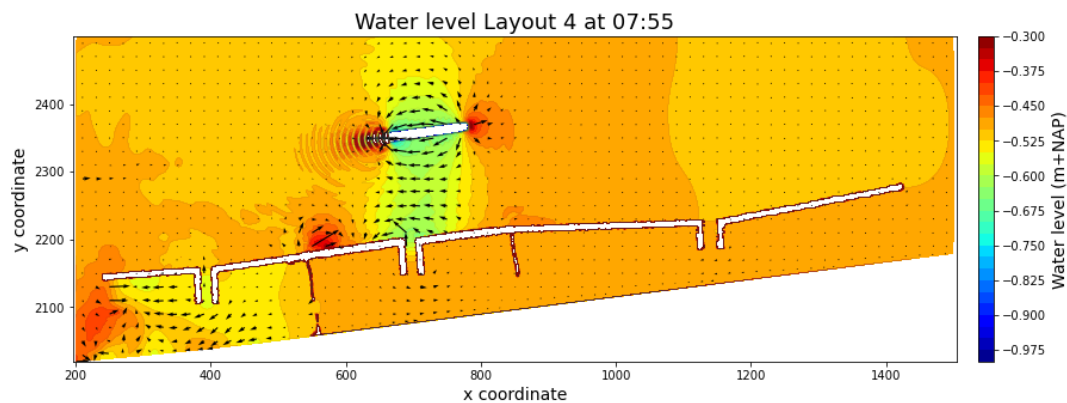


**Figure 5.5:** Water level around the groyne field at different moments in time while a vessel passes the groyne field considering layout 4. The colours represent the water level ranging from -1.8 to 0.0 meter +NAP. Initial (calm) Water level = -0.5 m. The black arrows show the flow direction at the corresponding points in time and indicate the magnitude. The vessel sails in the direction from left to right.

## 5.2. Alternative layout results

In Appendix D.4, all the water level and velocity magnitude signals are illustrated for locations 1 to 7 of the simulations of both Chapter 5 and Chapter 4. In this section, only the key takeaways for the different layouts are treated. By analysing variations between the different layouts, conclusions can be formulated for each element. The interesting elements that are considered are the number of openings in the groyne field, the kind of opening used and the emerged groynes compared to the submerged

ones. Additionally, the effect the layouts have on the oscillatory behaviour explained in Sections 2.4 and 4.2.1 is analysed.

### 5.2.1. General hydrodynamic behaviour

The analyses generally show that the alternative layouts cause less hydrodynamic activity in the groyne field. Figure 5.6 illustrates different vector plots at particular moments in time. It shows that in the basic situation, the water in the groyne field is more active. Additionally, this can be concluded by analysing the figures with water level and velocity signals in Appendix D.4. Here, the signals exemplify low amplitudes and low-velocity magnitudes compared to the basic simulation.

Figure 5.6 shows high dynamic activity in the west side of the groyne field in the basic simulation, which indicates the explanation for the difference in dynamic activity can be found somewhere in the geometry at the west side of the groyne field. The most obvious difference on the west side of the groyne field between the basic layout and the other layouts is the longitudinal dam in the neighbouring groyne field. This will be analysed more in the following sections.

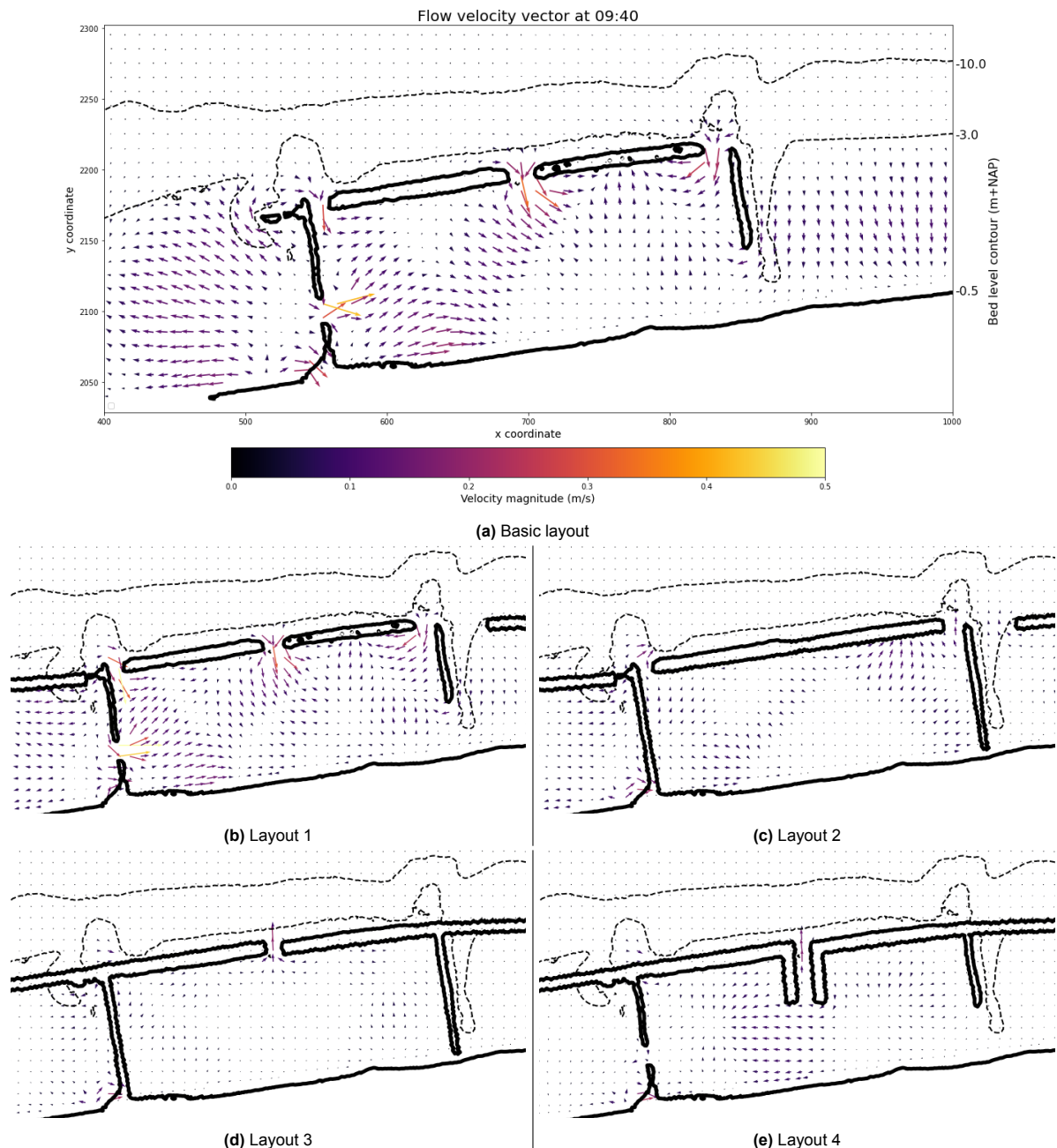


**Figure 5.6:** The water velocities of all the different layouts at the same point in time (09:40) after the vessels have passed the groyne field. The colours represent the velocity magnitude and the arrows show the flow direction. The black lines illustrate the bathymetry and layout in a simplified way.

### 5.2.2. Quantitative results

In order to quantify the water level and water velocity effects, tables containing information about the average and maximum water level amplitudes and velocities are created. The information for every location is located in Appendix D, but all the values from the different simulations at location 2 are shown in Table 5.1. All tables confirm the conclusions and observations done in this chapter concerning the differences between the layouts, for example, the high velocities at location 2 for the simulation with the original bed and the simulation of layout 4. The quantitative results in the tables show that the order of magnitude of velocity increases caused by vessel-induced waves is about 0.2 m/s for the vessel modelled in the models. The order of magnitude of the water level drawdown is different for the various layouts but is in the order of magnitude between 3 and 8 centimetres for the modelled vessel. This magnitude is similar for comparable vessels in the data analysis.

Layout	Mean amplitude (m)	Max amplitude (m)	Mean velocity (m/s)	Max velocity (m/s)
Basic simulation	0.011	0.058	0.046	0.187
Original bed	0.009	0.050	0.061	0.360
Layout 1	0.010	0.064	0.028	0.119
Layout 2	0.007	0.025	0.016	0.093
Layout 3	0.006	0.026	0.018	0.105
Layout 4	0.012	0.112	0.070	0.645

**Table 5.1:** Quantitative results from water level and velocity signals at location 2.

### 5.2.3. Effect of entrance configuration

Layouts 2 and 3 have similar geometries whereas the only difference is the connection to the waterway. The results, however, show limited differences in hydrodynamic activities. Only at location 7, the velocities are higher in the layout 2 simulation. This can be explained by the fact that location 7 is located in the northwest corner of the groyne field and layout 2 had an entrance in this corner while in layout 3 this entrance is closed off.

The effect of the elongated entrance is effectively conveyed in the signals from location 2. The velocity signals of all layouts, including layout 4, are depicted in Figure 5.7. It shows the velocity from the entrances at the second location is significantly higher in the fourth layout.

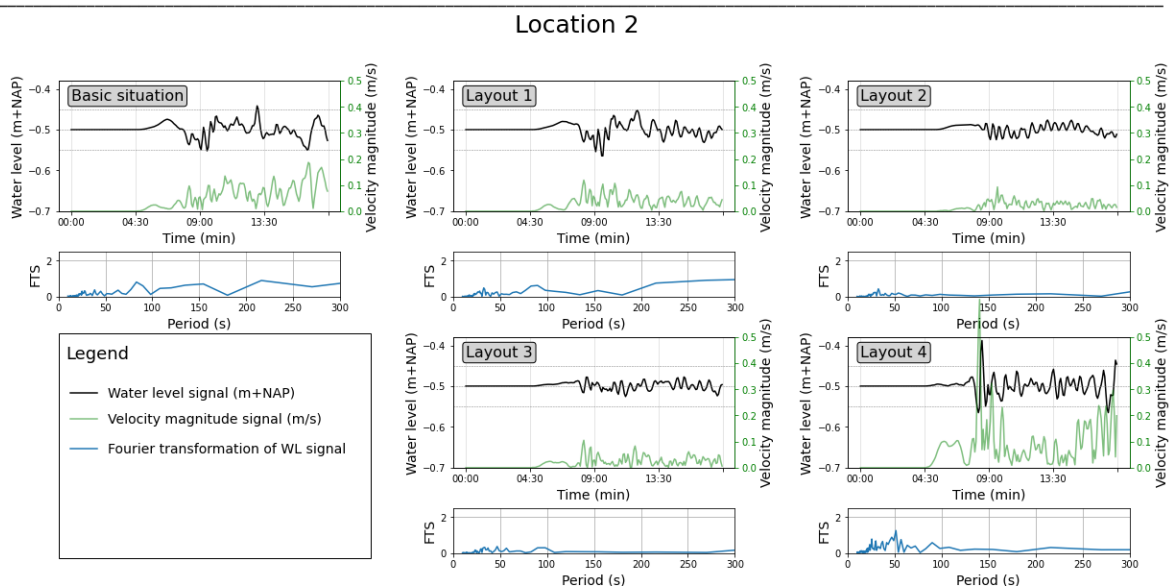


**Figure 5.7:** Signals of the different layouts at location 2. The exact location in the groyne field can be seen in Figure 4.1. The black line shows the water level signal, the green line shows the velocity magnitude and the blue line is a Fourier transformation on the black line.

### 5.2.4. Effect of emerged and submerged groynes

The results from the different simulations show that the groyne height has a significant impact on the hydrodynamic behaviour in the groyne field. The basic situation and the first layout have significantly higher amplitudes in the water level and velocity signals. The only exception is layout 4, which has submerged groynes but has moderate signal amplitudes. This can be described by the geometrical layout of the neighbouring groynes. In layout 4, the groyne fields each have a single connection to the channel. This reduces the water volume transport in and out the groyne fields which reduces the flow over and through the partially submerged groynes. Appendix D.4 is the best illustration for showing the difference between emerged and submerged groynes. While looking at Appendix D.4, it is important to remember that the basic situation and layout 1 contain submerged groynes and layout 2 and layout 3 contain emerged groynes.

### 5.2.5. Natural frequency

The second layout consists of emerged groynes and has two openings in the corners. This geometrical layout increases the validity of closed basin assumptions which are analysed in Chapter 4. To check if this layout will enhance natural oscillatory behaviour in the groyne field, a simulation is run with two vessels sailing 120 seconds behind each other. According to the resulting signals from the basic situation, this created oscillations with a period of around 150 seconds. Only locations 4 and 5 are checked because these visualised the most clear oscillations in the basic simulation. The resulting signals are illustrated in Figure 5.8.

The resulting signal from the second layout does not indicate a similar oscillatory behaviour. This is opposite to the proposed hypothesis as the layout was expected to create more suitable conditions for oscillatory movement. A theory is proposed to explain the absence of this oscillatory behaviour.

The animation of water level at different time steps in the simulation shows a lot of propagating waves rather than standing waves during the simulation. This could explain the highly frequent oscillations visible in the signal in Figure 5.8. It suggests that the water inside the groyne field does not have enough time to flow out of the groyne field. This creates water level drawdown only around the corner entrances that eventually propagate through the groyne field. A possible reason for the reduced outflow is the opening size, which is smaller in the second layout compared to the basic situation due to the emerged groyne. It shows that the oscillatory movement in the groyne field depends on the total entrance size and the ability of a large water volume to be transported through the groynes or longitudinal dams in a short period.

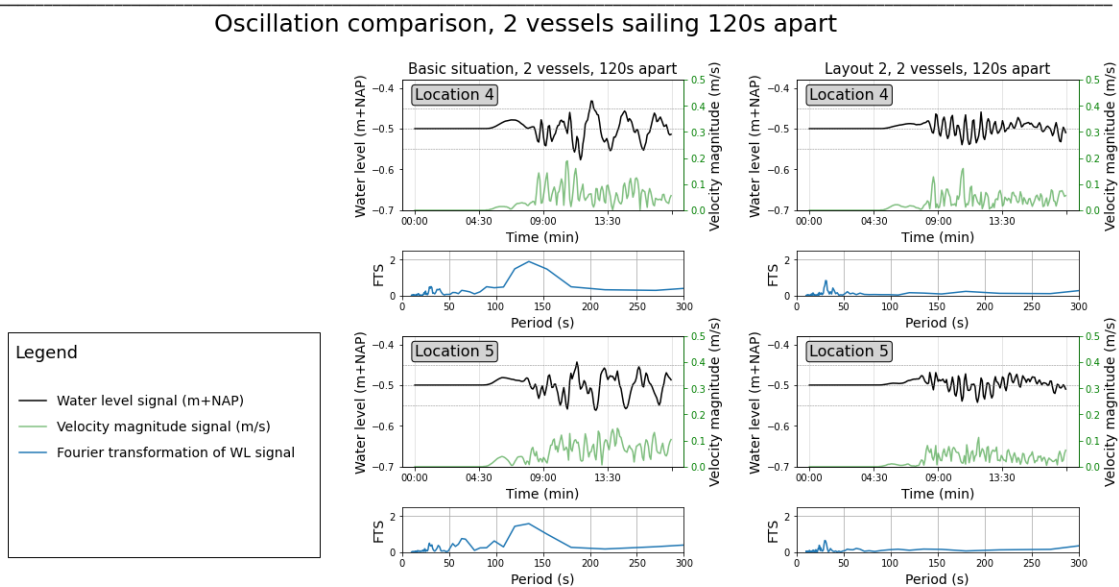


**Figure 5.8:** Signal comparison of two vessels sailing 120s behind each other between the basic situation and the second layout. The black line shows the water level signal, the green line shows the velocity magnitude and the blue line is a Fourier transformation on the black line.

## 5.3. Concluding remarks on the different layouts

To summarise the results from the different layout simulations, two main conclusions can be drawn. First, if the neighbouring groyne is relatively open by having a lot of entrances or no longitudinal dam at all, the groynes have a large impact on the hydrodynamic behaviour. A submerged groyne will result in more dynamics than an emerged groyne. This effect is much less if the neighbouring groyne has a relatively closed layout as well.

Secondly, it can be concluded that the number of openings and location of the openings in the longitudinal dam is of much less importance than the total size of the openings combined. A smaller opening will cause more propagating waves in the groyne field, while a larger opening surface will cause much larger, almost standing waves in the area. Next to this, by choosing an elongated opening, it becomes possible to choose locations where velocities will be higher and locations where velocities will be smaller.



# 6

## Discussion

The outcomes of this study have provided insight into the working principles of the primary vessel-induced waves. As one of the first studies, it combines the modelling of vessel-induced waves with the hydrodynamic effect on the river banks. The research contains two main parts. This chapter provides a reflection on both the data analysis and the numerical model.

### 6.1. Data analysis

In line with other studies on vessel drawdown, results from the data analysis indicate clear correlations between vessel dimensions, sailing velocities and water level drawdown. The analysis is done with a single large dataset, which means that flaws in the data could end up in the results, as explained in Chapter 2. However, most flaws are filtered out, resulting in a reliable data set containing 2685 input vessels. The large number of vessels in the data stabilises the results when adding a small amount of vessel data. Therefore, nothing indicates flaws in the data impact the results significantly.

Reliable data is used to create an empirical formula to describe the water level drawdown with the most important vessel characteristics. The formula is created in a similar way as done in the study of Almström and Larson (2020). Sensitivity analysis indicates that the severity of the water level drawdown can be described relatively well in other locations with the created empirical formula. Additionally, it shows that the differences can be explained by location-dependent properties. These findings make this study a good starting point for additional research. The comparison between these studies could be extended to various locations to be able to describe primary wave effects more effectively.

### 6.2. Numerical model

The numerical simulations indicate the fact that groyne field bathymetry and layout influence the hydrodynamics significantly. Despite making necessary assumptions in the model setup, the simulations represent reality as realistic as possible to gain as much knowledge about the hydrodynamic behaviour as possible. This study and the model can be used for hydrodynamic studies in busy waterways and can be used as literature for morphodynamic studies in the 'Nieuwe Waterweg'. In this study, the influence of assumptions is mostly limited, but before concluding, it is important to reflect on different elements of the numerical model. For clarity, different elements are discussed separately in this section.

#### 3D effects: Salinity and scour holes

The numerical calculations conducted in this research are based on the depth-averaged velocity assumption, which means that 3D effects are ignored. Groyne Field 9 has a complex bathymetry causing a lot of turbulent flow. This raises the question of whether or not including 3D effects would change the results of this research.

Salinity is one of the main natural effects that can not be considered using only 2D modelling. In the 'Nieuwe Waterweg', a salt wedge flows into the river mouth creating a water column with high salinity water near the riverbed and more fresh water at the top. In this situation, the velocity vectors can vary a significant amount within the water column, which is impossible for the current 2D model to comprehend. If 3D effects were used in the model, the computations would become much more expensive

for a relatively large domain used in this research. However, this study mainly focuses on the hydrodynamics inside the groyne field and a salt wedge would affect this location less, because fresh and saltwater is more mixed and homogeneous compared to the water columns in the deep channel. Additionally, the bathymetry of Groyne Field 9 contains deep scour holes near the openings in the longitudinal dams and the submerged parts of the groynes. The shape and steepness of these holes indicate that 3D effects occur inside the scour holes which may affect local hydrodynamic conditions. This research studies numerical simulations containing a simplified flat bed and therefore, the results are not affected significantly by scour holes. However, the results of the simulation conducted with the original bathymetry show a reduction of flow velocity at the scour holes. This can be explained by the depth-averaged velocity assumption and indicates an influence of this effect. In this case, the most important feature that is still unclear is the hydrodynamic behaviour inside the scour hole. This would become important when studying morphodynamics. The research conducted in this thesis mainly focuses on the larger-scale hydrodynamic behaviour in the groyne field. Therefore, the effects of 3D effects on the conclusions are limited.

### Tidal effects

A tidal period is multiple orders of magnitude larger compared to the period of a primary vessel wave. Combining these signals in a single simulation would make finding causalities in the results difficult. Additionally, it would make the model unnecessarily expensive. Therefore, the influence of tidal forcing on the hydrodynamics of Groyne Field 9 is studied separately. This simulation shows that the groyne height mainly guides the hydrodynamic behaviour inside the groyne field.

The decision has been made to primarily concentrate on the vessel waves during low water conditions because visual observations learned that this is the time the hydrodynamic activity is higher compared to high water conditions. Measurements show a similar drawdown during high and low tides, therefore the relative effect in water level reduction is higher during low tides. During the time it takes for the primary vessel wave to develop, travel and damp out, the water level has not risen significantly to affect the results significantly.

### Vessel design assumptions

The data analysis results in key findings on the effect of different vessel characteristics on the primary vessel wave. The purpose of the numerical model is to research the effect primary vessel waves have on Groyne Field 9. The decision is made to use one vessel configuration for all simulations to cancel out the effects of different vessel characteristics. In reality, as well as in the analysed data, the vessel characteristics are different for every individual vessel. The chosen simulated vessel represents an above-average-sized vessel sailing relatively fast to be able to obtain clear results. By uniforming the input parameters, the effects from different vessel sizes are not considered, which is less realistic. However, if all kinds of different vessel configurations are used, the causality between different characteristics and different results could not become clear. Therefore, the necessary assumption to uniform the vessel configuration increases the quality of the model for the desired purpose.

### Boundary conditions

Boundaries of the numerical domain are modelled in a sufficient and realistic way, as already explained in Chapter 3. However, closed boundaries like the river banks need some additional reflection. In reality, these boundaries contain open rock revetments to add friction and dampen waves. The bathymetry input does not take this into account and therefore the friction is modelled equal to the friction at every other surface. In theory, if the numerical model contained this extra friction at the boundaries, smaller secondary waves would be affected most by it. Despite this assumption, this study focuses on larger primary waves. The different friction at the boundaries would influence these longer waves much less. Therefore, adding friction to just the boundary areas of the dams and groynes would probably not affect the results significantly.

### Morphodynamic effects

The research has not been extended to the level where sediment is included in the analysis. Sediment is an important factor in natural development because stable sediment can serve as a place for plants to take root and for birds to feed themselves by the benthos on semi-dry flats. At the same time, unstable sediment could cause erosion which creates habitats for specific fish species. In December 2022,

sediment was nourished in the groyne field. During a visual fieldwork campaign in September 2023, researchers visually observed that the deposited sediment had transported slightly to the west of the groyne field, indicating sediment transport. During various fieldwork campaigns during a low water level, small ripples in the bed have been observed. On one occasion, sediment suspension and instability were observed in the groyne field at the time a vessel sailed by it. These observations prove qualitatively that the bathymetry changes, but to make conclusions, quantitative research is recommended. During this study, sediment samples have been collected from the groyne field bed and sieved to get an overview of the sediment composition. The sieve curves are not analysed in detail for this study and have been added to Appendix F, but on average, the 50-percentile grain size in the groyne field is 0.23 mm. The stability of sediment in the groyne field needs to be checked in future research but can roughly be estimated using the Shields theory for the initiation of motion of a sediment bed. Whether sediment is (un)stable depends more or less on the sediment size, the flow velocities near the bed and the turbulence of the water. A simple calculation to check stability:

$$d_c > \frac{u^2}{\psi_c \Delta C^2} \quad (6.1)$$

With:

$$C = 18 \log \frac{12h}{2d} \quad (6.2)$$

Assuming  $\psi_c = 0.035$  for significant sediment transport,  $h = 1.5$  m depth,  $d = d_{50} = 0.23$  mm grain size,  $\Delta = 1.6$  and  $u = 0.3$  m/s, the critical diameter of the sediment becomes 0.24 mm. This diameter is almost equal to the average  $d_{50}$  of the sample taken from the groyne field and this result indicates that for this velocity, unstable sediment would be a realistic phenomenon inside the groyne field. The Shields formula assumes laminar flow, but in the complex shallow water of the groyne field, turbulent flow occurs regularly. Secondary waves create even higher turbulent conditions, which in general, result in more unstable conditions for the sediment.

If vessel-induced velocities mobilise sediment, it is unclear if it is transported out of the groyne field or if the sediment flows back and forth along the wave cycle. In this situation, the change in bed level may be moderate, while the disturbance of the top is significant. This influences the conditions for benthos and vegetation growth. Next to this, smaller-scale morphodynamic effects, like ripple or dune forming, could have an effect on the bed friction, possibly resulting in a change in hydrodynamic behaviour.

### 6.3. Ecological considerations

The conducted research shows that primary vessel wave impact significantly impacts the hydrodynamic behaviour in the semi-closed groyne field. The sediment stability calculation shows that Groyne Field 9 is morphologically dynamic. The numerical study shows that by changing the layout of groynes and dams, the hydrodynamic behaviour can be changed significantly. Before conclusions can be drawn on what is the 'best' layout or solution, there need to be various additional discussions about different perspectives.

If a calm hydrodynamic environment is preferred, this study proposes effective solutions by emerging the groynes above the water level and limiting the total size of the entrances of the groyne field. Depending on the preferred level of dynamics in the groyne field, the layout can be changed. The resulting consequences on ecology are neglected in this study. However, the model can be used as a tool for ecologists to decide what could be the best solution from their perspective. Moreover, the effects on other elements must be taken into consideration. For example, various stakeholders prefer that the shipping performance in the channel is not affected by changes in the groyne field. If the water flow through the groyne field is obstructed, it is possible that the flow velocities in the main channel are affected as well. Additionally, this could influence the flood protection. Another possible limiting factor could be sediment transport back into the sailing channel. These possible elements need to be considered next to the ecological objectives before decisions are made.

# 7

## Conclusions

The report's main objective is: *How can primary vessel waves impact the hydrodynamics in the semi-closed Groyne Field 9 in the 'Nieuwe Waterweg' and how can the hydrodynamic conditions be modified with different structural layout designs?* To answer this question, the research mainly consists of two analyses. Measurement data has been analysed by combining Acoustic Doppler Velocimeter (ADV) data with Automatic Identification System (AIS) data to find correlations between water level drawdown and vessel parameters. Next to this, a numerical model has been developed to be able to control parameters and simplify the situation which helps to understand and explain the hydrodynamic effects considering a semi-closed groyne field. To be able to separate the study into different elements, the main question has been split into four sub-questions that all relate to a specific aspect of the research.

1. *What parameters are important for creating the primary vessel waves that impact semi-closed groyne fields, based on measurement data?*
2. *How can primary vessel waves be modelled numerically in a clear but realistic manner?*
3. *How does the hydrodynamic system behave in a semi-closed groyne field?*
4. *What geometrical adaptations can be done to manage the hydrodynamic system in a semi-closed groyne field?*

Measurement (ADV) data has been compared to the vessel data (AIS) from vessels sailing the 'Nieuwe Waterweg'. This research demonstrates that wavelet analysis is an efficient tool to distinguish vessel waves from other types of waves, which eventually results in the causality between vessel characteristics and resulting hydrodynamic effects, like water level drawdown. A thorough analysis of this data confirms the importance of the vessel's sailing velocity and dimensions. It shows that a water level drawdown caused by a vessel passage of fifteen centimetres is no exception. Empirical regression analysis shows how these parameters are correlated. Existing literature confirms the result that the vessel's sailing velocity parameter is dominant with respect to its dimensions. The empirical analysis generates a function to describe the water level drawdown that is sufficient to use in other locations as well. The empirical formulas created in this study and in the study by Almström and Larson (2020) predict the water level drawdown in the 'Nieuwe Waterweg' with a Mean Average Error (MAE) of respectively 0.024 and 0.027 meters. Differences in the empirical functions can be explained by the difference in location characteristics, data set and bathymetry around the measurement instrument.

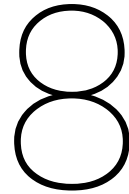
The numerical model developed in this research is one of the first models able to simulate the effects of a primary vessel wave on its environment by using the atmospheric pressure method. Using a local atmospheric pressure increase turns out to be an effective way to model a moving vessel in a water body. Additionally, the model contains advantages for future research such as easy vessel shape and characteristic variation possibilities. At the same time, the study domain is modelled in such a way, that various bathymetry layouts can be implemented. The flexible options for the vessel input as well as the bathymetrical layout input create a model that can be used in the future to run a large amount of additional scenarios.

A semi-closed groyne field with a flat bed is modelled in order to create a basic simplified simulation and to check the effect of the groynes and longitudinal dam on the hydrodynamic forces. It is compared to a simulation with the current complex bathymetry. From these simulations and measurements, we now know that the order of magnitude of flow increase caused by vessel-induced waves is about 0.2 m/s and we know that these magnitudes are most likely to occur near the entrances of the groyne field and near the groynes. In general, the complex bathymetry causes more friction and therefore damping of waves. On the other hand, locally, the velocities can be higher compared to a simple situation, because flow lines contract to flow around an island for example.

The analysis of primary waves in Groyne Field 9 with simple bathymetry shows that a standing wave can occur in the simplified groyne field with a period of around 150 seconds. In this situation, the groyne field can be assumed to be a closed basin where the water oscillates in the first natural frequency mode. To verify this conclusion, a layout with an adapted geometry is simulated. This layout is designed to make the closed-basin assumptions more accurate. However, this simulation has a contradictory outcome because no oscillations or standing waves are observed. The animation of this simulation shows waves travelling through the groyne field indicating that the opening is large enough for water to flow out during the time the vessel passes. It demonstrates that, to have a standing oscillating wave, the conditions on bathymetry, boundaries and opening sizes must be balanced.

In addition to understanding the system, the numerical model is used to check the effects different layout designs have on the hydrodynamic activity in the groyne field. The considered designs have different geometrical elements, for example, emerged or submerged groynes, one or two openings and in one particular layout, the entrance is elongated. One of the conclusions is that emerged groynes create much calmer dynamics in the groyne field. Typical velocity magnitudes for layouts with emerged groynes are, with local exceptions, around 50% lower than those with partly submerged groynes. In general, the number or location of the groyne field entrances does not give significant variation in the hydrodynamic properties between the layouts. However, the total size of all openings combined has a clear effect because if more water is able to flow in and out of the groyne field, the overall hydrodynamics will change. This also relates to whether or not the system is able to behave similarly to a closed basin system mentioned in the section above. The elongated entrance in the longitudinal dam results in a longer distance where the velocities are higher. Location 2 in the analysis in Chapter 5 represents a location in the middle of the groyne field, closer to the river bank. At this location, the effect of the elongated entrance is an increase in flow velocity of 350%.

It shows that different layouts concerning different geometrical elements have an influence on the hydrodynamics in the groyne field area. To apply this to other locations, a separate analysis needs to be done because local small-scale elements can influence the results significantly. Additional relevant questions could be answered by additional research which is discussed in Chapter 8.



# Recommendations

The discussion points considered in Chapter 6 induce questions for further research on primary vessel waves and their effect on semi-closed groyne fields. General applications that this study could contribute to and general recommendations are discussed in the first section of this chapter. The second section of this chapter focuses on the natural development considerations based on this study are discussed. Lastly, recommendations for further research are discussed.

## 8.1. General applications and recommendations

The research question of this thesis was composed to understand the vessel wave impact on a semi-closed groyne field. The results and conclusions can be applied in various research fields. In the research field of vessel wave impact, this thesis could serve as a reference project to analyse vessel waves from large data sets together with numerical models.

The other focus area of this thesis is the hydrodynamic behaviour of semi-closed groyne fields. The research concludes the most important factors that impact the behaviour in the groyne field. Therefore, projects with a river bank development objective can use this thesis as reference information. More specifically, a natural development at a river bank or in a groyne field is the perfect project that relates to this research topic, because, in this situation, vessel impact is relevant. The hydrodynamic model can develop by adding morphodynamics which is crucial for the research to natural development in the area.

The conducted research solely focuses on the hydrodynamic effects, which can be used as starting points for additional research on morphology and ecology. Next to these elements that influence the objectives of the projects 'Proeftuin Sediment Rijmond' and the 'Groene Poort', several different elements are relevant as well. Deciding on emerged or submerged groynes influences the general hydrodynamic behaviour in the area. However, higher groynes obstruct general flow in the waterway. A question that needs to be asked is whether or not flood risk increases with such measures. Maybe, the general tide-induced flow velocities in the main channel are higher due to the obstruction of part of the channel. In this study, groynes and dams with a stone topping are considered. If natural development is the objective, alternative solutions could be considered. For example, more natural groynes or open structured sewage pipes. In the same domain, concrete 'Reefy' blocks are tested as a habitat for coral and other sea life.

In theory, the research could be extended to other locations in the Rhine-Meuse estuary, but in most locations, the vessel intensity and tidal influence would not be as high as at the Groyne Field 9 location. Sediment nourishment in the groyne fields is something that needs to be monitored closely. After the nourishment works conducted in December 2022, the bathymetry has been monitored only once. If this is monitored more often, it can provide insight into whether sediment is flowing in the channel or not. This can better help indicate if disposing sediment in the system is more efficient compared to transporting the sediment to open sea.

## 8.2. Natural development

The motivations for conducting this research were the pilot projects 'Proeftuin Sediment Rijnmond' and the 'Groene Poort'. These projects aim for sediment management and natural development in the Rhine estuary and the 'Nieuwe Waterweg'. Parallel to this research, more fieldwork campaigns have been conducted. One of them is taking sediment samples to check the development of sediment content over time. Eventually, this will give an insight into how the sediment in the groyne field behaves in the long term. For example, in December 2022, sediment was deposited on the east side of the groyne field. In September 2023, during fieldwork in the location, it seemed like the sediment had relocated more in a westerly direction. This needs to be confirmed by regular measurements of the bed level.

For natural development, the quality of the sediment is a factor that needs to be considered. If it has the preferred composition for particular benthos.

A second fieldwork campaign conducted parallel to this research is the monitoring of how the fish population develops. Experts, like ecologists, need to study what conditions are preferable for the envisioned species. If the connection between the abiotic hydro- and morphodynamics and biotic effect is clear, the groyne fields can be developed into the desired situation. This thesis shows that different groyne field layouts can result in different hydrodynamic conditions.

For fish, deeper conditions are preferred, which means that the openings should create sufficient flow velocities to erode the bed. Creating deeper conditions can be enhanced by elongating the entrances, which is shown in the analysis of layout 4.

Future research needs to focus on the design of all the neighbouring groyne fields. Hypothetically, dedicate one groyne field as a fish resting place by creating conditions that develop a low bed level and then dedicate the next groyne field to green natural development by creating a calm environment and nourishing dredged sediment until conditions are ideal for particular vegetation.

Natural development is difficult to predict and it sometimes costs more time than expected. This should always be considered when natural development is the objective, but uncertainty can be limited by consulting ecology and biology experts.

## 8.3. Additional research

Considering the data analysis, it could be interesting to do the same measurements and analysis at other locations and see what the differences are. The AIS data and ADV data need to be processed in the same way, so that filtering certain vessels does not influence the results. Additionally, a measurement instrument needs to be located inside the waterway to avoid obstructions like dams or groynes from influencing the results.

Other field measurements that could measure flow patterns in the groyne field are drone videos or Acoustic Doppler Current Profiler (ADCP) measurements. ADCP measurements give an image of the flow patterns in the entire water column. Kouwenhoven (2023) conducted ADCP measurements, but these results were unreliable because of low velocities and depths during the campaign. Correct ADCP measurements could help validate the numerical model of (short-term) vessel wave effects.

The study in this thesis proves the causality between different vessel parameters in Chapter 2 and it shows that additional effects play a role. To investigate these different properties in more detail, laboratory research combined with a numerical model is a possibility. In this way, the model can run with different vessel parameters and hull shapes. In a scale model study, scale effects must be accounted for, which can be validated using field measurements. Following this, the validated scale model can be used to accurately validate a numerical model more .

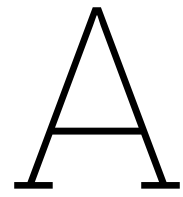
Considering the semi-closed groyne fields, as already mentioned, further research should focus on the sediment behaviour in a detailed way. Not just by applying Shield calculations on the flow velocities obtained by the model, but by considering other properties and scenarios. If the sediment becomes unstable, is it then transported or does it just flow back and forth? Are the high velocities the driving force for sediment to become unstable, or is it the amount of local turbulence in the groyne field? These questions can be asked with the inclusion of tidal flow as well. A scenario to investigate could be the hypothesis that sediment is mobilised by the vessel waves and transported by tidal flow. Or if averaged over a tidal cycle, what will be the remaining net transport of the sediment in and outside the groyne field? To summarise, the ideal research includes morphodynamic effects as well as hydrodynamic effects and includes tidal forcing together with river discharge.

# References

- Almström, B., & Larson, M. (2020). Measurements and analysis of primary ship waves in the Stockholm archipelago, Sweden. *Journal of Marine Science and Engineering*, 8(10), 743. <https://doi.org/10.3390/jmse8100743>
- Brouwers, S. (2022). *The effect of vessels on the flow pattern inside a groyne field* (Master's thesis). Delft University of Technology. Delft, The Netherlands.
- Chavarrias, V., Sloff, K., & Mosselman, E. (2020). *Final evaluation longitudinal training walls wp10: Morphology, operation and maintenance draft* (Technical Report 11204644012ZWS0001). Deltares, Delft.
- Collas, F., Flores, N., van Aalderen, R., Bosman, F., Schoor, M., Verbrugge, L., Romeijn, W., Van Kessel, N., Achterkamp, B., Liefveld, W., Buijse, A., & Leuven, R. (2020). *Rapportage natuurgegevens langsdammen waal 2016 - 2020* (Report). Radboud Universiteit, Rijkswaterstaat, Sportvisserij Nederland, Hengelsport Federatie Midden Nederland, Deltares, Bureau Waardenburg, Universiteit Twente.
- Collas, F., Buijse, A. D., Van Den Heuvel, L. P., Van Kessel, N., Schoor, M. M., Eerden, H., & Leuven, R. S. E. W. (2018). Longitudinal training dams mitigate effects of shipping on environmental conditions and fish density in the littoral zones of the River Rhine. *Science of The Total Environment*, 619-620, 1183–1193. <https://doi.org/10.1016/j.scitotenv.2017.10.299>
- Deltares. (2018). *Delft3dflow user manual version 3.15: Simulation of multidimensional hydrodynamic flows and transport phenomena including sediments*. Deltares.
- Deltares. (2022). *Delft3dflow user manual version 2022.02: Computational cores and user interface*. Deltares.
- Dempwolff, L.-C., Melling, G., Windt, C., Lojek, O., Martin, T., Holzwarth, I., Bihs, H., & Goseberg, N. (2022). Loads and effects of ship-generated, drawdown waves in confined waterways - a review of current knowledge and methods. *Journal of Coastal and Hydraulic Structures*, 2. <https://doi.org/10.48438/jchs.2022.0013>
- Engineering, B. -. F. W., & of Germany, R. I. (2010). *Principles for the design of bank and bottom protection for inland waterways (gbb): Code of practice* (tech. rep.). Federal Waterways Engineering and Research Institute of Germany. Karlsruhe, Germany. [https://izw.baw.de/publikationen/merkblaetter/0/BAWCodeofPractice\\_Principles\\_Bank\\_Bottom\\_Protection\\_Inland\\_Waterways\\_GBB\\_2010.pdf](https://izw.baw.de/publikationen/merkblaetter/0/BAWCodeofPractice_Principles_Bank_Bottom_Protection_Inland_Waterways_GBB_2010.pdf)
- Hiddema, P., W., Z., van Leeuwen, J., & van Zonneveld, G. (2013). *Groene poort waterweg* (Ontwerpbeschrijving). Rijkswaterstaat, Port of Rotterdam, Gemeente Rotterdam, and Wereldnatuurfonds.
- Hiddema, P., Zwakhals, W., Van Leeuwen, J., & Van Zonneveld, G. (2013). *Groene poort waterweg van grijs naar groen: Ontwerpbeschrijving* (Technical report). Rijkswaterstaat.
- Juez, C., & Navas-Montilla, A. (2022). Numerical characterization of seiche waves energy potential in river bank lateral embayments. *Renewable Energy*, 186, 143–156. <https://doi.org/10.1016/j.renene.2021.12.125>
- Kouwenhoven, T. (2023). *The effect of modifications to a groyne area in the nieuwe waterweg* (Master's thesis). Delft University of Technology. Delft, The Netherlands.
- Meile, T., Boillat, J.-L., & Schleiss, A. (2011). Water-surface oscillations in channels with axi-symmetric cavities. *Journal of Hydraulic Research*, 49(1), 73–81. <https://doi.org/10.1080/00221686.2010.534671>
- of Rotterdam, P. (2019). *Verdieping nieuwe waterweg*. <https://www.portofrotterdam.com/nl/bouwen-aan-de-haven/lopende-projecten/verdieping-nieuwe-waterweg>
- of Rotterdam, P. (2022). *Room for nature in the port of rotterdam* (Vision report). Port of Rotterdam. Rotterdam, Netherlands.
- Parlement, E., & council, E. (2000). *Richtlijn 2000/60/eg van het europees parlement en de raad*. Retrieved 2023, from <https://www.rivm.nl/sites/default/files/2018-11/KaderrichtlijnWater.pdf>



- Samaras, A. G., & Karambas, T. V. (2021). Numerical simulation of ship-borne waves using a 2DH post-Boussinesq model. *Applied Mathematical Modelling*, 89, 1547–1556. <https://doi.org/10.1016/j.apm.2020.08.034>
- Schiereck, G. J. (1993). *Introduction to bed bank and shore protection*. A.A. Balkema Publishers.
- Simons, J., Bakker, C., & Sorber, A. (2000). *Evaluatie nevengeulen opijnen en beneden-leeuwen 1993-1998* (Report No. 2000.040). RIZA. Lelystad.
- Sloff, K., Sligte, R. V. D., Huisman, Y., & Fuhrhop, H. (2012). *Morphological model of the rhine-meuse delta* (tech. rep. No. 1205961001). Deltares. Delft.
- Soomere, T. (2007). Nonlinear components of ship wake waves. *Applied Mechanics Reviews*, 60(3), 120–138. <https://doi.org/10.1115/1.2730847>
- Stelling, G. S. (1984). *On the construction of computational methods for shallow water flow problems* (Doctoral dissertation). Rijkswaterstaat. <http://resolver.tudelft.nl/uuid:d3b818cb-9f91-4369-a03e-d90c8c175a96>
- Talebi, S. (2020). *Time series, signals, and the fourier transform*. Retrieved June 12, 2023, from <https://towardsdatascience.com/time-series-signals-the-fourier-transform-f68e8a97c1c2>
- Ten Brinke, W. (2003). *De sedimenthuishouding van kribvakken langs de Waal: Resultaten van de monitoring in 2002* (tech. rep.). Rijkswaterstaat, Dienst Weg- en Waterbouwkunde. The Netherlands.
- van Infrastructuur en Milieu, M. (2015). *Stroomgebiedbeheerplan rijn 2016-2021* (Government report). <https://www.helpdeskwater.nl/onderwerpen/wetgevingbeleid/kaderrichtlijnwater/20162021/>
- Yossef, M. (2005). *Morphodynamics of rivers with groynes* (PhD thesis). Delft University of Technology.



# Study area

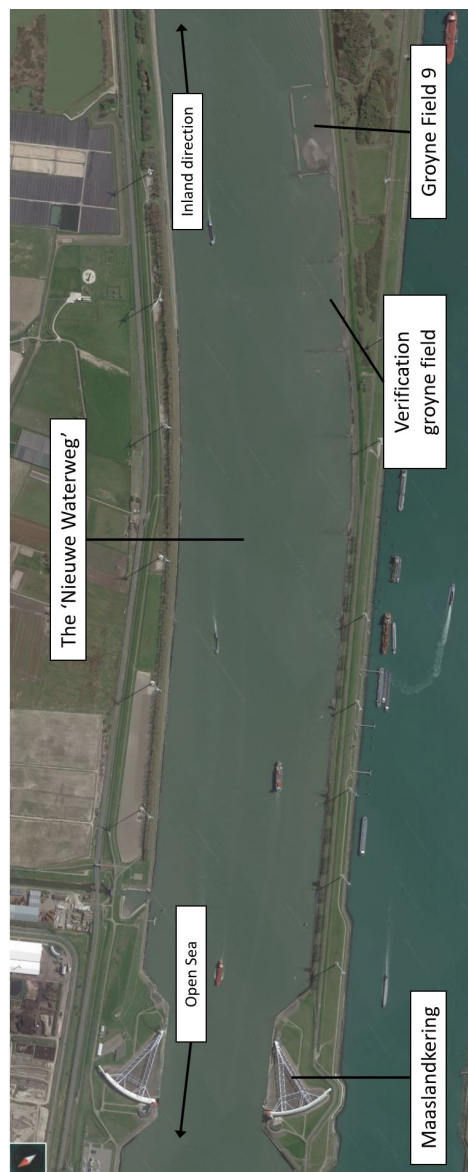


**Figure A.1:** A satellite image of the different elements around Groyne Field 9.

# B

## Data analysis appendix

### B.1. Wavelet signals

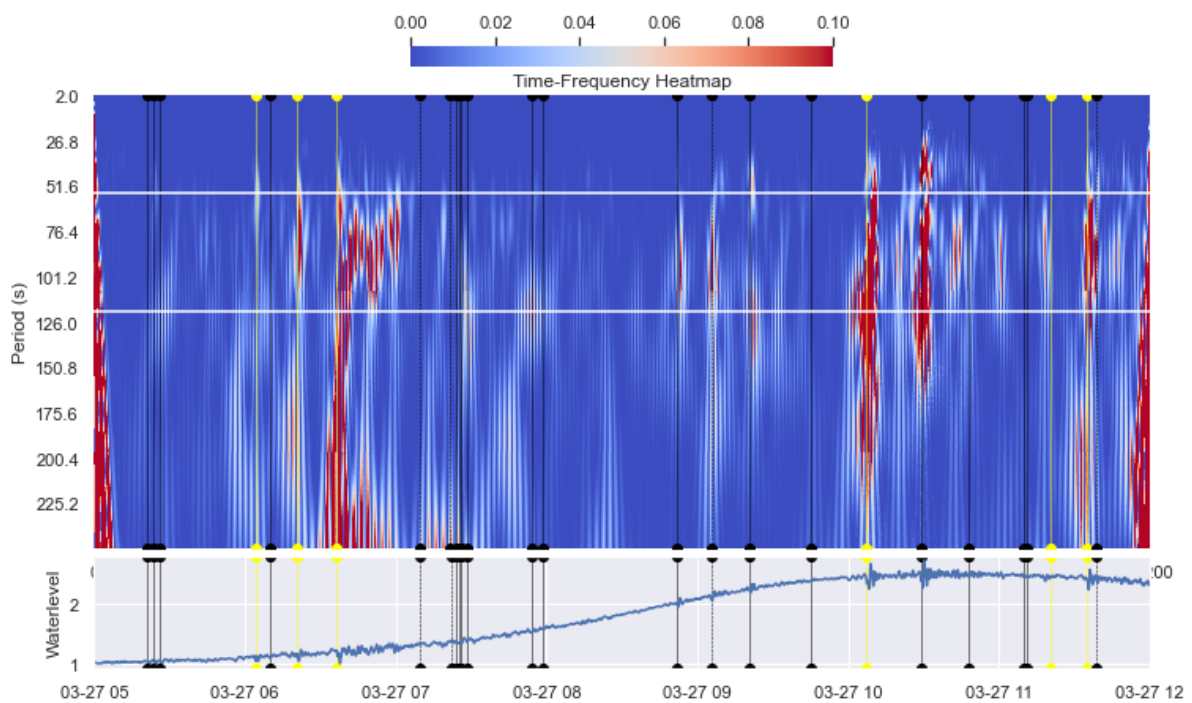


**Figure B.1:** Frequency to time heat map of the pressure signal from ADV3 created by wavelet analysis. The y-axis is transposed to wave period instead of frequency. Red spots correspond to the presence of the corresponding wave period in the water level signal at this location in the signal. Yellow lines represent vessels longer than 170 meter.

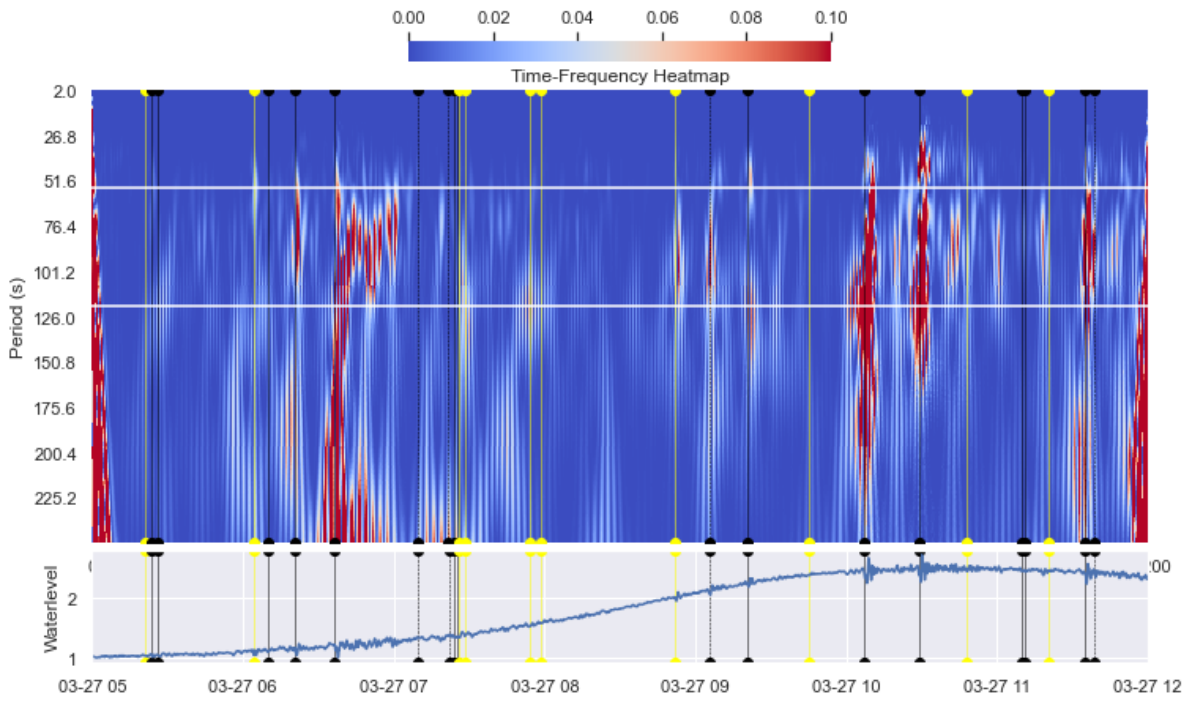


**Figure B.2:** Frequency to time heat map of the pressure signal from ADV3 created by wavelet analysis. The y-axis is transposed to wave period instead of frequency. Red spots correspond to the presence of the corresponding wave period in the water level signal at this location in the signal. Yellow lines represent vessels further away than 0.15 km

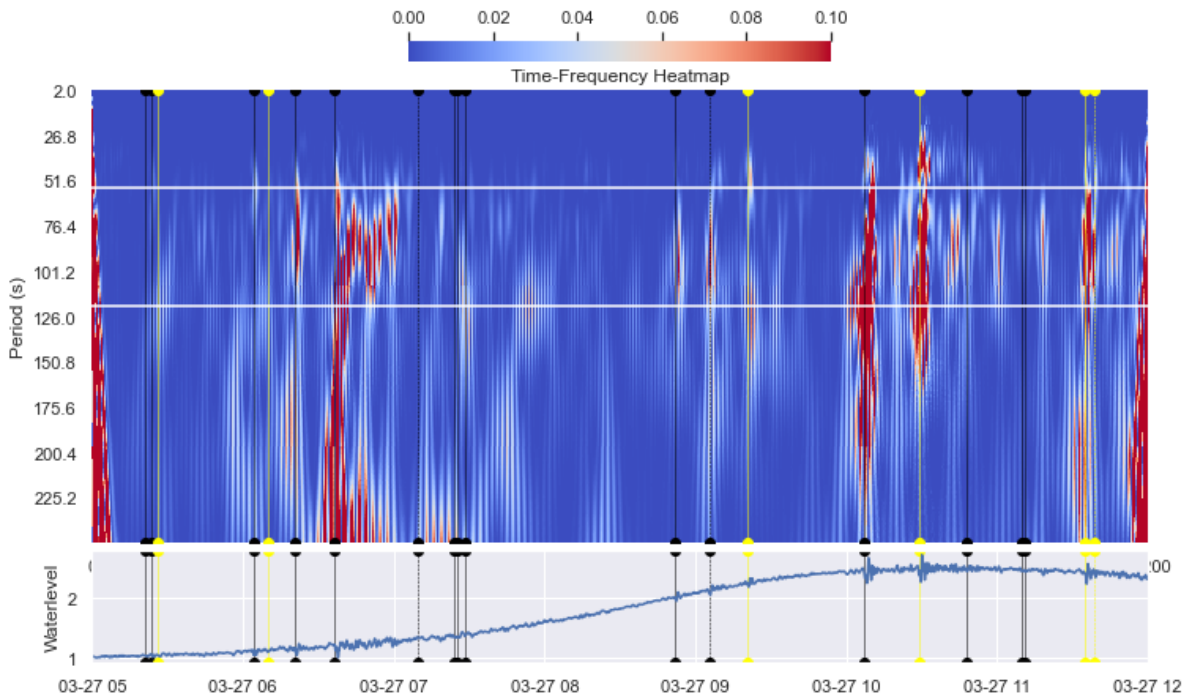


**Figure B.3:** Frequency to time heat map of the pressure signal from ADV3 created by wavelet analysis. The y-axis is transposed to wave period instead of frequency. Red spots correspond to the presence of the corresponding wave period in the water level signal at this location in the signal. Yellow lines represent vessels with a higher draught than 7 meters. (Some vessels lack this information)

## B.2. Verification selection data

This appendix shows all the signals of Selection 1.

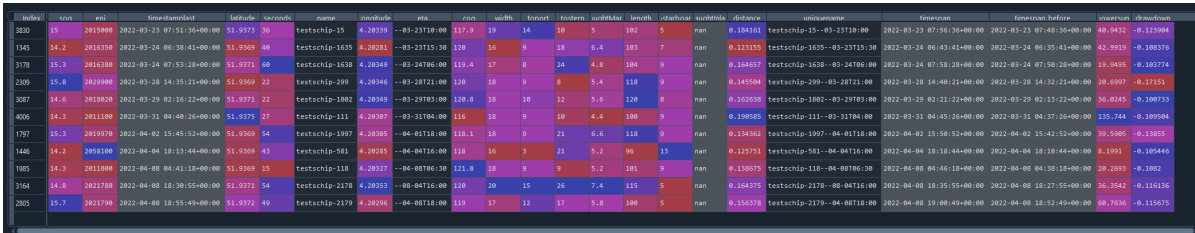


Figure B.4: Overview table of all the vessels used in the verification process

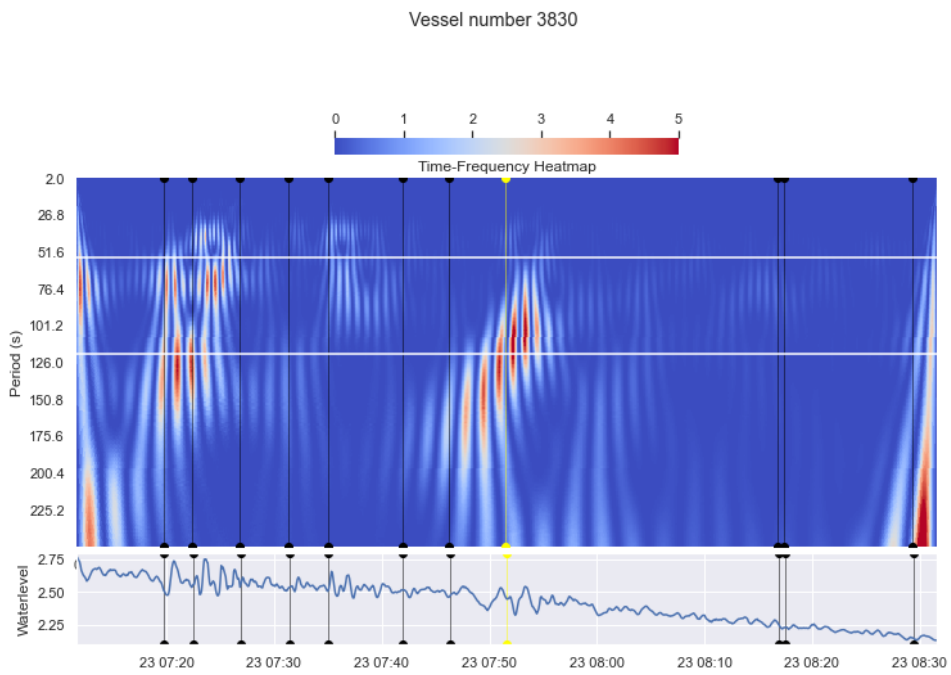
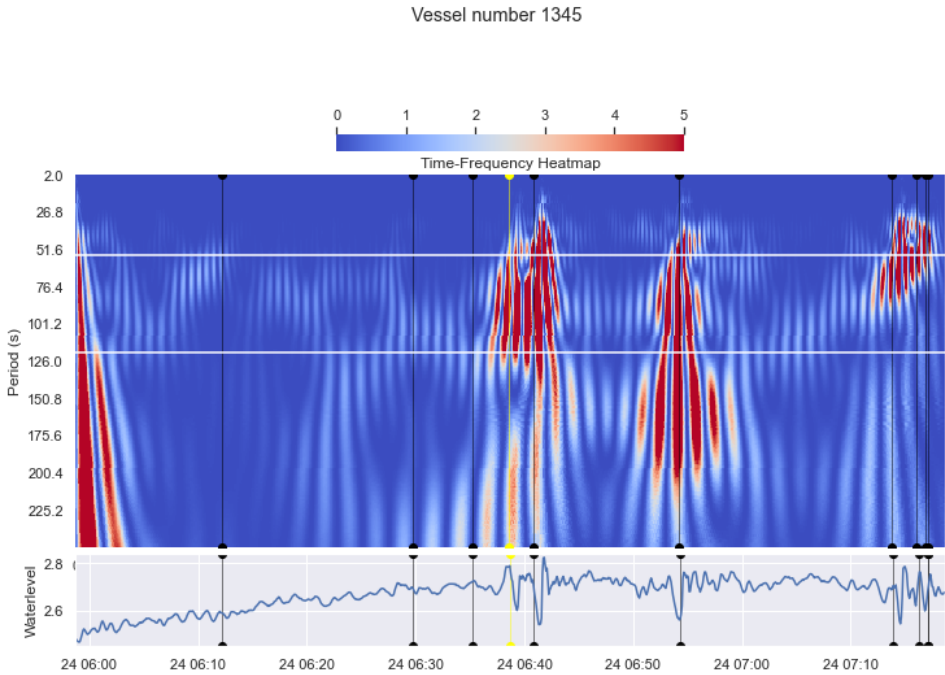
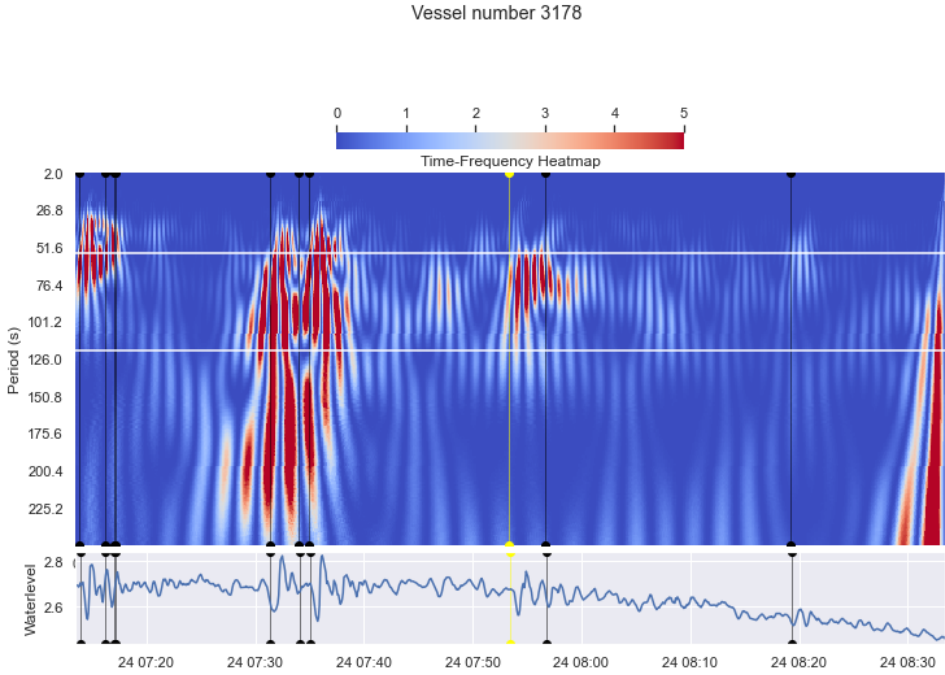


Figure B.5: Signal and wavelet signal for vessel 3830. Frequency to time heat map of the pressure signal from ADV3 created by wavelet analysis. The y-axis is transposed to wave period instead of frequency. Red spots correspond to the presence of the corresponding wave period in the water level signal at this location in the signal.



**Figure B.6:** Signal and wavelet signal vessel 1345. Frequency to time heat map of the pressure signal from ADV3 created by wavelet analysis. The y-axis is transposed to wave period instead of frequency. Red spots correspond to the presence of the corresponding wave period in the water level signal at this location in the signal.



**Figure B.7:** Signal and wavelet signal vessel 3178. Frequency to time heat map of the pressure signal from ADV3 created by wavelet analysis. The y-axis is transposed to wave period instead of frequency. Red spots correspond to the presence of the corresponding wave period in the water level signal at this location in the signal.

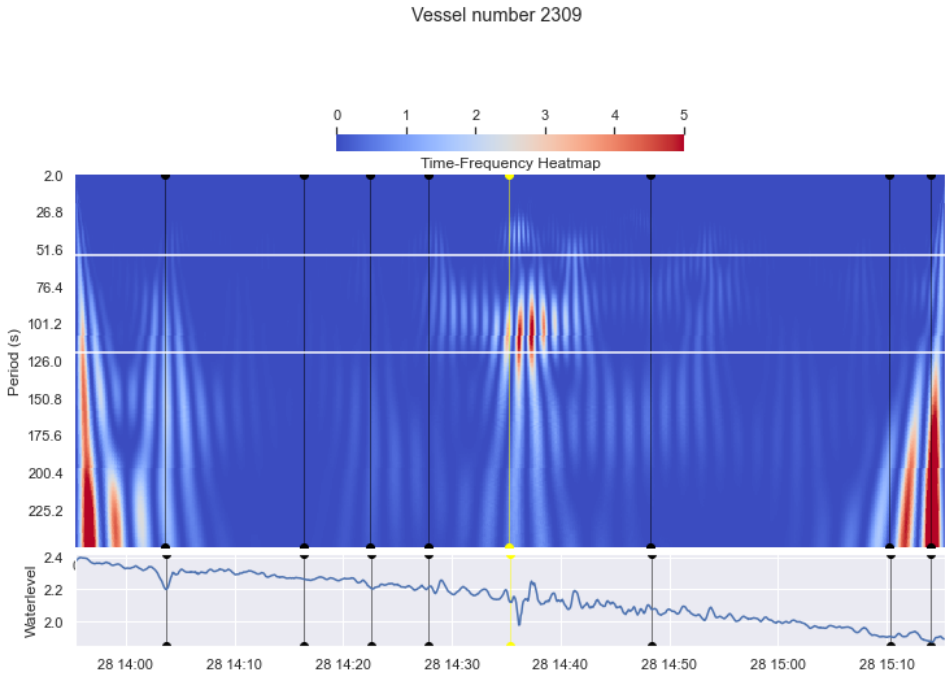


**Figure B.8:** Signal and wavelet signal vessel 2309. Frequency to time heat map of the pressure signal from ADV3 created by wavelet analysis. The y-axis is transposed to wave period instead of frequency. Red spots correspond to the presence of the corresponding wave period in the water level signal at this location in the signal.

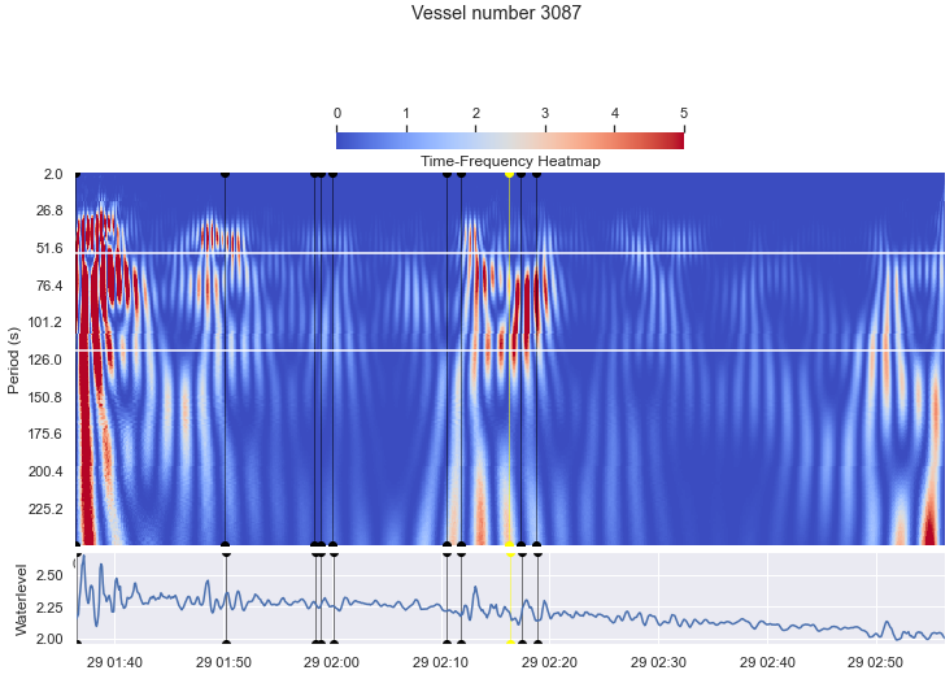


**Figure B.9:** Signal and wavelet signal vessel 3087. Frequency to time heat map of the pressure signal from ADV3 created by wavelet analysis. The y-axis is transposed to wave period instead of frequency. Red spots correspond to the presence of the corresponding wave period in the water level signal at this location in the signal.

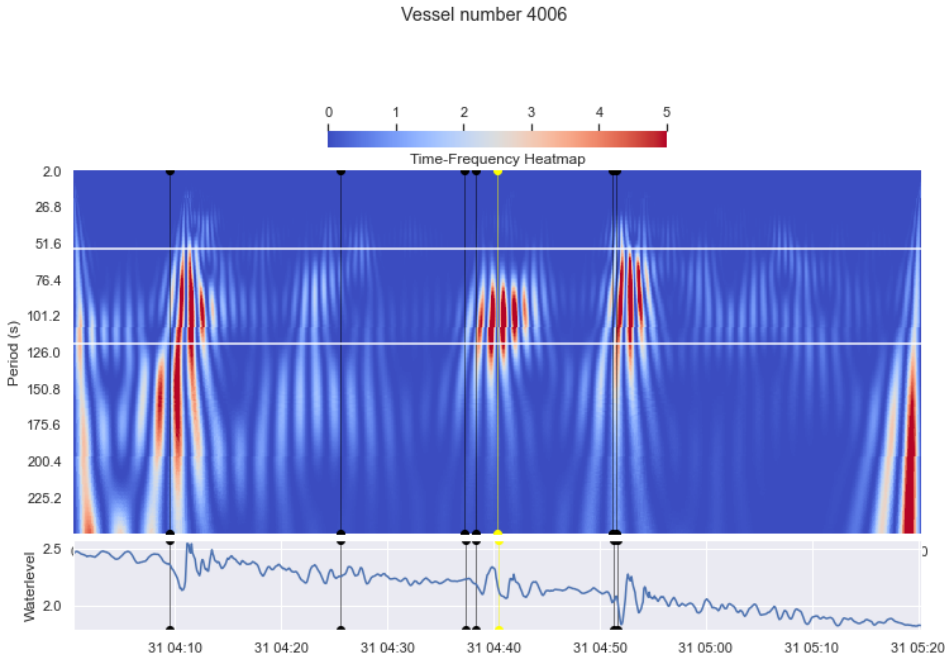


Figure B.10: Signal and wavelet signal vessel 4006. Frequency to time heat map of the pressure signal from ADV3 created by wavelet analysis. The y-axis is transposed to wave period instead of frequency. Red spots correspond to the presence of the corresponding wave period in the water level signal at this location in the signal.

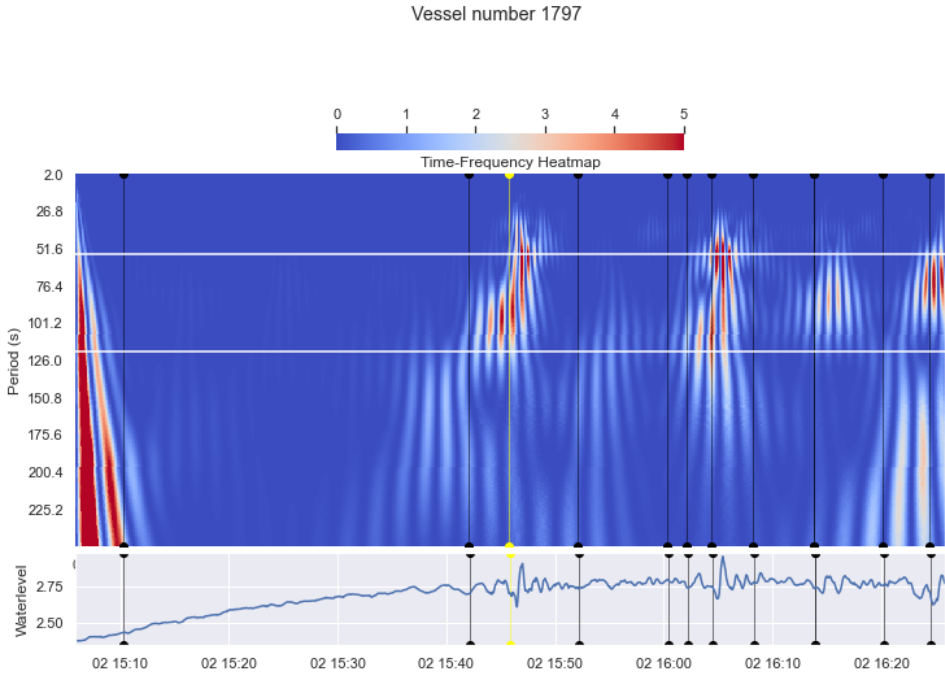
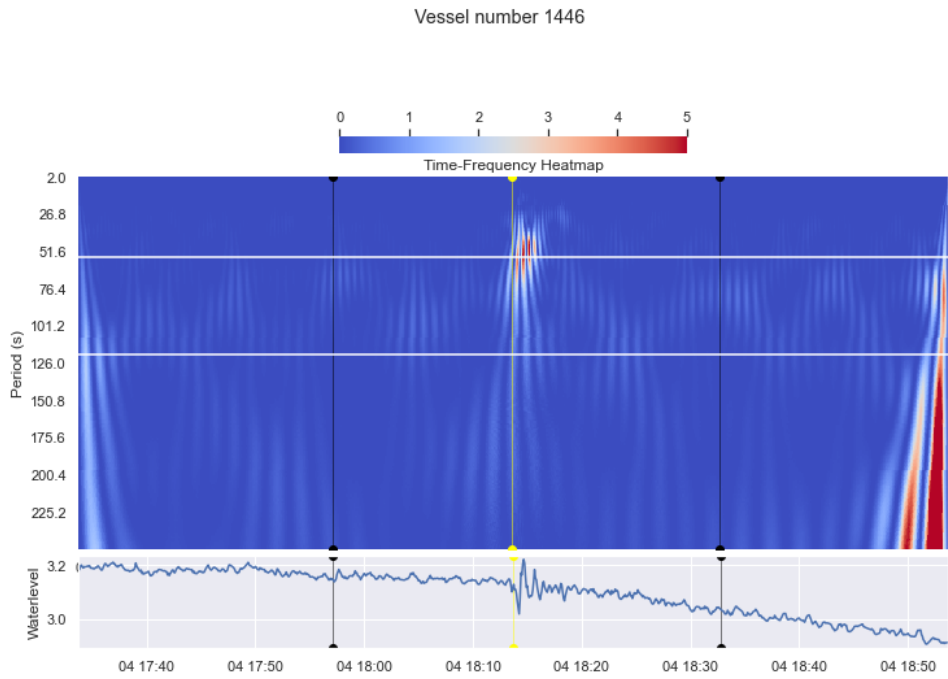
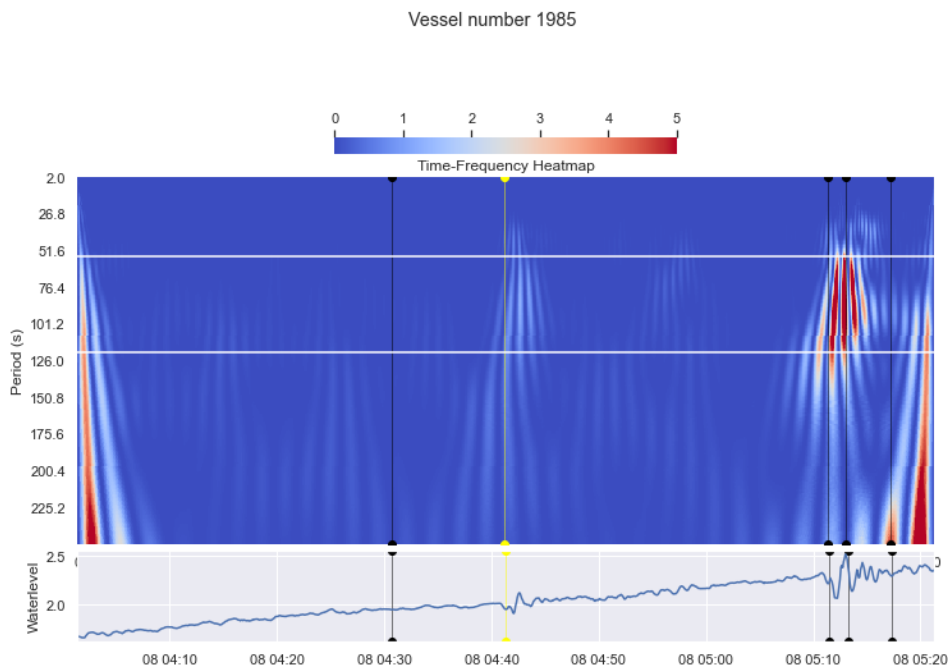


Figure B.11: Signal and wavelet signal vessel 1797. Frequency to time heat map of the pressure signal from ADV3 created by wavelet analysis. The y-axis is transposed to wave period instead of frequency. Red spots correspond to the presence of the corresponding wave period in the water level signal at this location in the signal.





**Figure B.12:** Signal and wavelet signal vessel 1446. Frequency to time heat map of the pressure signal from ADV3 created by wavelet analysis. The y-axis is transposed to wave period instead of frequency. Red spots correspond to the presence of the corresponding wave period in the water level signal at this location in the signal.



**Figure B.13:** Signal and wavelet signal vessel 1985. Frequency to time heat map of the pressure signal from ADV3 created by wavelet analysis. The y-axis is transposed to wave period instead of frequency. Red spots correspond to the presence of the corresponding wave period in the water level signal at this location in the signal.

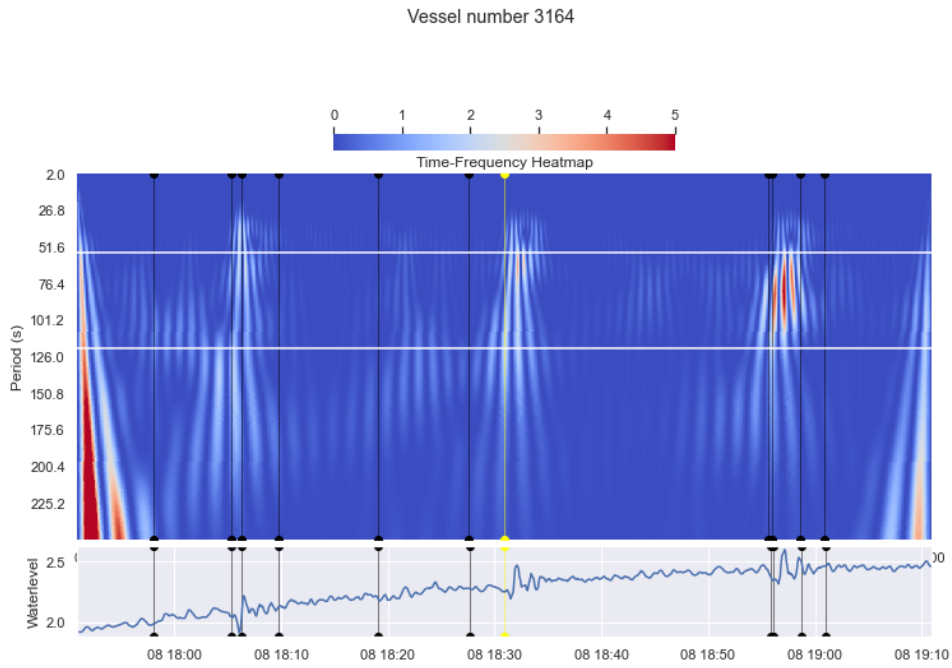


**Figure B.14:** Signal and wavelet signal vessel 3164. Frequency to time heat map of the pressure signal from ADV3 created by wavelet analysis. The y-axis is transposed to wave period instead of frequency. Red spots correspond to the presence of the corresponding wave period in the water level signal at this location in the signal.

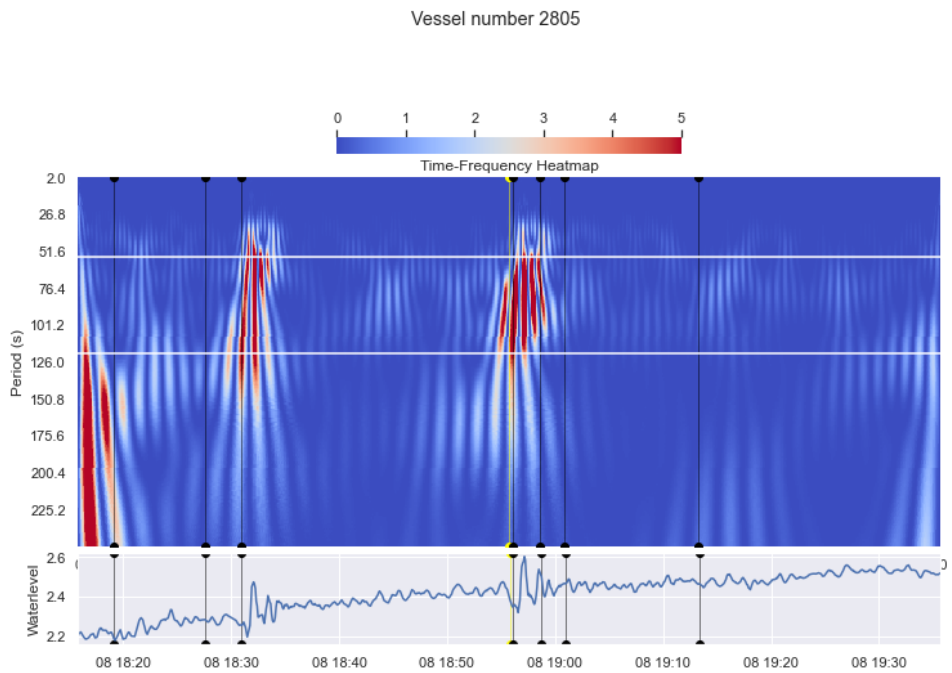
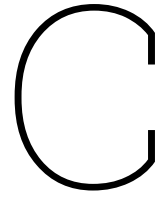


**Figure B.15:** Signal and wavelet signal vessel 2805. Frequency to time heat map of the pressure signal from ADV3 created by wavelet analysis. The y-axis is transposed to wave period instead of frequency. Red spots correspond to the presence of the corresponding wave period in the water level signal at this location in the signal.



# Numerical methodology

Various parameters are used based on expert opinion and on Delft3D Flexible Mesh default settings. The most important parameters are shown in Table C.1.

Parameter	Value
Uniform horizontal eddy viscosity	0.1
Uniform horizontal eddy diffusivity	0.1
Uniform vertical eddy viscosity	5E-5
Uniform vertical eddy diffusivity	5E-5
Uniform friction coefficient	0.023

**Table C.1:** Overview of parameters required for the numerical model.

The Grid of the model is depicted in Figure C.1.

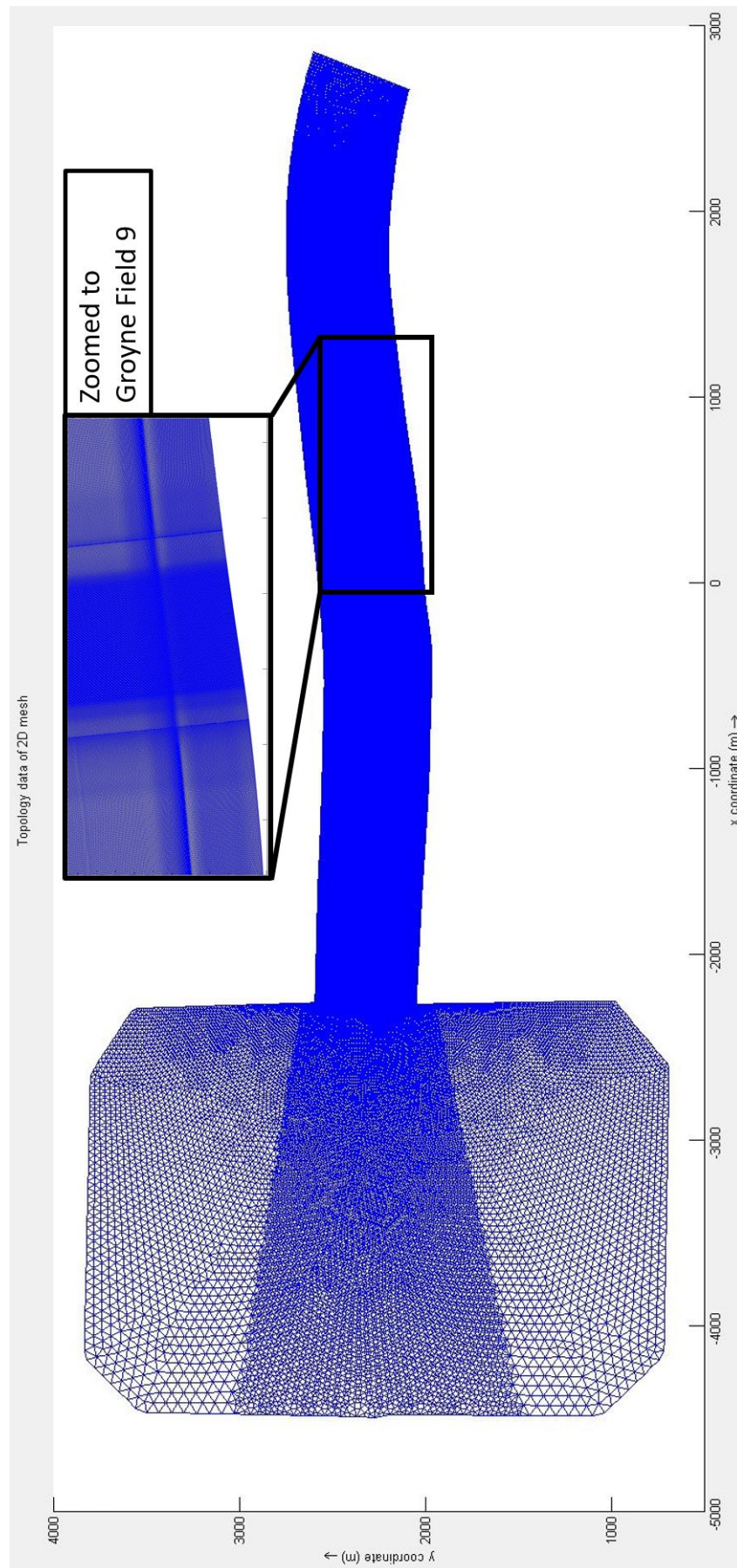


**Figure C.1:** The grid used in the numerical models. It shows that the grid size varies from course in the western open sea area and is very fine (around 1 meter x 1 meter) around the Groyne Field 9 area.

# D

## Numerical simulations

Layout/situation	Vessel configuration
Basic situation	1 vessel
	2 vessels (60s in between)
	2 vessels (120s in between)
	2 vessels (180s in between)
Additional	2 vessels (150s in between)
Complex-bathymetry situation (current situation)	1 vessel
	2 vessels (60s in between)
	2 vessels (120s in between)
	2 vessels (180s in between)
Tidal background (Flat bed)	0 vessels
Tidal Background (Current bed)	0 vessels
Basic simulation	1 vessel
Layout 1	1 vessel
Layout 2	1 vessel
Layout 3	1 vessel
Layout 4	1 vessel

**Table D.1:** Overview of the different simulations ran for this appendix

## D.1. Basic (flat bed) situation

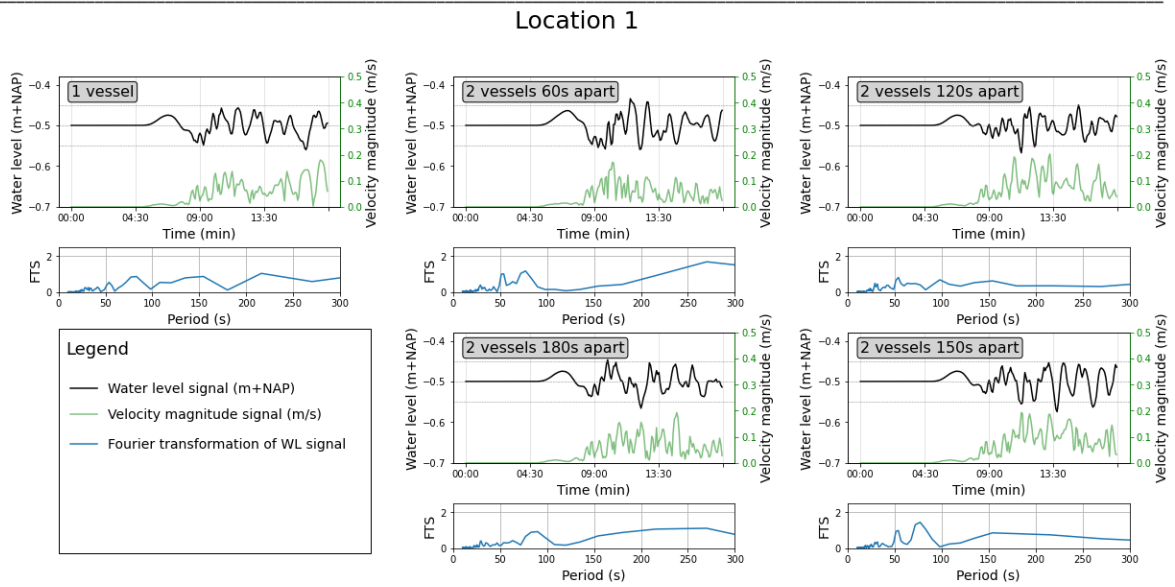


**Figure D.1:** Signal from location 1 of the model with a flat bathymetry in the groyne field. The figure compares different simulations of 1 vessel passage or 2 vessel passages with different amounts of time in between. The black and green lines show respectively water level and velocity magnitude. The blue line plots the Fourier analysis of the black water level line.

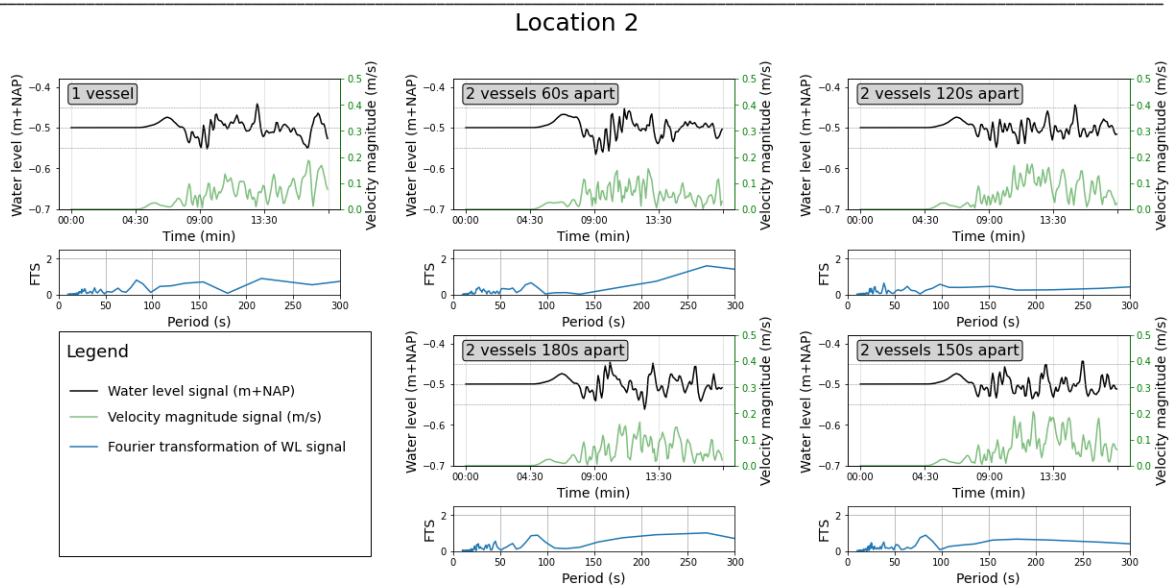


**Figure D.2:** Signal from location 2 of the model with a flat bathymetry in the groyne field. The figure compares different simulations of 1 vessel passage or 2 vessel passages with different amounts of time in between. The black and green lines show respectively water level and velocity magnitude. The blue line plots the Fourier analysis of the black water level line.

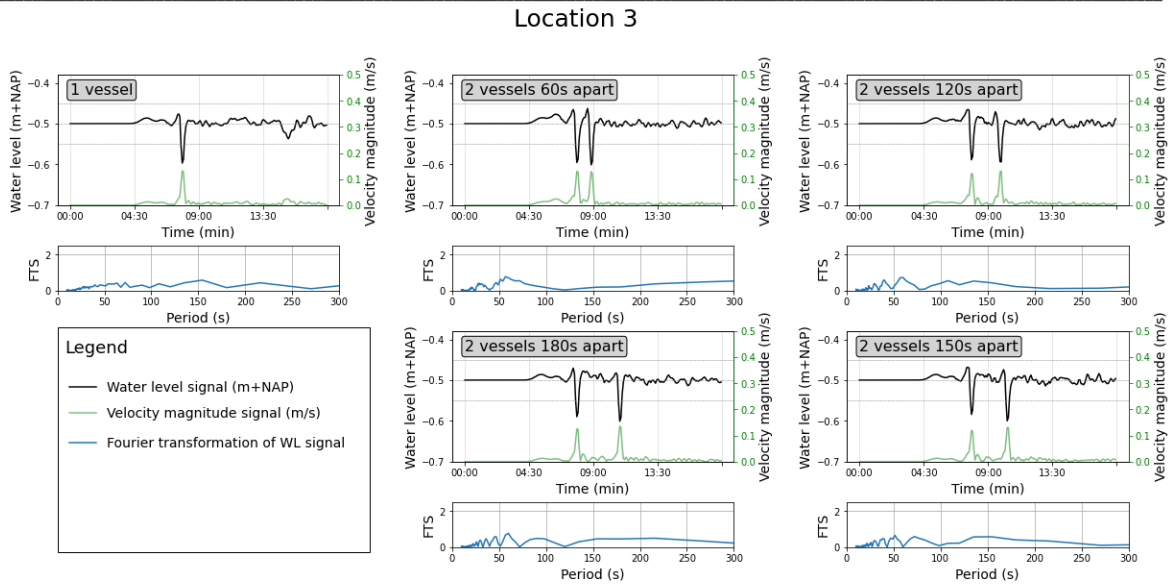


**Figure D.3:** Signal from location 3 of the model with a flat bathymetry in the groyne field. The figure compares different simulations of 1 vessel passage or 2 vessel passages with different amounts of time in between. The black and green lines show respectively water level and velocity magnitude. The blue line plots the Fourier analysis of the black water level line.

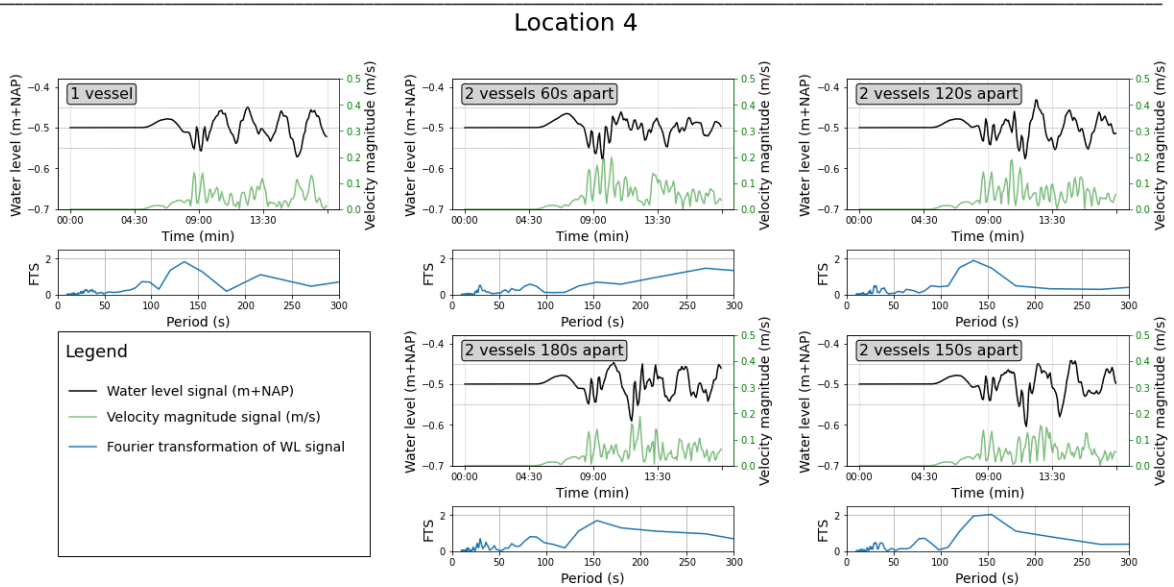


**Figure D.4:** Signal from location 4 of the model with a flat bathymetry in the groyne field. The figure compares different simulations of 1 vessel passage or 2 vessel passages with different amounts of time in between. The black and green lines show respectively water level and velocity magnitude. The blue line plots the Fourier analysis of the black water level line.

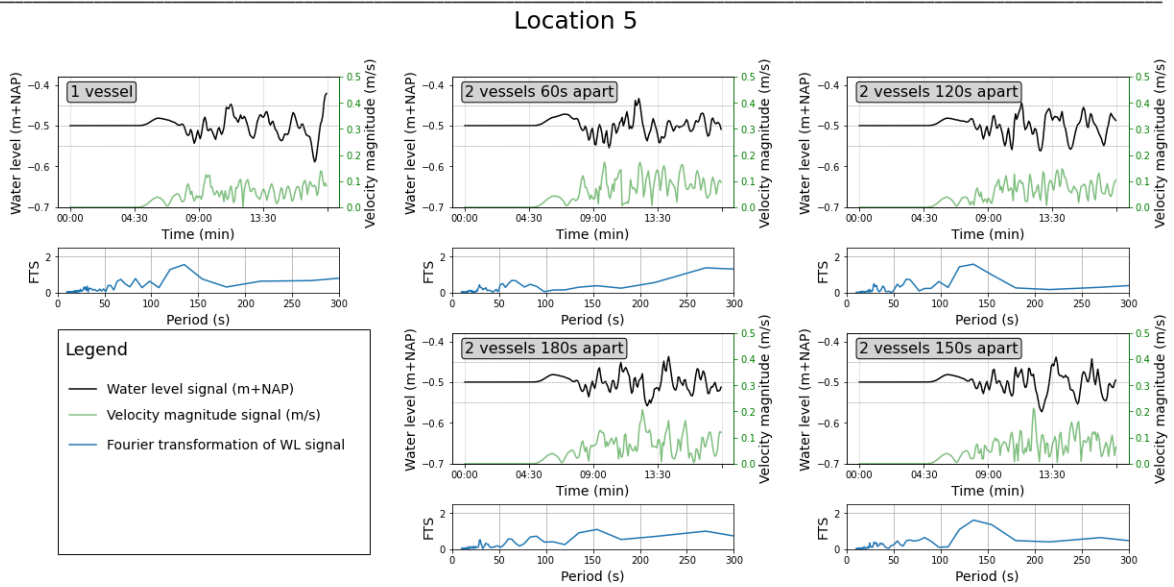


**Figure D.5:** Signal from location 5 of the model with a flat bathymetry in the groyne field. The figure compares different simulations of 1 vessel passage or 2 vessel passages with different amounts of time in between. The black and green lines show respectively water level and velocity magnitude. The blue line plots the Fourier analysis of the black water level line.

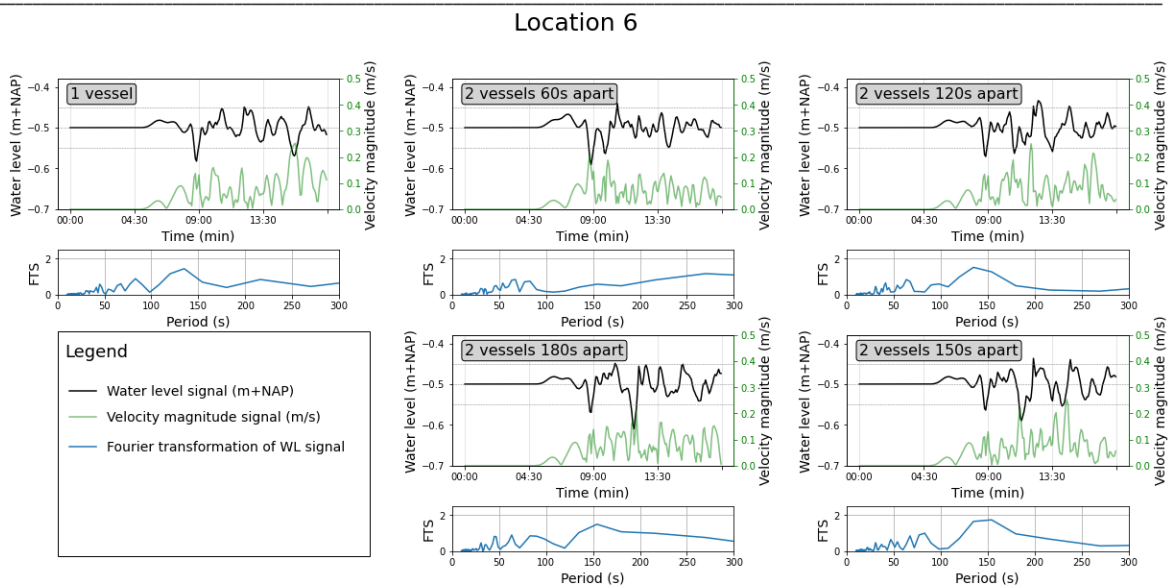


**Figure D.6:** Signal from location 6 of the model with a flat bathymetry in the groyne field. The figure compares different simulations of 1 vessel passage or 2 vessel passages with different amounts of time in between. The black and green lines show respectively water level and velocity magnitude. The blue line plots the Fourier analysis of the black water level line.



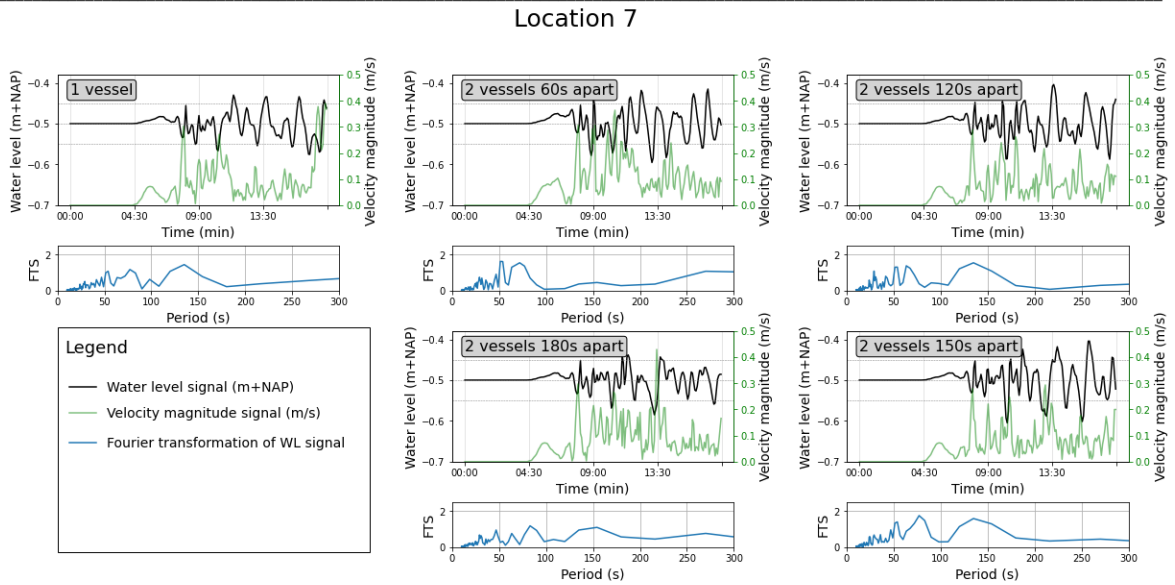


**Figure D.7:** Signal from location 7 of the model with a flat bathymetry in the groyne field. The figure compares different simulations of 1 vessel passage or 2 vessel passages with different amounts of time in between. The black and green lines show respectively water level and velocity magnitude. The blue line plots the Fourier analysis of the black water level line.

## D.2. Current (original bed) situation

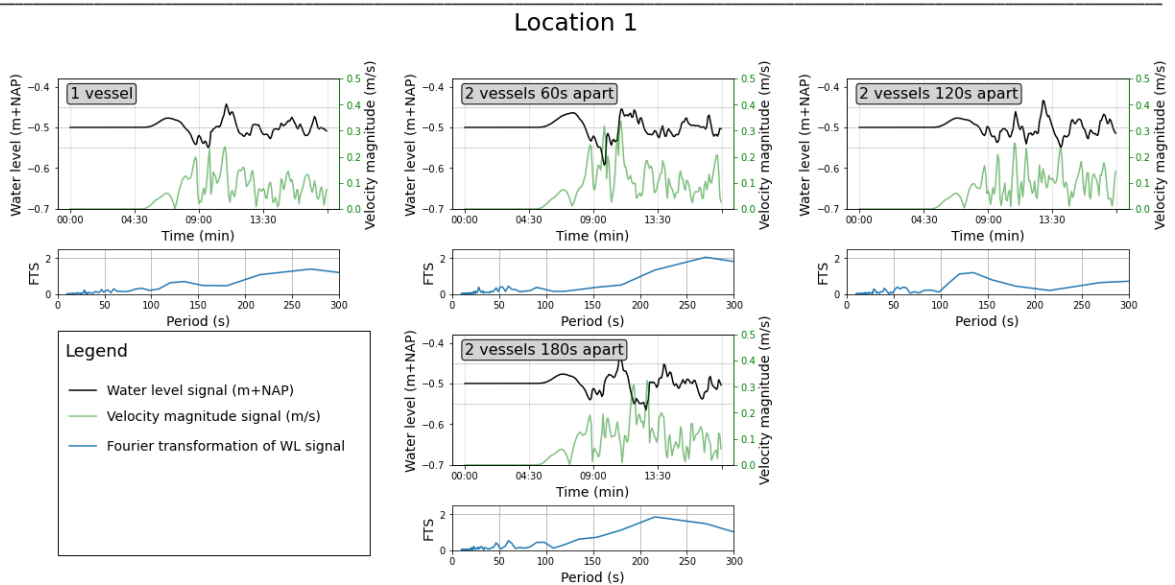


**Figure D.8:** Signal from location 1 of the model with the current bathymetry in the groyne field. The figure compares different simulations of 1 vessel passage or 2 vessel passages with different amounts of time in between. The black and green lines show respectively water level and velocity magnitude. The blue line plots the Fourier analysis of the black water level line.

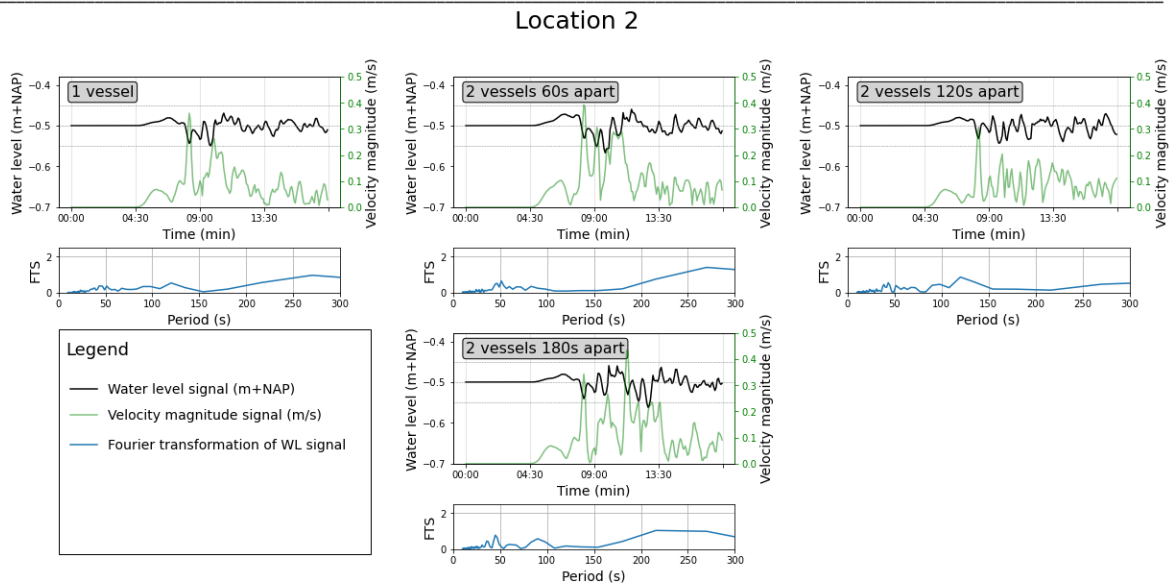


**Figure D.9:** Signal from location 2 of the model with the current bathymetry in the groyne field. The figure compares different simulations of 1 vessel passage or 2 vessel passages with different amounts of time in between. The black and green lines show respectively water level and velocity magnitude. The blue line plots the Fourier analysis of the black water level line.

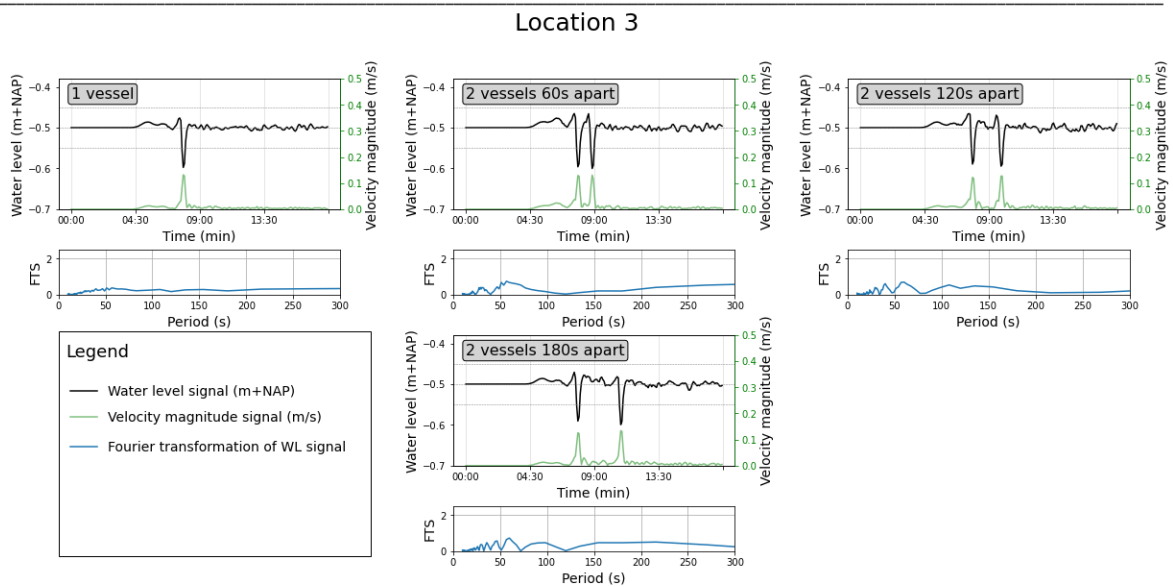


**Figure D.10:** Signal from location 3 of the model with the current bathymetry in the groyne field. The figure compares different simulations of 1 vessel passage or 2 vessel passages with different amounts of time in between. The black and green lines show respectively water level and velocity magnitude. The blue line plots the Fourier analysis of the black water level line.

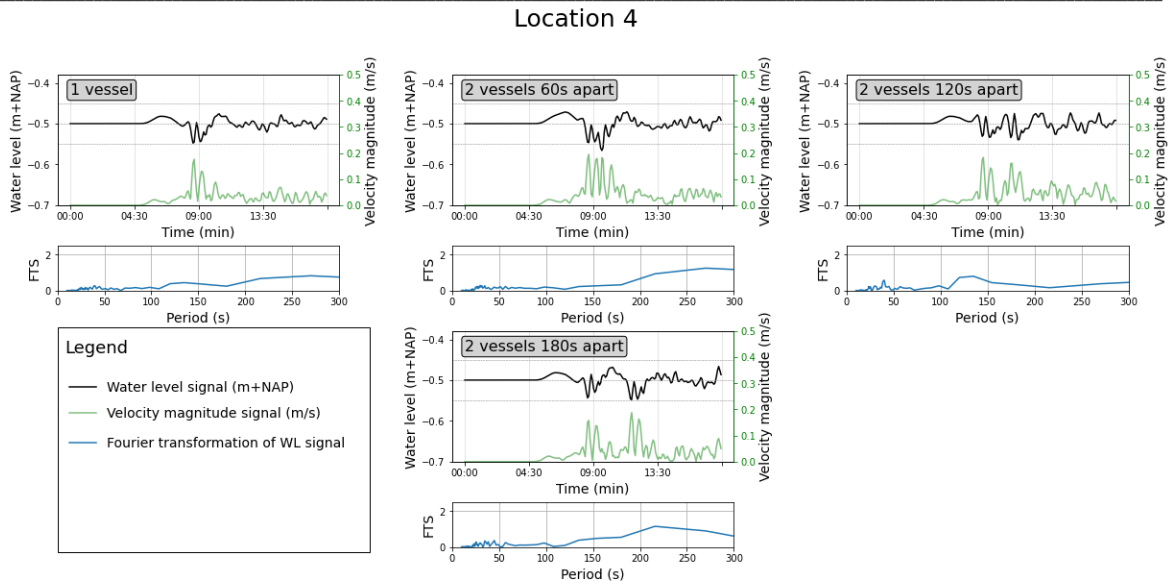


**Figure D.11:** Signal from location 4 of the model with the current bathymetry in the groyne field. The figure compares different simulations of 1 vessel passage or 2 vessel passages with different amounts of time in between. The black and green lines show respectively water level and velocity magnitude. The blue line plots the Fourier analysis of the black water level line.

**Figure D.12:** Signal from location 5 of the model with the current bathymetry in the groyne field. The figure compares different simulations of 1 vessel passage or 2 vessel passages with different amounts of time in between. The black and green lines show respectively water level and velocity magnitude. The blue line plots the Fourier analysis of the black water level line.

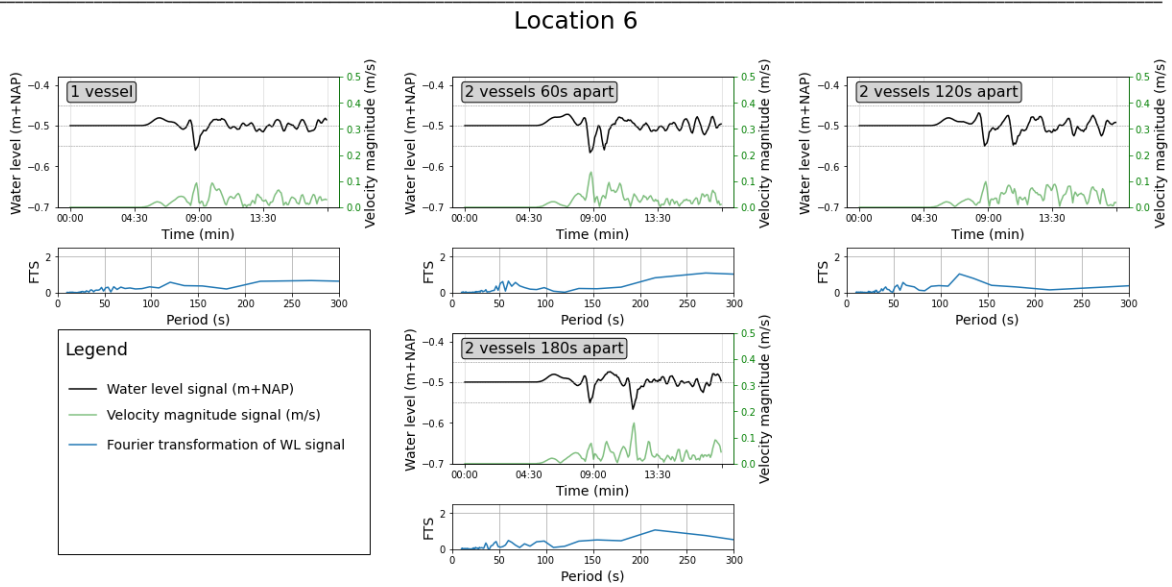


**Figure D.13:** Signal from location 6 of the model with the current bathymetry in the groyne field. The figure compares different simulations of 1 vessel passage or 2 vessel passages with different amounts of time in between. The black and green lines show respectively water level and velocity magnitude. The blue line plots the Fourier analysis of the black water level line.

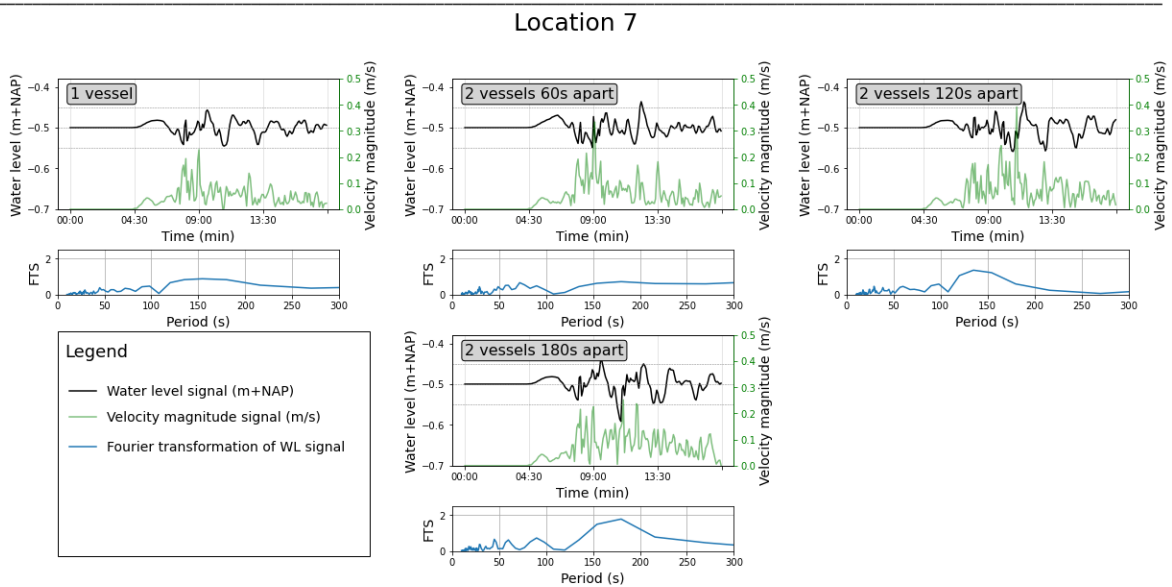


**Figure D.14:** Signal from location 7 of the model with the current bathymetry in the groyne field. The figure compares different simulations of 1 vessel passage or 2 vessel passages with different amounts of time in between. The black and green lines show respectively water level and velocity magnitude. The blue line plots the Fourier analysis of the black water level line.

### D.3. Tidal flow analysis

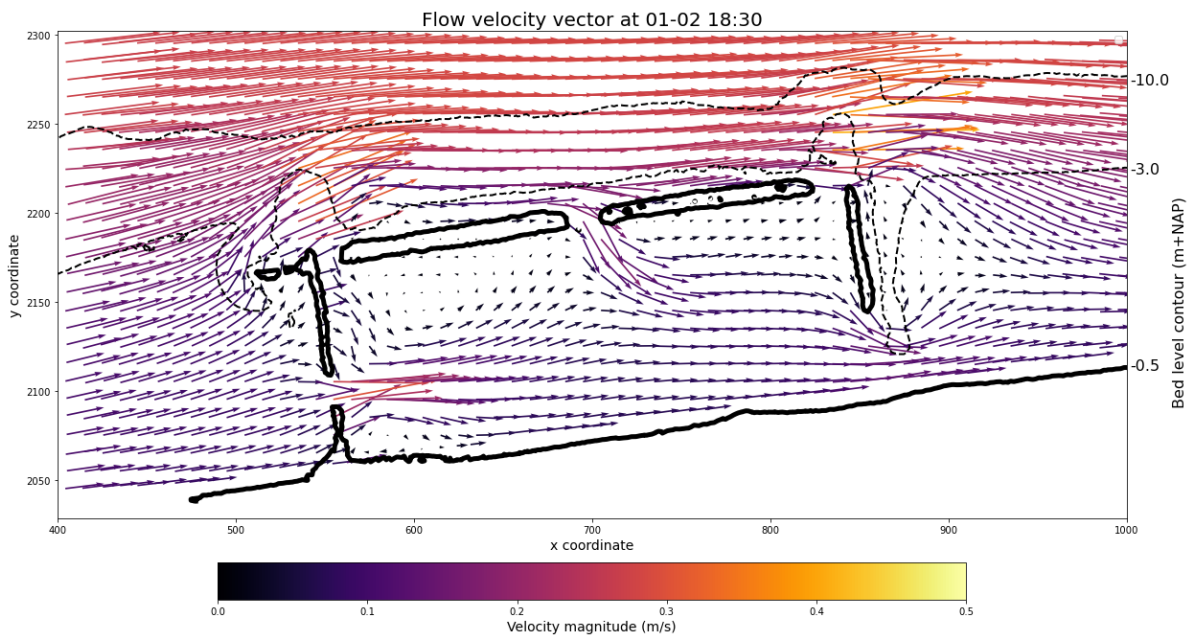


**Figure D.15:** Detailed vector plot depicting the flow during flood tide, the arrows show the velocity direction and the colour scale represents the velocity magnitude. The black lines show a simple bathymetry overview.

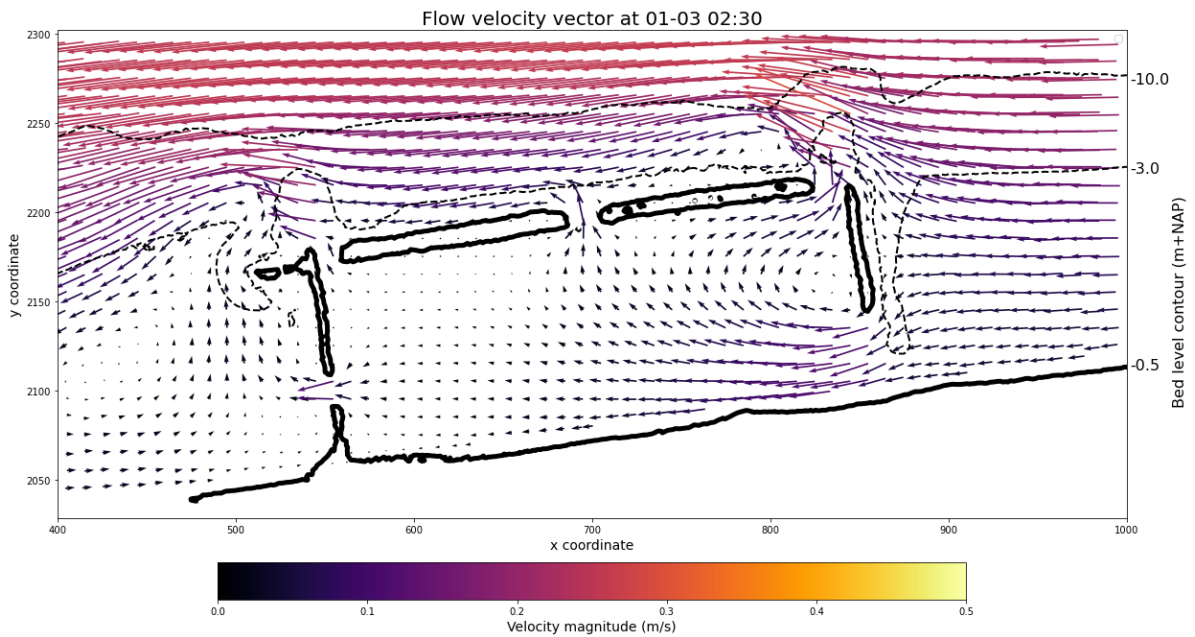


**Figure D.16:** Detailed vector plot depicting the flow during ebb tide, the arrows show the velocity direction and the colour scale represents the velocity magnitude. The black lines show a simple bathymetry overview.

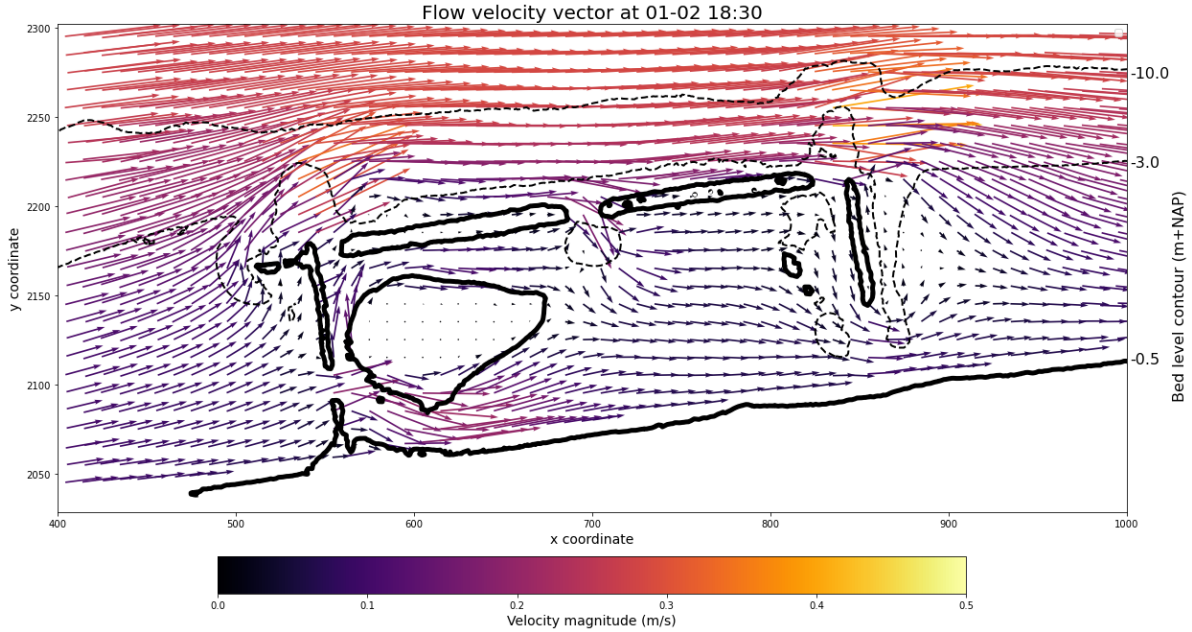


Figure D.17: Detailed vector plot depicting the flow during flood tide, the arrows show the velocity direction and the colourscale represents the velocity magnitude. The black lines show a simple bathymetry overview.

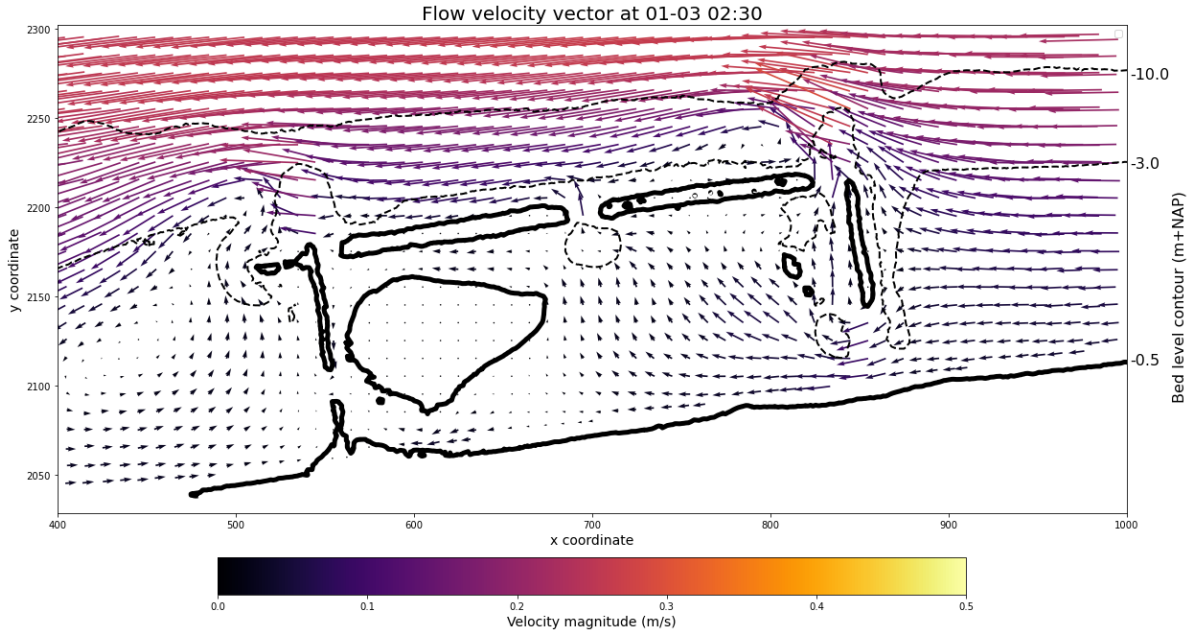
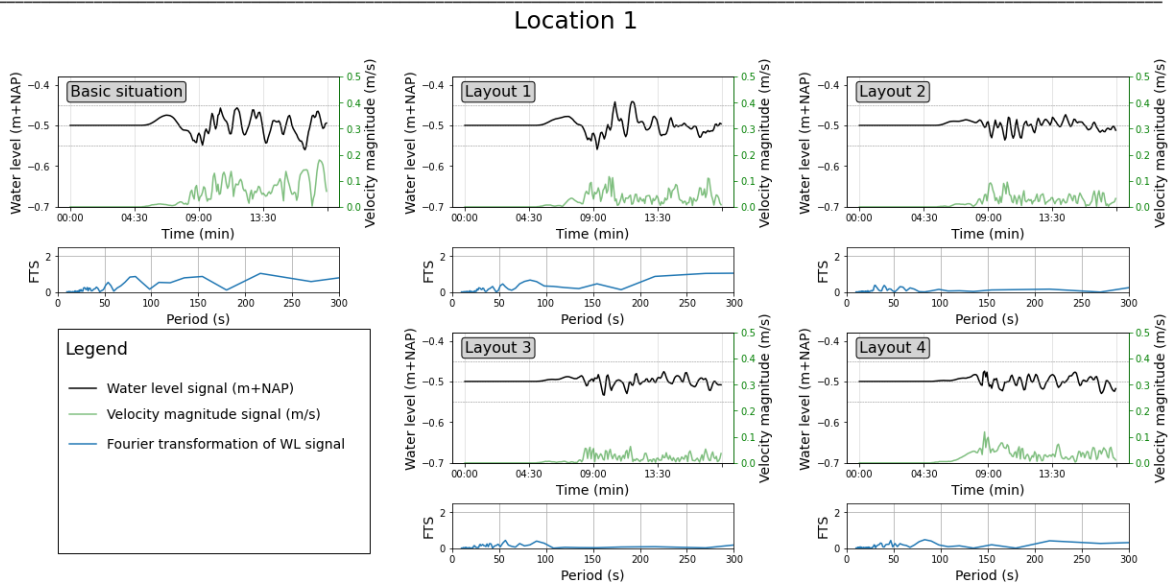
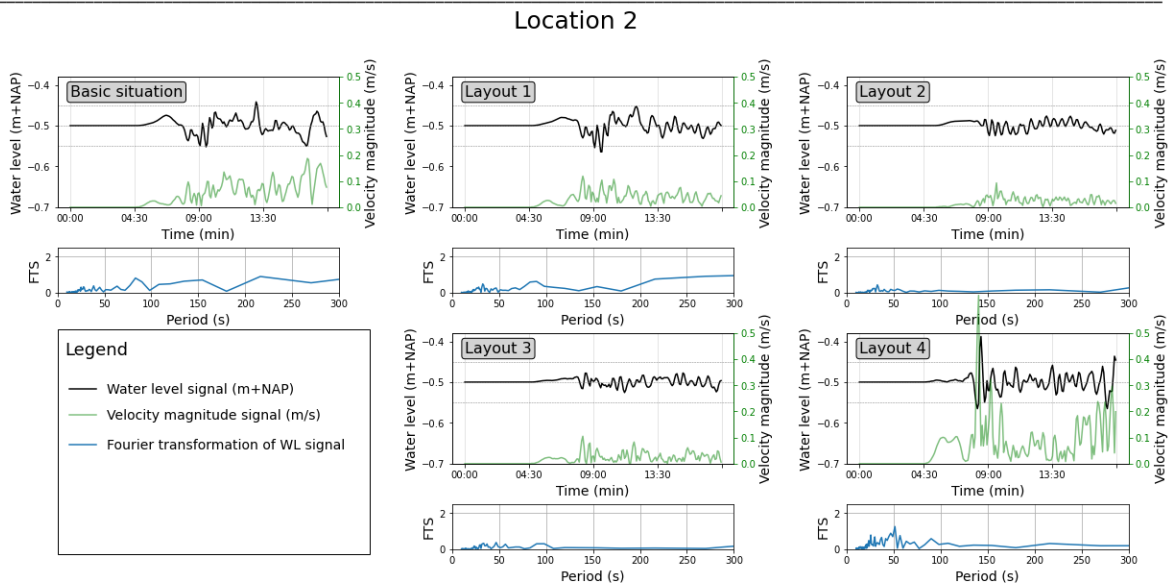


Figure D.18: Detailed vector plot depicting the flow during ebb tide, the arrows show the velocity direction and the colour scale represents the velocity magnitude. The black lines show a simple bathymetry overview.

## D.4. Different layout simulations



**Figure D.19:** Signal from location 1 of the model with the different layout bathymetries. The figure compares different simulations of 1 vessel in the basic simulation compared to the different layout simulations. The black and green lines show respectively water level and velocity magnitude. The blue line plots the Fourier analysis of the black water level line.



**Figure D.20:** Signal from location 2 of the model with the different layout bathymetries. The figure compares different simulations of 1 vessel in the basic simulation compared to the different layout simulations. The black and green lines show respectively water level and velocity magnitude. The blue line plots the Fourier analysis of the black water level line.

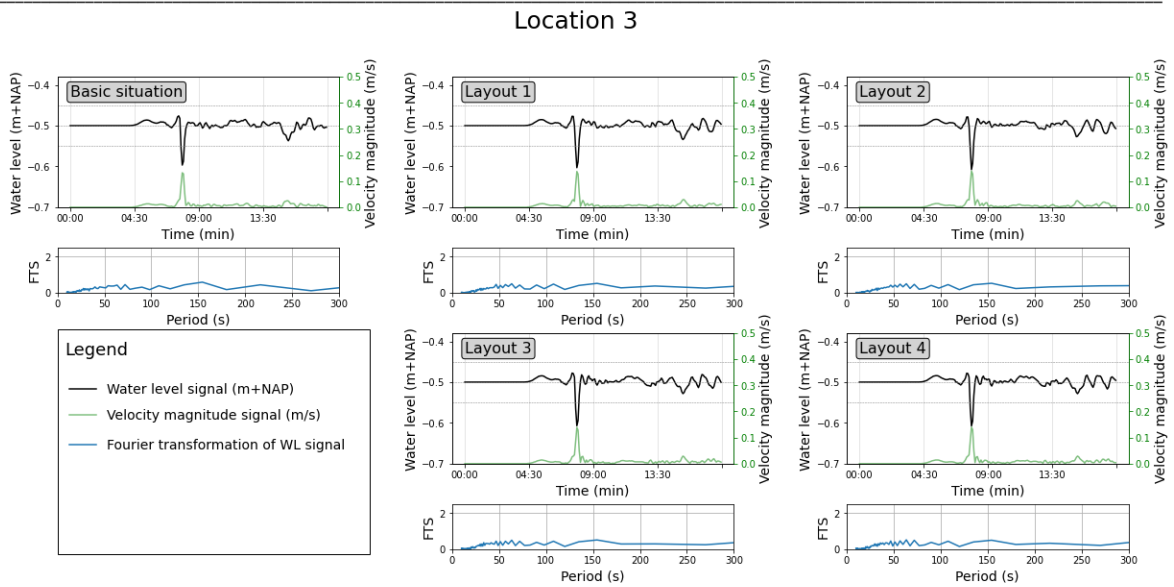


**Figure D.21:** Signal from location 3 of the model with the different layout bathymetries. The figure compares different simulations of 1 vessel in the basic simulation compared to the different layout simulations. The black and green lines show respectively water level and velocity magnitude. The blue line plots the Fourier analysis of the black water level line.

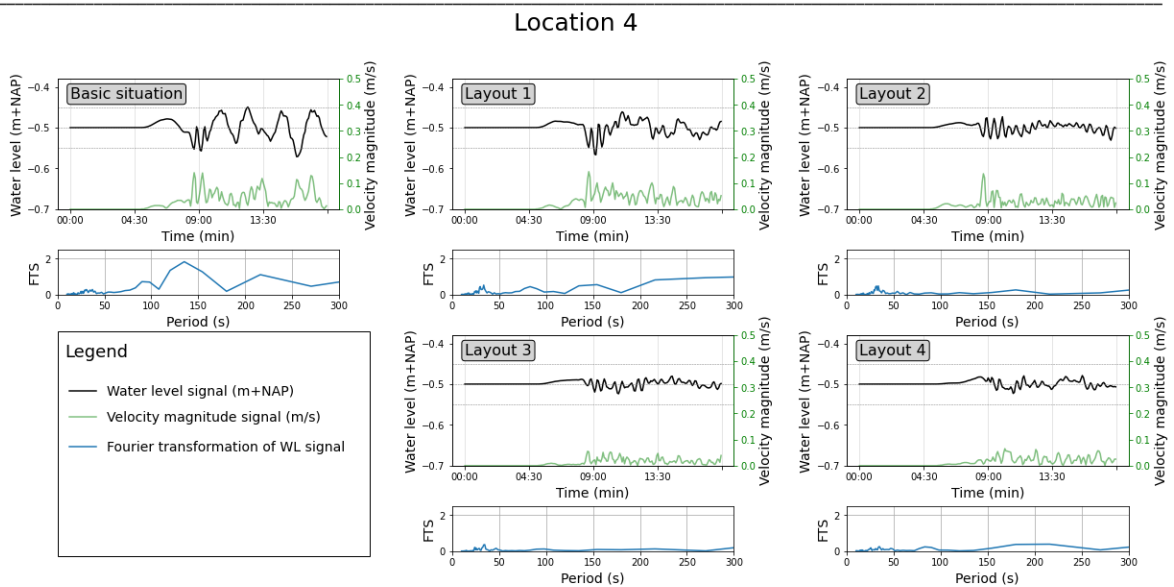


**Figure D.22:** Signal from location 4 of the model with the different layout bathymetries. The figure compares different simulations of 1 vessel in the basic simulation compared to the different layout simulations. The black and green lines show respectively water level and velocity magnitude. The blue line plots the Fourier analysis of the black water level line.



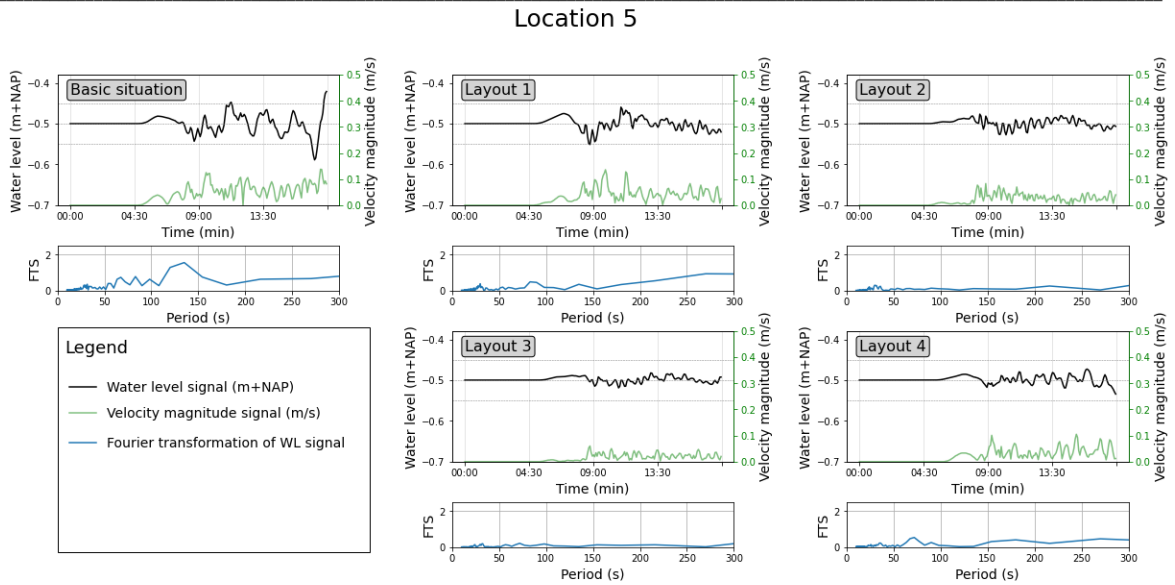


**Figure D.23:** Signal from location 5 of the model with the different layout bathymetries. The figure compares different simulations of 1 vessel in the basic simulation compared to the different layout simulations. The black and green lines show respectively water level and velocity magnitude. The blue line plots the Fourier analysis of the black water level line.

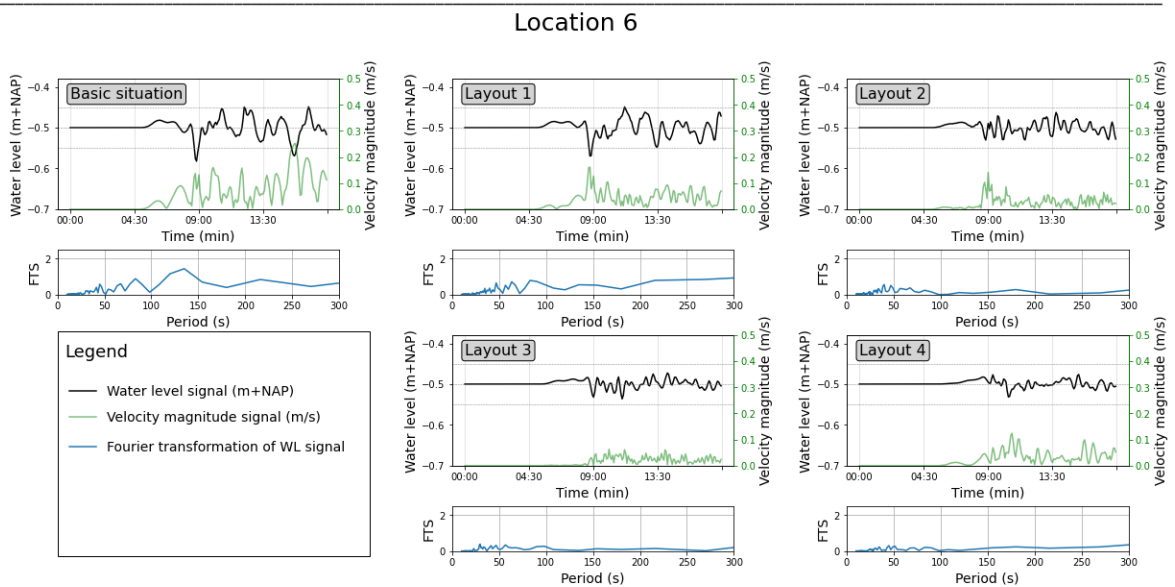


**Figure D.24:** Signal from location 6 of the model with the different layout bathymetries. The figure compares different simulations of 1 vessel in the basic simulation compared to the different layout simulations. The black and green lines show respectively water level and velocity magnitude. The blue line plots the Fourier analysis of the black water level line.

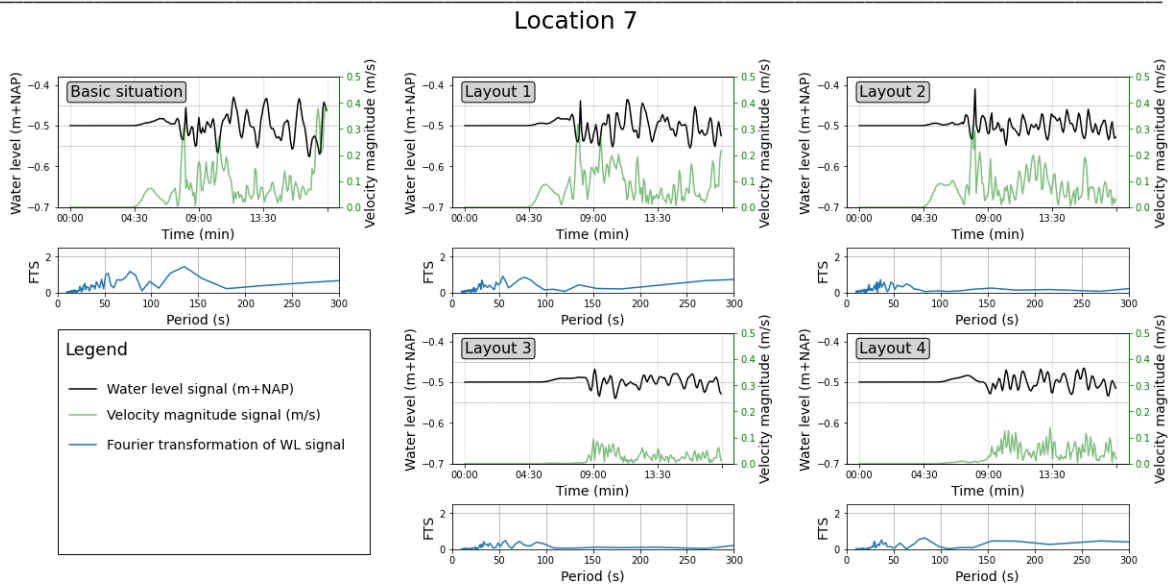


**Figure D.25:** Signal from location 7 of the model with the different layout bathymetries. The figure compares different simulations of 1 vessel in the basic simulation compared to the different layout simulations. The black and green lines show respectively water level and velocity magnitude. The blue line plots the Fourier analysis of the black water level line.

## D.5. Quantification tables

Location	Mean amplitude (m)	Max amplitude (m)	Mean velocity (m/s)	Max velocity (m/s)
1	0.011	0.057	0.059	0.238
2	0.009	0.050	0.061	0.360
3	0.005	0.098	0.006	0.132
4	0.007	0.048	0.025	0.176
5	0.271	0.271	0.000	0.000
6	0.007	0.060	0.021	0.093
7	0.010	0.045	0.038	0.228

**Table D.2:** Quantified average and maximum values of the water level and velocity magnitude signals in the simulation containing the current complex bed. (one vessel passage)

Location	Mean amplitude (m)	Max amplitude (m)	Mean velocity (m/s)	Max velocity (m/s)
1	0.014	0.060	0.043	0.180
2	0.011	0.058	0.046	0.187
3	0.007	0.097	0.008	0.132
4	0.016	0.071	0.031	0.140
5	0.015	0.089	0.040	0.138
6	0.013	0.082	0.055	0.252
7	0.017	0.075	0.069	0.391

**Table D.3:** Quantified average and maximum values of the water level and velocity magnitude signals in the simulation containing the basic flat bed. (One vessel passage)

Location	Mean amplitude (m)	Max amplitude (m)	Mean velocity (m/s)	Max velocity (m/s)
1	0.011	0.059	0.024	0.116
2	0.010	0.064	0.028	0.119
3	0.007	0.103	0.008	0.137
4	0.010	0.066	0.029	0.144
5	0.009	0.051	0.030	0.136
6	0.012	0.070	0.030	0.161
7	0.014	0.064	0.065	0.318

**Table D.4:** Quantified average and maximum values of the water level and velocity magnitude signals in the simulation containing Layout 1.

Location	Mean amplitude (m)	Max amplitude (m)	Mean velocity (m/s)	Max velocity (m/s)
1	0.007	0.036	0.018	0.095
2	0.007	0.025	0.016	0.093
3	0.007	0.108	0.008	0.139
4	0.006	0.031	0.019	0.136
5	0.006	0.027	0.019	0.083
6	0.008	0.037	0.018	0.141
7	0.010	0.090	0.061	0.310

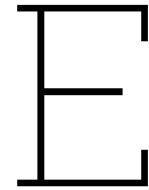
**Table D.5:** Quantified average and maximum values of the water level and velocity magnitude signals in the simulation containing Layout 2.

Location	Mean amplitude (m)	Max amplitude (m)	Mean velocity (m/s)	Max velocity (m/s)
1	0.006	0.034	0.013	0.063
2	0.006	0.026	0.018	0.105
3	0.007	0.107	0.008	0.139
4	0.005	0.024	0.012	0.055
5	0.005	0.019	0.013	0.060
6	0.006	0.036	0.013	0.063
7	0.007	0.040	0.016	0.093

**Table D.6:** Quantified average and maximum values of the water level and velocity magnitude signals in the simulation containing Layout 3.

Location	Mean amplitude (m)	Max amplitude (m)	Mean velocity (m/s)	Max velocity (m/s)
1	0.007	0.030	0.024	0.119
2	0.012	0.112	0.070	0.645
3	0.007	0.107	0.008	0.140
4	0.005	0.023	0.015	0.065
5	0.006	0.034	0.023	0.105
6	0.005	0.032	0.022	0.124
7	0.008	0.034	0.027	0.139

**Table D.7:** Quantified average and maximum values of the water level and velocity magnitude signals in the simulation containing Layout 4.



# Python sheets

## E.1. Wavelets

This python sheet was used to create the wavelet power spectrum for the water level signal.

```
1 start_time = '2022-03-30T12:00:00'
2 end_time = '2022-03-30T13:30:00'
3
4 sampling_period = 5 # seconds
5
6 filepath1 = r'C:/Users/broeders/OneDrive - Stichting Deltares/Documents/Data/Python files/
   InstrumentProcessing/ADV/ADV3/Sander/tailored/ADV302_pilot_tailored_all_5sec_1.nc'
7 filepath2 = r'C:/Users/broeders/OneDrive - Stichting Deltares/Documents/Data/Python files/
   InstrumentProcessing/ADV/ADV3/Sander/tailored/ADV302_pilot_tailored_all_5sec_2.nc'
8 filepath3 = r'C:/Users/broeders/OneDrive - Stichting Deltares/Documents/Data/Python files/
   InstrumentProcessing/ADV/ADV3/Sander/tailored/ADV302_pilot_tailored_all_5sec_3.nc'
9
10 data1 = xr.open_dataset(filepath1)
11 data2 = xr.open_dataset(filepath2)
12 data3 = xr.open_dataset(filepath3)
13 alldata = xr.concat([data1, data2, data3], dim='t')
14
15 dat_sel = alldata.sel(t=slice(start_time, end_time))
16 dat_sel = dat_sel.resample(t='5S').interpolate()
17 signal = dat_sel.zsmean # Signal (with or without .values??)
18
19 water_level_data = signal
20 normalized_data = (water_level_data - np.mean(water_level_data)) / np.std(water_level_data)
21
22 wavelet = 'morl' # Choose the wavelet type, e.g., Morlet
23
24 min_scale = 0.4 # Minimum scale (corresponds to max freq)
25 max_scale = 50 # Maximum scale (corresponds to min freq)
26 num_scales = 200 # Number of scales
27
28 scales = np.arange(min_scale, max_scale, (max_scale-min_scale)/num_scales)
29
30 coefficients, frequencies = pywt.cwt(normalized_data, scales, wavelet, sampling_period)
31 power = (np.abs(coefficients)) ** 2 # Calculate the power of the coefficients
32
33 # Generate a time-frequency heatmap using seaborn
34 sns.set() # Set seaborn style
35 fig, (ax, ax2) = plt.subplots(2, 1, figsize=(12, 8), gridspec_kw={'height_ratios': [5, 1]}) #
   2 plots Adjust the figure size as needed
36
37 ax = sns.heatmap(power, cmap='coolwarm', xticklabels=False, yticklabels=False, vmin = 0, vmax
   = 0.1, ax=ax, cbar_kws={'orientation': 'horizontal', 'shrink': 0.4, 'location': 'top'})
38
39 # Add time and frequency labels
40 num_time_points = len(normalized_data)
41 num_scales = len(scales)
42
```

```

43 # Set the x-axis labels (time)
44 xticklabels_step = num_time_points // 10 # Adjust the step based on the number of time
    points
45 xticks = np.arange(0, num_time_points, xticklabels_step)
46 xticklabels = np.arange(0, num_time_points * 5, xticklabels_step * 5) # Assuming 5-second
    sampling period
47 ax.set_xticks(xticks)
48 ax.set_xticklabels(xticklabels)
49
50 ax.yaxis.set_major_formatter(plt.FormatStrFormatter('%1f'))
51 # # Set the y-axis labels (scale)
52 yticklabels_step = num_scales // 10 # Adjust the step based on the number of scales
53 yticks = np.arange(0, num_scales-1, yticklabels_step)
54 yticklabels = (scales[:, yticklabels_step] * sampling_period).round(1) # Calculate frequency
    or period values
55 ax.set_yticks(yticks)
56 ax.set_yticklabels(yticklabels)
57
58 AISpd = pd.read_pickle(r'C:/Users/broeders/OneDrive - Stichting Deltares/Documents/Data/AIS (
    schepen)/aisdata.pkl')
59 aisdata_all = AISpd
60 aisdata_range = aisdata_all[(end_time > aisdata_all['timestamplast']) & (aisdata_all['
    timestamplast'] > start_time)]
61 aisdata_range['powersum'] = 0
62 aisdata_range['drawdown'] = 0
63 for n in aisdata_range.index.values:
64     aisdatatime = aisdata_range['timestamplast'][n].replace(tzinfo = None)
65     pointintime = aisdatatime - dat_sel.t[0].values
66     point2 = pointintime.total_seconds()
67     previousindex = np.where(aisdata_all.index == n)[0][0] - 1
68     timediff = aisdata_range['timestamplast'][n] - aisdata_all['timestamplast'].iloc[
        previousindex]
69
70     # Sailing velocity criterium
71     if aisdata_range['draughtMarine'][n] < 7: ## The course is 300 degrees (seaward)
72         col = 'black'
73     else:
74         col = 'yellow'
75
76     if 200 < aisdata_range['cog'][n]:
77         linestyle = '--'
78     else:
79         linestyle = '-'
80
81     alpha = 1
82     ax.axvline(x = point2//sampling_period, color= col, marker = 'o', linestyle = linestyle,
        linewidth= '0.5', label = aisdata_range['sog'][n], alpha = alpha)
83     ax2.axvline(x = aisdatatime, color = col, marker = 'o', linestyle =linestyle, linewidth =
        '0.5', alpha = alpha)
84     ax.legend(loc='lower right')
85
86     upbound = np.int((55-sampling_period*min_scale)*num_scales/(sampling_period*(max_scale-
        min_scale)))
87     lowbound = np.int((120-sampling_period*min_scale)*num_scales/(sampling_period*(max_scale-
        min_scale)))
88     powersum = np.sum(power[upbound:lowbound, np.int(point2//sampling_period):np.int(point2//
        sampling_period)+10])
89     aisdata_range['powersum'][n] = powersum
90
91     locinterval = aisdata_range['timestamplast'][n]+pd.to_timedelta('1.5min') , aisdata_range
        ['timestamplast'][n]-pd.to_timedelta('0.5min')
92     end = locinterval[0].strftime('%Y-%m-%dT%H:%M:%S.%f')
93     start = locinterval[1].strftime('%Y-%m-%dT%H:%M:%S.%f')
94
95     wl = water_level_data.sel(t=slice(start, end))
96     if wl.size ==0:
97         aisdata_range = aisdata_range.drop(n)
98     else:
99         wlmin = np.min(wl)
100
101         wlmintime = wl.t[wl == wlmin]

```

```

102     datmean = water_level_data.resample(t='10T', loffset='5T').mean() # average over 10
103         minutes
104
105     wlmean_interp = np.interp(wl.t, datmean.t, datmean)
106
107     diff = wl - wlmean_interp
108     if all(diff.isnull()):
109         aisdata_range = aisdata_range.drop(n)
110     else:
111         drawdown = np.min(diff).values
112         aisdata_range['drawdown'][n] = drawdown
113
114 ax.axhline((55-sampling_period*min_scale)*num_scales/(sampling_period*(max_scale-min_scale)),
115           color='w')
116 ax.axhline((120-sampling_period*min_scale)*num_scales/(sampling_period*(max_scale-min_scale))
117           , color='w')
118 ax.set_xlabel('Time (seconds)')
119 ax.set_ylabel('Period (s)')
120 ax.set_title('Time-Frequency Heatmap')
121
122 ax2.plot(dat_sel.t, water_level_data)#signal)
123 ax2.set_ylabel('Waterlevel')
124 ax2.set_xlim(dat_sel.t.min(), dat_sel.t.max())
125
126 plt.subplots_adjust(hspace=0.02)
127 plt.show()

```

## E.2. Atmospheric pressure (vessel) input file

The python sheet below creates the .amp file used in the Delft3D software to model the vessel as atmospheric pressure moving through the domain.

```

1 -----
2 Create Trajectory
3 -----
4 import numpy as np
5 import matplotlib.pyplot as plt
6 from scipy.interpolate import CubicSpline
7
8 def interpolate_trajectory(coordinates, num_points):
9     """
10     Interpolates a trajectory using cubic spline interpolation.
11     Returns the interpolated trajectory as a list of coordinates.
12     """
13     # Separate x and y coordinates
14     x = [coord[0] for coord in coordinates]
15     y = [coord[1] for coord in coordinates]
16
17     # Perform cubic spline interpolation
18     t = np.linspace(0, 1, len(coordinates))
19     interp_func_x = CubicSpline(t, x)
20     interp_func_y = CubicSpline(t, y)
21
22     # Generate the interpolated trajectory
23     t_interp = np.linspace(0, 1, num_points)
24     x_interp = interp_func_x(t_interp)
25     y_interp = interp_func_y(t_interp)
26     interpolated_trajectory = list(zip(x_interp, y_interp))
27
28     return interpolated_trajectory
29
30 import numpy as np
31 from scipy.spatial import distance
32
33 def reorder_coordinates_equal_distance(coordinates):
34     # Convert coordinates to NumPy arrays
35     coordinates = np.array(coordinates)
36

```

```

37 # Calculate the cumulative distances along the path
38 distances = np.cumsum([0] + [distance.euclidean(coord1, coord2) for coord1, coord2 in zip
    (coordinates[:-1], coordinates[1:])])
39
40 # Calculate the total distance along the path
41 total_distance = distances[-1]
42
43 # Determine the target distance between each point
44 target_distance = total_distance / (len(coordinates) - 1)
45
46 # Initialize the reordered coordinates with the start point
47 reordered_coordinates = [coordinates[0]]
48
49 # Iterate through the cumulative distances to select points at equal intervals
50 current_distance = target_distance
51 for i in range(1, len(distances)):
52     while distances[i] > current_distance:
53         # Interpolate the coordinates at the current distance
54         t = (current_distance - distances[i-1]) / (distances[i] - distances[i-1])
55         interpolated_coord = (1 - t) * coordinates[i-1] + t * coordinates[i]
56         reordered_coordinates.append(interpolated_coord)
57         current_distance += target_distance
58
59 return reordered_coordinates
60
61 def plot_trajectory(trajectory):
62     """
63     Plots a trajectory given as a list of coordinates.
64     """
65     # Separate x and y coordinates
66     x = [coord[0] for coord in trajectory]
67     y = [coord[1] for coord in trajectory]
68
69     # Create a scatter plot of the trajectory
70     plt.scatter(x, y, color='b', label='Original')
71
72     # Create a line plot of the interpolated trajectory
73     plt.plot(x, y, color='b', linestyle='dashed', label='Interpolated')
74
75     # Set the x and y axis labels
76     plt.xlabel('X')
77     plt.ylabel('Y')
78     plt.xlim(0, 6000)
79     plt.ylim(0, 500)
80     plt.axis('equal')
81     plt.axhline(450)
82     # Add a legend
83     plt.legend()
84
85     # Show the plot
86     plt.show()
87
88
89 coordinates = [(51.95588208314513, 4.162455167528892), (51.95389012676021, 4.166501374856782)
    , (51.950224397606625, 4.174087807482804), (51.94540815527047, 4.184352879254348)
90     , (51.94186430952298, 4.193590922356478), (51.93948013111301, 4.200358914375027)
    , (51.93720281686141, 4.207399609261002)
91     , (51.93494067209952, 4.213523030724143), (51.93243383793713, 4.218729178449067)
    , (51.92945296871419, 4.223860952669008)
92     , (51.926762373214885, 4.227381300111996), (51.919798203958585,
    4.231972522559489)
93     , (51.90958302520583, 4.2557657918836895)]
94
95 import pyproj as proj
96
97 zero_coord = (51.920281, 4.156407) # for the 5.36km coordinates
98
99 ### For rotation of the coordinates to align with grid
100 angle_degrees = 37
101 angle_rad = angle_degrees * (3.14159 / 180.0)
102 x00 = 71500

```

```

103 y00 = 438000
104
105 # setup your projections
106 crs_wgs = proj.Proj(init='epsg:4326') # assuming you're using WGS84 geographic
107 crs_bng = proj.Proj(init='EPSG:28992') # use a locally appropriate projected CRS
108 x0, y0 = proj.transform(crs_wgs, crs_bng, zero_coord[1], zero_coord[0])
109
110
111 for i in range(len(coordinates)):
112     # then cast your geographic coordinate pair to the projected system
113     x, y = proj.transform(crs_wgs, crs_bng, coordinates[i][1], coordinates[i][0])
114     print(x, y)
115     new_x = (x-x00) * np.cos(angle_rad) - (y-y00) * np.sin(angle_rad)
116     new_y = (x-x00) * np.sin(angle_rad) + (y-y00) * np.cos(angle_rad)
117
118     coordinates[i] = (new_x+4000, new_y-2250)
119
120 num_points = 1075*2 #10*(len(coordinates)-1) # Number of points for the interpolated
    trajectory
121
122 coordinates2 = reorder_coordinates_equal_distance(coordinates)
123
124 # Interpolate the trajectory
125 interpolated_trajectory = interpolate_trajectory(coordinates2, num_points)
126
127 # Plot the trajectory
128 plot_trajectory(interpolated_trajectory)
129 -----
130 Vessel shape inclusion
131 -----
132
133 import matplotlib.pyplot as plt
134 from matplotlib.patches import Rectangle
135
136 #Vessel dimensions:
137 Breath = 30
138 Length = 90
139 Draft = 5
140 Lfac = 1 #Change manually
141 Bfac = 1 # Change manually
142
143 def plot_square(center_x, center_y, angle, w=Length/Lfac, h=Breath/Bfac):
144     """
145     Plots a square object on a Cartesian grid given the coordinates of its center and side
        length.
146     """
147     # Calculate the corner coordinates of the square
148     x = center_x - w / 2
149     y = center_y - h / 2
150
151     # Create a rectangle patch with the calculated coordinates
152     rect = Rectangle((x, y), 1.35*w, h, linewidth=1, angle = angle, edgecolor='black',
        facecolor='none')
153
154     return rect, x, y
155 -----
156 This function makes a vessel shape and changes the grid
157 -----
158 import numpy as np
159 import matplotlib.pyplot as plt
160 from matplotlib.patches import Rectangle
161 from matplotlib.transforms import Affine2D
162
163 def set_matrix_values_within_rotated_rectangle(matrix, x, y, angle, width = Length/Lfac,
    height= Breath/Bfac, D = Draft):
164     """
165     Sets the values within a rotated rectangle in a matrix.
166     The value at each point within the rectangle is dependent on its location.
167     """
168     rect_transform = Affine2D().translate(width/2, height/2).rotate_deg_around(x, y, angle)
169

```



```

170     x_start = x - width/2
171     y_start = y - height/2
172
173     # Create a grid of indices corresponding to the matrix
174     rows, cols = matrix.shape
175     x_grid, y_grid = np.meshgrid(np.arange(cols), np.arange(rows))
176
177     transformed_grid = rect_transform.inverted().transform(np.column_stack((x_grid.ravel(),
178                                     y_grid.ravel())))
179     transformed_x_grid = transformed_grid[:, 0].reshape((rows, cols))
180     transformed_y_grid = transformed_grid[:, 1].reshape((rows, cols))
181     # print(np.shape(transformed_x_grid))
182     # print(np.shape(matrix))
183     Ds = D # m draft
184     Dp = Ds*10**4
185     Lp = Length
186     Bp = Breath
187     a = 16
188     cl = 2
189     cb = 16
190
191     x = transformed_x_grid - x_start
192     y = transformed_y_grid - y_start
193
194     value = Dp*(1 - cl*((x-0.5*Lp/Lfac)/Lp)**4)*(1 - cb*((y-0.5*Bp/Bfac)/Bp)**2)*np.exp(-a*((
195     y-0.5*Bp/Bfac)/Bp)**2)
196     print(np.shape(value))
197     # Check if the transformed indices are within the rectangle and set the corresponding
198     values
199     mask = (transformed_x_grid >= x_start) & (transformed_x_grid < x_start + width) & \
200           (transformed_y_grid >= y_start) & (transformed_y_grid < y_start + height)
201     matrix[mask] = value[mask]
202     for i in range(len(matrix)):
203         for j in range(len(matrix[i])):
204             if matrix[i, j] < 0:
205                 matrix[i, j] = 0
206             else:
207                 matrix[i, j] = matrix[i, j]
208
209     return matrix
210
211 -----
212 This Function creates the input file for the Delft3D FM model for 2 vessels sailing 120s
213 apart
214 -----
215 timestep = np.linspace(0, 0.5*(len(interpolated_trajectory)), (len(interpolated_trajectory)
216 +1))
217
218 print(timestep)
219 with open('NWlongfinerot_2(2ships)_120sapart_seastart_100.amp', 'w') as file:
220     file.write(f'### START OF HEADER' + '\n')
221     file.write(f'### This file is created by Deltares' + '\n')
222     file.write(f'### Additional comments' + '\n')
223     file.write(f'FileVersion = 1.03' + '\n')
224     file.write(f'filetype = meteo_on_equidistant_grid' + '\n')
225     file.write(f'NODATA_value = -9999.0' + '\n')
226     file.write(f'n_cols = 6000' + '\n')
227     file.write(f'n_rows = 450' + '\n')
228     file.write(f'grid_unit = m' + '\n')
229     file.write(f'x_llcenter = {-4000}' + '\n')
230     file.write(f'y_llcenter = {+2100}' + '\n')
231     file.write(f'dx = 1' + '\n')
232     file.write(f'dy = 1' + '\n')
233     file.write(f'n_quantity = 1' + '\n')
234     file.write(f'quantity1 = air_pressure' + '\n')
235     file.write(f'unit1 = Pa' + '\n')
236     file.write(f'### END OF HEADER' + '\n')
237     for i in range(len(interpolated_trajectory)):
238         if i == len(interpolated_trajectory) - 1:
239             angle = np.arctan((interpolated_trajectory[i][1] - interpolated_trajectory[i-1][1]) /
240                               (interpolated_trajectory[i][0] - interpolated_trajectory[i-1][0]))

```

```

235     else:
236         angle = np.arctan((interpolated_trajectory[i+1][1] - interpolated_trajectory[i
237         ] [1]) / (interpolated_trajectory[i+1][0] - interpolated_trajectory[i][0]))
238         angle_deg = np.degrees(angle)
239
240     matrix = np.zeros((450, 6000)) # Example matrix filled with zeros
241     rect = plot_square(interpolated_trajectory[i][0], interpolated_trajectory[i][1],
242         angle = angle_deg, w=Length/Lfac, h=Breath/Bfac)[0]
243
244     fmat = set_matrix_values_within_rotated_rectangle(matrix, rect.get_x(), rect.get_y(),
245         rect.get_angle(), rect.get_width(), rect.get_height(),D = Draft)
246
247     flipmatrix = np.flip(fmat, axis = 0)
248
249     text = f'TIME = {timestep[i]} seconds since 2001-01-02 00:00:00 +00:00'
250     file.write(text + '\n')
251     flipmatrix2 = np.zeros((450, 6000))
252     if timestep[i] <= 120:
253         flipmatrix2 = np.zeros((450, 6000))
254         factor =np.arange(1/100,1+1/100,1/100)
255         if i < 100:
256             flipmatrix = factor[i]*flipmatrix
257         else:
258             flipmatrix = 1*flipmatrix
259             finalflipmatrix = flipmatrix + flipmatrix2
260             np.savetxt(file, finalflipmatrix, fmt='%d', delimiter=' ')
261     else:
262         matrix = np.zeros((450, 6000)) # Example matrix filled with zeros
263         angle = np.arctan((interpolated_trajectory[i-240+1][1] - interpolated_trajectory[
264         i-240][1]) / (interpolated_trajectory[i-240+1][0] - interpolated_trajectory[i
265         -240][0]))
266         angle_deg = np.degrees(angle)
267         rect = plot_square(interpolated_trajectory[i-240][0], interpolated_trajectory[i
268         -240][1], angle = angle_deg, w=Length/Lfac, h=Breath/Bfac)[0]
269
270         fmat2 = set_matrix_values_within_rotated_rectangle(matrix, rect.get_x(), rect.
271         get_y(), rect.get_angle(), rect.get_width(), rect.get_height(),D = Draft)
272
273         flipmatrix3 = np.flip(fmat2, axis = 0)
274
275         factor =np.arange(1/100,1+1/100,1/100)
276         if i < 100+240:
277             flipmatrix3 = factor[i -240]*flipmatrix3
278         else:
279             flipmatrix3 = 1*flipmatrix3
280             finalflipmatrix = flipmatrix + flipmatrix3
281             np.savetxt(file, finalflipmatrix, fmt='%d', delimiter=' ')
282 plt.imshow(finalflipmatrix, cmap='hot');
283 plt.colorbar() # Optional colorbar
284 plt.show()

```

## E.3. Bedlevel file changer

This python file is used to change the .xyz-files, necessary for the bathymetry input, to the desired layouts.

```

1 import matplotlib
2 import numpy as np
3 from matplotlib import pyplot as plt
4 import pandas as pd
5 import sys # curvilinear file
6 import matplotlib
7 import numpy as np
8 from matplotlib import pyplot as plt
9 import pandas as pd
10 import sys # curvilinear file
11 #%%
12 def open_txtfile_as_matrix(filepath):
13     matrix = []
14     with open(filepath, 'r') as file:

```

```

15     for line in file:
16         # Split the line by a delimiter (e.g., space, comma) to separate values
17         values = line.strip().split()
18         if values[2] == '-nan(ind)':
19             del values
20         else:
21             values[2] = values[2]
22             #
23             print(values)
24             # Convert the values to integers or floats if needed
25             row = [float(value) for value in values]
26             # Append the row to the matrix
27             matrix.append(row)
28
29     # Convert the matrix to a NumPy array for convenient manipulation
30     matrix = np.array(matrix)
31
32     return matrix
33
34 filepath = 'P:/studenten-riv/03_Work/Sander_Broeders/3_7(1ship)/dflowfm/
35           bedlevelrotated_flat_3.xyz'
36 mat = open_txtfile_as_matrix(filepath)
37 #%%
38 import pandas as pd
39 m = pd.DataFrame(mat)
40
41 # m = m[m.iloc[:,0] <= 6000-3000] #basis
42 # m = m[m.iloc[:,0] >= 0-3000] #basis
43
44 m = m[m.iloc[:,0] <= 1000]
45 m = m[m.iloc[:,0] >= 200]
46 m = m[m.iloc[:,1] <= 2300]
47
48 # m = m[m.iloc[:,1] <= 500+2000]
49 # m = m[m.iloc[:,1] >= 0+2000]
50 # mat = mat[65000 <= mat[:,0] <= 80000]
51 import matplotlib.pyplot as plt
52 x = m.iloc[:,0]
53 y = m.iloc[:,1]
54 z = m.iloc[:,2]
55 plt.scatter(x, y, c=z)
56 cbar = plt.colorbar()
57 cbar.set_label('Bed level')
58 plt.xlabel('X')
59 plt.ylabel('Y')
60 plt.title('Check starting bl')
61 plt.axis('equal')
62
63 # Display the plot
64 plt.show()
65 #%%
66 m = pd.DataFrame(mat)
67
68 import pandas as pd
69
70 # Assuming your data is stored in a pandas DataFrame called 'data' with columns [x, y, z]
71
72 # m = m[m.iloc[:,0] <= 6000-3000] #basis
73 # m = m[m.iloc[:,0] >= 0-3000] #basis
74
75 # m = m[m.iloc[:,0] <= 1000]
76 # m = m[m.iloc[:,0] >= 400]
77 # m = m[m.iloc[:,1] <= 2300]
78
79 m = m[m.iloc[:,0] <= 3000] #basis
80 m = m[m.iloc[:,0] >= -5000] #basis
81 m = m[m.iloc[:,1] >= 500]
82 m = m[m.iloc[:,0] >= -2250]
83
84 # m = m[m.iloc[:,0] <= 1500]
85 # m = m[m.iloc[:,0] >= 100]
86 # m = m[m.iloc[:,1] <= 2400]

```

```

85 # m = m[m.iloc[:,1] >= 1900]
86
87 # polygon_points = [[(270, 2150), (385, 2160),(385, 2150), (270, 2140)], # Neighbouring
    groyne fields closed
88 #         [(400, 2160), (525, 2170), (525, 2160),(400, 2150) ],
89 #         [(890, 2220), (1130, 2230), (1130, 2220),(890, 2210)],
90 #         [(1150, 2230), (1370, 2270), (1370, 2260),(1150, 2220)],
91 #         [(1420, 2280), (1430, 2284), (1445, 2184),(1435, 2180)],
92 #         [(240, 2150), (250, 2152), (260, 2077),(250, 2075)]]
93
94 # polygon_points = [[(270, 2150), (525, 2170),(525, 2160), (270, 2140)], # Lay out 2
95 #         [(890, 2220), (1370, 2270), (1370, 2260),(890, 2210)],
96 #         [(1420, 2280), (1430, 2284), (1445, 2184),(1435, 2180)],
97 #         [(240, 2150), (250, 2152), (270, 2025),(260, 2025)],
98 #         [(562, 2181), (822, 2219), (823, 2209), (563, 2171)],
99 #         [(540, 2174), (545, 2174), (565, 2058), (560, 2058)],
100 #         [(843, 2211), (848, 2211), (864, 2102), (859, 2102)]]
101
102 # polygon_points = [[(240, 2150), (385, 2160),(385, 2150), (240, 2140)], # Lay out 3
103 #         [(400, 2160), (687, 2203), (689, 2193),(400, 2150) ],
104 #         [(703, 2202), (842, 2220), (844, 2210),(705, 2192)],
105 #         [(842, 2220), (1130, 2230), (1130, 2220),(844, 2210)],
106 #         [(1420, 2280), (1430, 2284), (1445, 2184),(1435, 2180)],
107 #         [(1150, 2230), (1425, 2283), (1425, 2273),(1150, 2220)],
108 #         [(240, 2150), (250, 2152), (270, 2025),(260, 2025)],
109 #         [(540, 2174), (545, 2174), (565, 2058), (560, 2058)],
110 #         [(843, 2211), (848, 2211), (864, 2102), (859, 2102)]]
111
112 polygon_points = [[(240, 2150), (385, 2160),(385, 2150), (240, 2140)], # Lay out 4
113 #         [(400, 2160), (687, 2203), (689, 2193),(400, 2150) ],
114 #         [(703, 2202), (842, 2220), (844, 2210),(705, 2192)],
115 #         [(842, 2220), (1130, 2230), (1130, 2220),(844, 2210)],
116 #         [(1420, 2280), (1430, 2284), (1445, 2184),(1435, 2180)],
117 #         [(1150, 2230), (1425, 2283), (1425, 2273),(1150, 2220)],
118 #         [(240, 2150), (250, 2152), (270, 2025),(260, 2025)],
119 #         [(375, 2155), (385, 2155), (387, 2105), (377, 2105)],
120 #         [(400, 2155), (410, 2155), (412, 2105), (402, 2105)],
121 #         [(677, 2198), (687, 2198), (691, 2148), (681, 2148)],
122 #         [(703, 2197), (713, 2197), (717, 2148), (707, 2148)],
123 #         [(1120, 2225), (1130, 2225), (1130, 2185), (1120, 2185)],
124 #         [(1150, 2225), (1160, 2225), (1160, 2185), (1150, 2185)]]
125 #         [(540, 2174), (545, 2174), (565, 2058), (560, 2058)], #higher groynes
126 #         [(843, 2211), (848, 2211), (864, 2102), (859, 2102)]]
127
128 for k in range(len(polygon_points)):
129     for index, row in m.iterrows():
130         x = row[0]
131         y = row[1]
132         is_inside_polygon = False
133
134         # Define the polygon using four points
135 #         polygon_points = [(557, 2170), (840, 2210), (860, 2100), (565, 2060)]
136
137         j = len(polygon_points[k]) - 1
138         for i in range(len(polygon_points[k])):
139             if ((polygon_points[k][i][1] < y <= polygon_points[k][j][1]) or
140                 (polygon_points[k][j][1] < y <= polygon_points[k][i][1])) and \
141                 (x < (polygon_points[k][j][0] - polygon_points[k][i][0]) *
142                  (y - polygon_points[k][i][1]) / (polygon_points[k][j][1] -
143                  polygon_points[k][i][1]) + polygon_points[k][i][0]):
144                 is_inside_polygon = not is_inside_polygon
145                 j = i
146
147             if is_inside_polygon:
148                 m.at[index, 2] = 1.0
149                 print('halfway')
150
151 # Print the updated DataFrame
152 print(m)
153 x = m.iloc[:,0]
154 y = m.iloc[:,1]

```

```
154 z = m.iloc[:,2]
155 plt.scatter(x, y, c=z, marker = '.')
156 cbar = plt.colorbar()
157 cbar.set_label('Bed level')
158 plt.xlabel('X')
159 plt.ylabel('Y')
160 plt.title('Final resulting map')
161 plt.axis('equal')
162
163 # Display the plot
164 plt.show()
165 %%
166 m.to_csv('bedlevelrotated_Layout3_flat_3.xyz', sep='\t', index=False, line_terminator='\n')
167 m.to_csv('P:/studenten-riv/03_Work/Sander_Broeders/Bedlevels/Bedlevel_layout4_flat3_progress.
xyz', sep='\t', index=False, line_terminator='\n')
168 %%
169
170 m = m[m.iloc[:,0] <= 1500]
171 m = m[m.iloc[:,0] >= 100]
172 m = m[m.iloc[:,1] <= 2400]
173 m = m[m.iloc[:,1] >= 1900]
174 import matplotlib.pyplot as plt
175 x = m.iloc[:,0]
176 y = m.iloc[:,1]
177 z = m.iloc[:,2]
178 plt.scatter(x, y, c=z, marker = '.')
179 cbar = plt.colorbar()
180 cbar.set_label('Bed level')
181 plt.xlabel('X')
182 plt.ylabel('Y')
183 plt.title('Final resulting map')
184 plt.axis('equal')
185
186 # Display the plot
187 plt.show()
```

# F

## Sediment analysis

Several sediment samples have been taken from Groyne Field 9 during several visits. Morphology is not considered in this study. However, the samples have been sieved. The sieve curves are shown below.

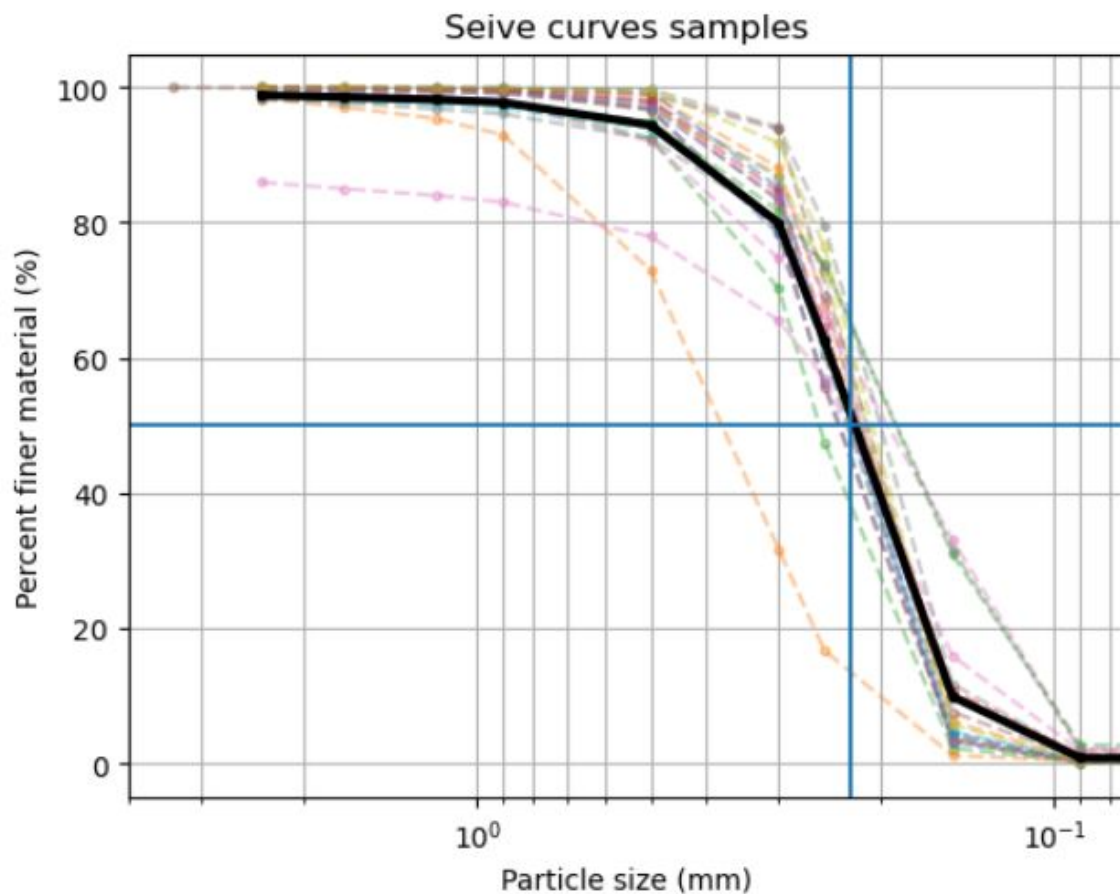


**Figure F.1:** The colours represent the sieve curves of different samples and the black line represents the average results. The horizontal and vertical blue line shows the 50-percentile grain size.

Samples	Naam	Datum
1	1-Top	2022-12-27
2	2	2022-12-27
3	3	2022-12-27
4	4	2022-12-27
5	1	2023-01-06
6	2 Top	2023-01-06
7	3 Oever zijde	2023-01-06
8	4 ZW zijde	2023-01-06
9	1 Kop Bovenstr	2023-01-25
10	2 Top	2023-01-25
11	3 Staart beneden	2023-01-25
12	1 Bij langsdam midden opening	2023-02-26
13	2: Naast ijzeren staaf westgeul	2023-02-26
14	3: Zeezijde eiland dwarsgeul	2023-02-26
15	4: midden eiland	2023-02-26
16	5: Voorkant oostzijde (opening krib)	2023-02-26
17	1	2023-03-22
18	2	2023-03-22
19	3	2023-03-22

**Figure F.2:** This figure shows the labelling of the different samples which indicates the location in the groyne field. Information about the sampling date is also included.